AD NUMBER

AD864115

LIMITATION CHANGES

TO:

Approved for public release; distribution is unlimited.

FROM:

**Distribution authorized to U.S. Gov't. agencies and their contractors;
Administrative/Operational Use; OCT 1969. Other requests shall be referred to Army Aviation Materiel Labs., Fort Eustis, VA.**

AUTHORITY

USAAMRDL ltr 18 Jun 1971

AD

USAAVLABS TECHNICAL REPORT 69-71

GROUND-BASED FLIGHT SIMULATION OF THE CH-47C HELICOPTER

By

Nicholas Albion
John R. Leet
P. Austin Mollenkof

October 1969

U. S. ARMY AVIATION MATERIEL LABORATORIES
FORT EUSTIS, VIRGINIA

CONTRACT DAAJ02-69-C-0047
VERTOL DIVISION
THE BOEING COMPANY
PHILADELPHIA, PENNSYLVANIA

156

DISCLAIMERS

The findings in this report are not to be construed as an official Department of the Army position unless so designated by other authorized documents.

When Government drawings, specifications, or other data are used for any purpose other than in connection with a definitely related Government procurement operation, the United States Government thereby incurs no responsibility nor any obligation whatsoever; and the fact that the Government may have formulated, furnished, or in any way supplied the said drawings, specifications, or other data is not to be regarded by implication or otherwise as in any manner licensing the holder or any other person or corporation, or conveying any rights or permission, to manufacture, use, or sell any patented invention that may in any way be related thereto.

DISPOSITION INSTRUCTIONS

Destroy this report when no longer needed. Do not return it to the originator.

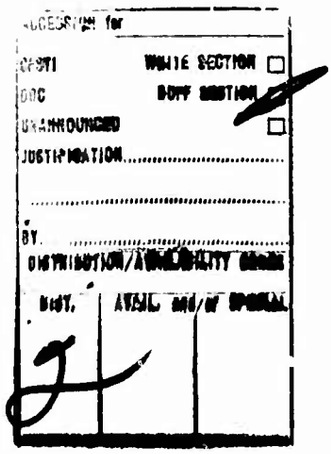

DEPARTMENT OF THE ARMY
U. S. ARMY AVIATION MATERIEL LABORATORIES
FORT EUSTIS, VIRGINIA 23604

This report has been reviewed by the U. S. Army Aviation Materiel Laboratories and is considered to be technically sound. The work was performed under Contract DAAJ02-69-C-0047 to program, set up, and validate a full maneuvering simulation of the CH-47 helicopter. The contract also required programming of an Advanced Flight Control Concept (AFCC).

The report is published for the dissemination and application of information and the stimulation of ideas in the area of simulation technology, with emphasis on handling qualities research.

Task 1F162204A14233
Contract DAAJ02-69-C-0047
USAAVLABS Technical Report 69-71
October 1969

GROUND-BASED FLIGHT SIMULATION OF THE CH-47C HELICOPTER

Final Report

D8-2418-1

by

Nicholas Albion
John R. Leet
P. Austin Mollenkof

Prepared by

Vertol Division
The Boeing Company
Philadelphia, Pennsylvania

for

U. S. ARMY AVIATION MATERIEL LABORATORIES
FORT EUSTIS, VIRGINIA

ABSTRACT

A ground-based simulation of the CH-47C tandem-rotor helicopter was constructed and evaluated. The mathematical model provided a fully coupled, large-perturbation representation of the aircraft which was used in conjunction with a five-degree-of-freedom motion base and a wide-angle point light source visual display. The mathematical model was validated by comparing its static and dynamic characteristics with flight test data. A test pilot flew the simulated aircraft to determine the degree of realism achieved and to evaluate the accuracy with which the CH-47 was represented. Representative data and pilot comments are presented in support of the evaluation. The simulation was found to possess sufficient fidelity to be used for investigating control system concepts and the associated handling qualities of the CH-47C.

FOREWORD

This research was performed by the Vertol Division of Boeing, under the sponsorship of the Army Aviation Materiel Laboratories (Contract DAAJ02-69-C-0047, DA Task 1F162204A14233). The research was monitored by Mr. Robert P. Smith of the Army Aviation Materiel Laboratories.

The research was conducted by Nicholas Albion, John R. Leet, and P. Austin Mollenkof of Boeing and John B. Sinacori of Northrop Corporation.

BLANK PAGE

TABLE OF CONTENTS

	Page
ABSTRACT	iii
FOREWORD	v
LIST OF ILLUSTRATIONS	ix
LIST OF TABLES	xiii
LIST OF SYMBOLS	xiv
INTRODUCTION	1
Background	1
Approach	1
Work Performed	4
IMPLEMENTATION OF THE SIMULATION WITH CONVENTIONAL FLIGHT CONTROL SYSTEM	7
General Description of the Simulation	7
Capabilities and Limitations of the Simulation	7
Definition of Mathematical Model	9
Ground-Based Simulator Configuration	18
Analog Computer Programming	32
Operating Procedures	33
SIMULATION VALIDATION WITH CONVENTIONAL FLIGHT CONTROL SYSTEM STATIC CHECKOUT	35
Dynamic Check	46
Pilot Evaluation	50
IMPLEMENTATION OF SIMULATION WITH ADVANCED FLIGHT CONTROL CONCEPT	56
Modeling of AFCC	56
Analog Computer Programming for AFCC	56
Simulator Cockpit Configuration for AFCC	56
ADVANCED FLIGHT CONTROL CONCEPT VALIDATION	58
CONCLUSIONS	59
RECOMMENDATIONS	61

	Page
LITERATURE CITED	63
GLOSSARY	64
APPENDIXES	
I. Pilot Comments	66
II. Isolated Rotor and Static Trim Data . . .	77
III. Unpiloted Dynamic Data	104
IV. Pilot Validation Data	117
DISTRIBUTION	139

LIST OF ILLUSTRATIONS

Figure		Page
1	Sketch of Ground-Based Simulator	2
2	CH-47C Three-view	3
3	Sidearm Controller	6
4	Ground-Based Simulation Block Diagram . . .	8
5	Equation Block Diagram	11
6	Aircraft Body Axis System	13
7	Instrument Display	19
8	Cockpit Instrument	20
9	Simulator X-Axis Frequency Response	23
10	Simulator Y-Axis Frequency Response	24
11	Simulator Z-Axis Frequency Response	25
12	Simulator Pitching Frequency Response . . .	26
13	Simulator Rolling Frequency Response	27
14	Simulator Yawing Frequency Response	28
15	Visual Display	30
16	Vibration Simulation	31
17	Audio Simulation	31
18	Torque Versus Thrust for CH-47C	36
19	Forward Flight Trim	38
20	Forward Flight Trim	39
21	Forward Flight Trim	40
22	Forward Flight Trim	41
23	Forward Flight Trim	42
24	Sideward Flight Trim	43

Figure		Page
25	Sideward Flight Trim	44
26	Sideward Flight Trim	45
27	Autorotation Rate of Descent	47
28	Dynamic Responses - Longitudinal Pulse . . .	49
29	Simulator Cockpit	57
30	Torque Versus Thrust for CH-47C	79
31	Torque Versus Thrust for CH-47C	80
32	H Force Versus Thrust for CH-47C	81
33	H Force Versus Torque for CH-47C	82
34	Static Trim Data	84
35	Static Trim Data	85
36	Static Trim Data	86
37	Static Trim Data	87
38	Static Trim Data	88
39	Static Trim Data	89
40	Static Trim Data	90
41	Static Trim Data	91
42	Static Trim Data	92
43	Static Trim Data	93
44	Static Trim Data	94
45	Static Trim Data	95
46	Static Trim Data	96
47	Static Trim Data	97
48	Static Trim Data	98
49	Static Trim Data	99

Figure		Page
50	Static Trim Data	100
51	Static Trim Data	101
52	Isolated Rotor Dynamics	103
53	Dynamic Responses - Longitudinal Pulse . . .	106
54	Dynamic Responses - Longitudinal Pulse . . .	107
55	Dynamic Responses - Lateral Pulse	108
56	Dynamic Responses - Pitch SAS Failure . . .	
57	Dynamic Responses - Roll SAS Failure	110
58	Dynamic Responses - Yaw SAS Failure	111
59	Dynamic Responses - Single-Engine Failure .	112
60	Dynamic Responses - Directional Pulse . . .	113
61	Dynamic Responses - Lateral Pulse	114
62	Dynamic Responses - Longitudinal Pulse . . .	115
63	Dynamic Responses - Collective Step	116
64	Pilot Validation - Conventional Control System (Pitch SAS Failure)	120
65	Pilot Validation - Conventional Control System (Roll SAS Failure)	121
66	Pilot Validation - Conventional Control System (Yaw SAS Failure)	122
67	Pilot Validation - Conventional Control System (Hover at 10 Degrees Nose Down) . . .	123
68	Pilot Validation - Conventional Control System (Hover to 10 Knots)	124
69	Pilot Validation - Conventional Control System (Forward Flight 10 Degrees Nose Down)	126
70	Pilot Validation - Conventional Control System (Acceleration).	127

Figure		Page
71	Pilot Validation - Conventional Control System (Deceleration)	129
72	Pilot Validation - Conventional Control System (Autorotation)	131
73	Pilot Validation - Conventional Control System (Climb)	132
74	Pilot Validation - Conventional Control System (Spot Turn)	133
75	Pilot Validation - Conventional Control System (SAS Off)	134
76	Pilot Validation - Conventional Control System (Forward Flight SAS On)	135
77	Pilot Validation - Conventional Control System (Moderate Turbulence)	136
78	Pilot Validation - Conventional Control System (Lateral Start - Stop)	137
79	Pilot Validation - Conventional Control System (Acceleration Through Transition)	138

LIST OF TABLES

Table		Page
I	Cockpit Instruments	21
II	Cockpit Control Travel	22
III	Equipment List	32
IV	Control Power and Stability Derivatives . . .	48
V	Isolated Rotor Characteristics	78
VI	Static Trim Data	83
VII	Isolated Rotor Dynamics	102
VIII	Dynamic Data	105
IX	Pilot Conventional Validation	118

LIST OF SYMBOLS

A_{ICFR}	front rotor lateral cyclic - wind axes, radians
A_{ICRR}	rear rotor lateral cyclic - wind axes, radians
AGL	above ground level
ALT	density altitude, ft
A/S	airspeed, kn
B_{ICFR}	front rotor - wind axes, radians
B_{ICRR}	rear rotor - wind axes, radians
C_T	rotor thrust coefficient
DFG	diode function generator
f(H)	ground effect altitude variation factor
f	landing gear body axis force, lb
f_o	oscillator basic frequency, Hz
G	input to motion and display systems
G (ω)	simulator amplitude ratio, db
g	acceleration due to gravity, ft/sec^2
H	rotor drag force perpendicular to shaft in down wind direction, lb
H	altitude of rotor hub, ft
H_D	density altitude, ft
H_{FW}	height of the main landing gear - looking parallel to helicopter z axis, ft.
H_{RW}	height of the aft landing gear - looking parallel to helicopter z axis, ft
IGE	in ground effect
IAS	indicated airspeed
I_{xx}	helicopter moment of inertia about x axis, $slug\text{-}ft^2$

I_{yy}	helicopter moment of inertia about y axis, slug-ft^2
I_{zz}	helicopter moment of inertia about z axis, slug-ft^2
I_{xz}	helicopter product of inertia in x-z plane, slug-ft^2
L	total rolling moment about helicopter cg, ft-lb
L_H	lateral rotor hub moment, ft-lb
L_P	change in rolling moment per unit change in roll rate, $\frac{\text{radians/sec}^2}{\text{radians/sec}}$
L_{δ_S}	change in rolling moment per unit change in lateral stick, $\frac{\text{radians/sec}^2}{\text{in.}}$
M	total pitching moment about helicopter cg, ft-lb
M_H	longitudinal rotor hub moment, ft-lb
M_Q	change in pitching moment per unit change in pitch rate, $\frac{\text{radians/sec}^2}{\text{radians/sec}}$
M_{δ_B}	change in pitching moment per unit change in longitudinal stick, $\frac{\text{radians/sec}^2}{\text{in.}}$
m	helicopter mass, slugs
N	total yawing moment about helicopter cg, ft-lb
N_R	rotor speed, rpm
N_R	change in yawing moment per unit change in yaw rate, $\frac{\text{radians/sec}^2}{\text{radians/sec}}$
N_{δ_R}	change in yawing moment per unit change in directional pedals, $\frac{\text{radians/sec}^2}{\text{in.}}$
OGE	out of ground effect
P	component of helicopter angular rotation rate about x axis, radians/sec
$\dot{P}$	aircraft angular acceleration about x-axis, radians/sec^2
Q	component of helicopter angular rotation rate about y axis, radians/sec

$\dot{Q}$	aircraft angular acceleration about y axis, radians/sec^2
Q_{AERO}	torque required, ft-lb
Q_G	rotor governor torque, ft-lb
R	component of helicopter angular rotation rate about z axis, radians/sec
$\dot{R}$	aircraft angular acceleration about z axis, radians/sec^2
R/C	rate of climb, fpm
T	rotor thrust force parallel to shaft, lb
u'	component of free-stream velocity
u	component of inertial velocity along x axis, ft/sec
$\dot{u}$	aircraft acceleration component along x axis, ft/sec^2
V	total free-stream velocity, ft/sec
VCO	voltage-controlled oscillator
v'	component of free-stream velocity along y axis, ft/sec
v	component of inertial velocity along y axis, ft/sec
$\dot{v}$	aircraft acceleration component along y axis, ft/sec^2
w	component of inertial velocity along z axis, ft/sec
$\dot{w}$	aircraft acceleration component along the z body axis
X	total force along helicopter x axis, lb
$\dot{X}_B$	velocity of helicopter cg along the x axis, ft/sec
(X, Y, Z)	inertial axis coordinates
Y	total force along helicopter y axis, lb
Y	rotor side force perpendicular to shaft and downwind direction, lb
$\dot{Y}_B$	velocity of helicopter cg along the y axis, ft/sec

Z	total force along helicopter z axis, lb
Z_w	change in z force per unit change in free-stream velocity component, $\frac{ft/sec^2}{ft/sec}$
Z_{δ_C}	change in z force per unit change in collective pitch control, $\frac{ft/sec^2}{in.}$
$\dot{z}_B$	velocity of helicopter cg along the z axis, ft/sec
α_R	angle of attack of rotor plane, deg
β	fuselage sideslip angle, radians
β'	rotor sideslip angle, radians
β'_F	sideslip angle of front rotor, radians
δ_B	longitudinal control, in.
δ_C	collective control, in.
δ_R	directional control, in.
δ_S	lateral control, in.
θ_o	root collective pitch, radians
$\theta_{.75}$	three-quarter blade radius collective pitch, deg
λ	rotor inflow ratio
λ'	component of inflow ratio due to free-stream velocity
μ	rotor advance ratio
(ϕ,θ,ψ)	yaw, pitch, roll Euler axis components
(ϕ',θ',ψ')	yaw, roll, pitch Euler axis components
Ω	rotor rotational speed, radians/sec
Ω_0	initial rotor rotational speed, radians/sec
$\nabla\Omega_p$	pilot engine beep, radians/sec
ρ	air density, slug/ft^3
ρ_0	air density at sea level, slug/ft^3
ΣQ_{AERO}	summation of front and rear rotor torque required

LIST OF SUBSCRIPTS

B	about aircraft center of gravity
CO	cockpit
D	visual display
DCPT	differential collective pitch trim
F	front rotor or landing gear
g	gust
FUS	fuselage
L	left landing gear
M	motion base
P	pilot
pe	pilot eye
R	rear rotor or landing gear
R	right landing gear
SAS	stability augmentation system
w	steady wind
x	x body axis component
y	y body axis component
z	z body axis component

INTRODUCTION

This report describes a ground-based simulation of the CH-47B/C helicopter. The simulation was performed under USAAVLABS Contract DAAJ02-69-C-0047, in which The Boeing Company, Vertol Division, contracted to program, set up, and validate a large-perturbation simulation of the CH-47. The facilities used for this program were the ground-based simulator (Figure 1) and the analog computers located at the Northrop-Norair Research Laboratories in Hawthorne, California. The contract also called for programming the Advanced Flight Control Concept (AFCC), which is described in a Boeing internal report.[1]

BACKGROUND

The CH-47C is a tandem-rotor, medium-lift, troop and cargo transport helicopter. It is powered by two turboshaft engines which can deliver up to 6,000 horsepower. The designed cruise speed is 130 knots; maximum speed capability is 170 knots. The weight ranges from an empty weight of 22,000 pounds to a maximum loaded weight of 46,000 pounds. A power-operated hydraulic flight control system, supplemented by the SAS, provides the helicopter with flight characteristics suitable for both visual flight rules (VFR) and instrument flight rules (IFR) operation. Figure 2 gives a three-view which shows the exterior geometry and overall dimensions of the CH-47C.

Boeing has had experience in the past with successful simulation of the tandem-rotor helicopter configuration. During the year preceding this program, three complex simulations using a fully coupled, large-perturbation mathematical model were conducted. In each simulation the aim was to accurately represent the aircraft for continuous flight from maximum power to autorotation. These simulations included the necessary subsystems, such as the engine governor and stability augmentation system (SAS). Flight test data correlation and test pilot opinion showed that these simulations provided a realistic representation of the aircraft.

APPROACH

In this program the objective was to set up and validate a realistic ground-based simulation of the CH-47C. The simulation was to be suitable for evaluating flight control system concepts and their associated handling qualities, rather than for operational pilot training. These objectives were to be achieved as closely as possible within the constraints imposed by the facility to be used.

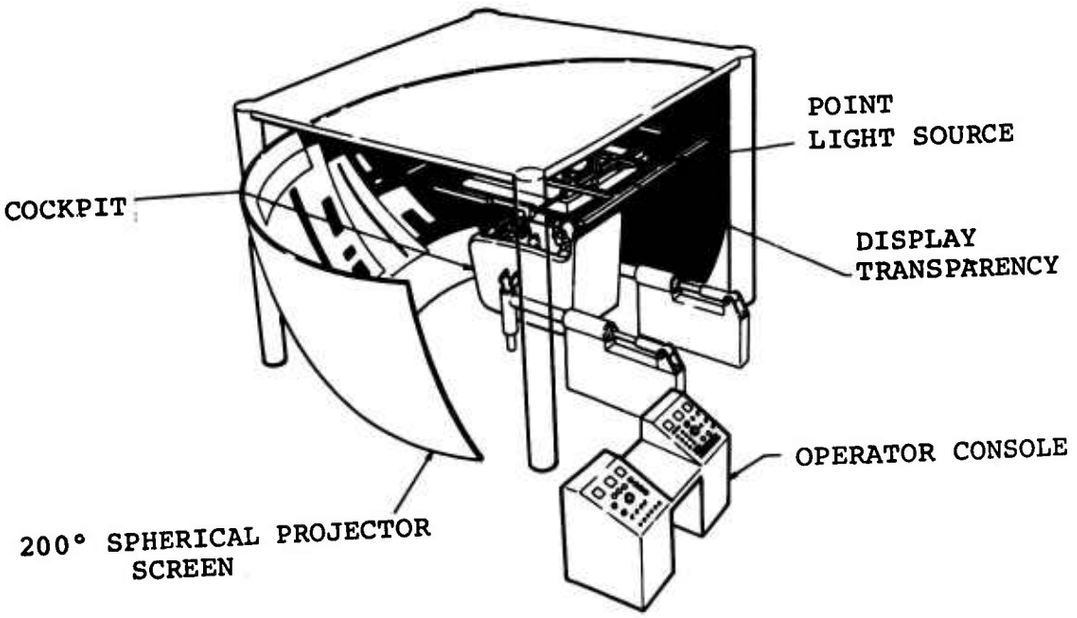

Figure 1. Sketch of Ground-Based Simulator.

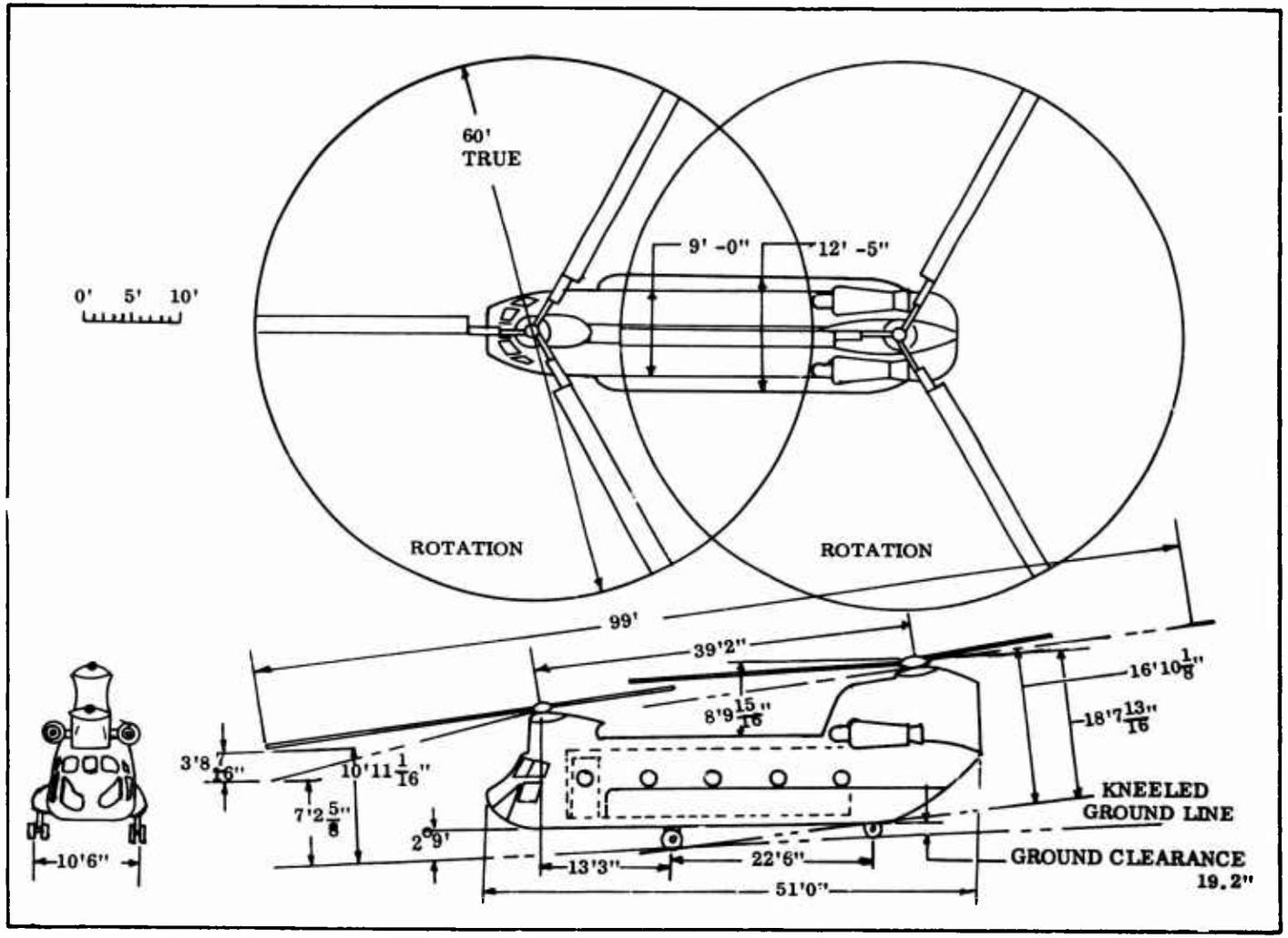

Figure 2. CH-47C Three-View.

The approach used was to provide a mathematical model suitable for the full maneuvering envelope defined in the CH-47C Operator's Manual.[2] In the equations, account was taken of rotor-rotor interference, blade stall, atmospheric turbulence, and ground effect. Test pilot opinion guided the development of the proper blend of kinesthetic and visual cues. When reasonable maneuverability was possible with normal operation of the motion system, the motion base was allowed to be the limit of maneuverability. Additional techniques were used to provide acceptable motion cues only when the normal motion system operation would have placed unreasonable limits on maneuverability.

The mathematical model was validated by comparing it to flight test data and to results from previously validated digital computer programs. Four comparisons were made:

1) The trim characteristics of the analog program were determined to confirm that the static derivatives were correct.

2) The dynamic derivatives were measured to confirm the inertial and quasi-static characteristics of the mathematical model.

3) Dynamic responses to control pulses and augmentation failures were compared with flight test data to confirm the accuracy of the dynamic models of the control system, the SAS, and the rotor.

4) A current CH-47 test pilot flew the completed ground-based simulation to evaluate the overall representation of the aircraft.

WORK PERFORMED

Mathematical models for subsystems not included in previous simulations were developed prior to arriving at the simulator facility. Eighteen weeks were required to complete the program. Fourteen weeks were spent in programming the analog computers and validating the mathematical model; the remaining four weeks were used primarily for pilot evaluation of the simulation.

The simulation incorporated the following effects and vehicle subsystems:

1) Rotor-rotor interference
2) Ground
3) Atmospheric turbulence, steady wind, and wind shear
4) Cockpit noise and vibration
5) Cockpit instrument panel

6) Conventional CH-47 flight control system
7) Governor and engine dynamics
8) Landing gear

The simulation was validated by static, dynamic, and pilot tests. Where possible, the simulation characteristics were compared with other theoretical methods and with flight test data. The static tests consisted of longitudinal and lateral trim speed sweeps, an autorotation speed sweep, and measurement of control power and stability derivatives. The responses to control pulses and single SAS and engine failures were compared to flight test data in the dynamic validation of the mathematical model.

The pilot evaluated the simulation characteristics throughout the flight envelope, including gust response, SAS failure, and SAS off. Maneuvers performed included spot turns, lateral start-stops, climbs, autorotation, sideslips, and coordinated turns.

The mathematical model for the advanced flight control concept (AFCC) was programmed[1], and necessary changes were made in the simulator cockpit. The operation of the AFCC was checked and evaluated by test pilots. Modifications to the simulator cockpit were made for evaluation of a sidearm controller (Figure 3) in conjunction with the AFCC. Development and study of the sidearm controller were part of USAAVLABS Contract DAAJ02-68-C-0019 with Northrop-Norair.

The remaining sections of this report contain a description of the mathematical model and hardware used in the simulation followed by a detailed evaluation of the simulation. Detailed descriptions of the mathematical model and the AFCC are not included in this report but can be found in Boeing reports.[1,3]

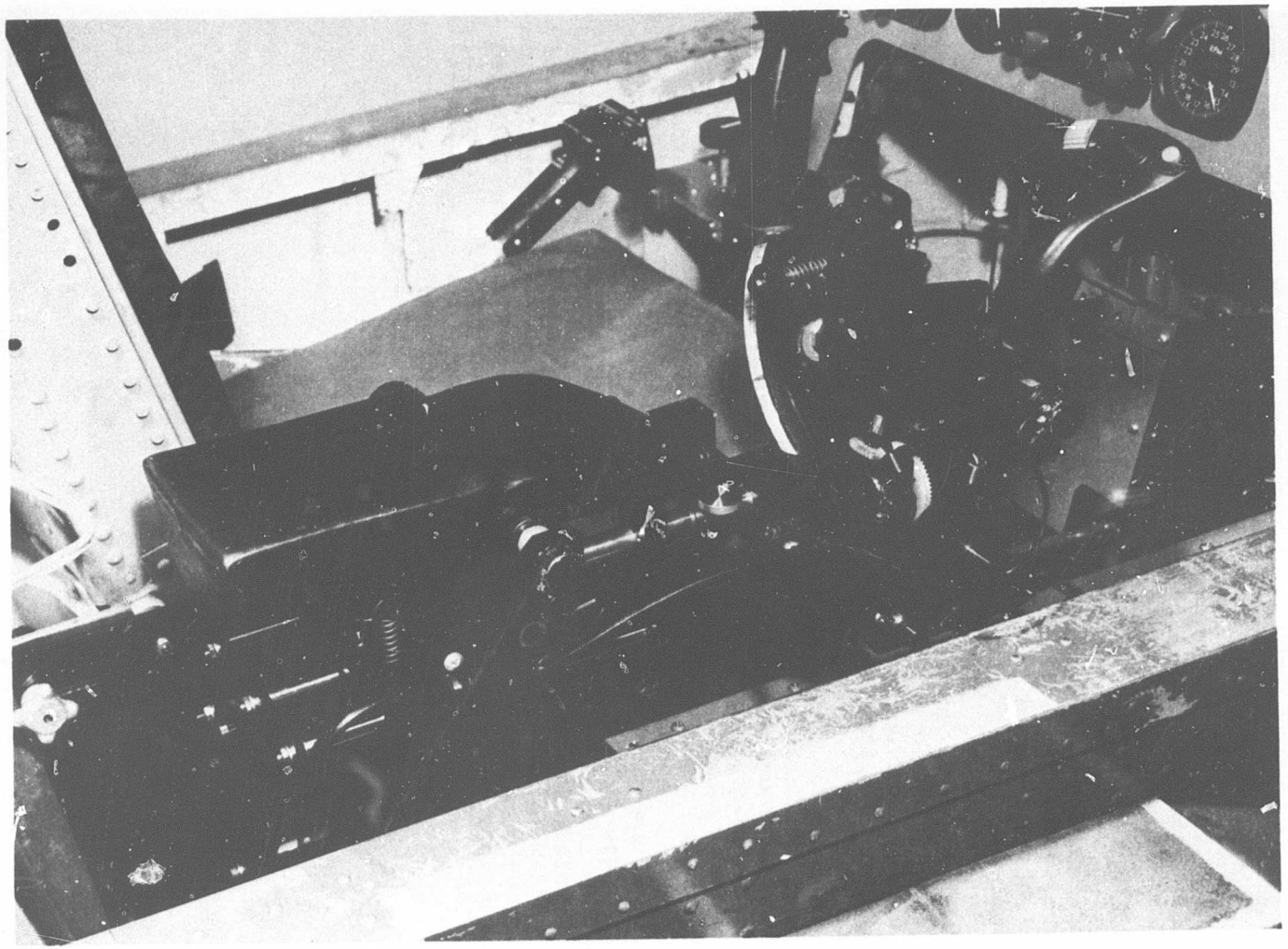

Figure 3. Sidearm Controller.

IMPLEMENTATION OF THE SIMULATION WITH CONVENTIONAL FLIGHT CONTROL SYSTEM

GENERAL DESCRIPTION OF THE SIMULATION

The block diagram in Figure 4 shows the major components of the simulation and the flow of information between them. The pilot controlled the simulated aircraft in response to cues from the visual display, motion base, and cockpit instruments. The pilot-controled inputs to the aircraft equations of motion produced changes in the simulated aircraft state variables. These changes were then used as inputs to the visual display, motion base, and cockpit instruments.

The mathematical model was implemented using seven analog computers. The simulator hardware consisted of a de Florez point light source visual display and a motion base. The point light source projection system produced a continuous six-degree-of-freedom, wide-angle visual display which presented to the pilot appropriate perspective, size, and position. Images were projected in color, showing terrain texture and three-dimensional objects. The motion base was located below the point light source, which was at the center of a 12-foot-radius hemispherical screen.

CAPABILITIES AND LIMITATIONS OF THE SIMULATION

The simulation can be used to investigate control system concepts and handling qualities of the CH-47C. The mathematical model permits simulated continuous flight in any direction for all hover and low-speed maneuvers within the operating limits of the CH-47C. In forward flight, the simulation can be flown continuously from maximum power climbs through autorotation with representative changes in rotor speed. No provisions are made for simulating continuous variation in air density as altitude varies. Continuous heading change is possible, but pitch and roll are limited by the visual display to $\pm$ 25 and $\pm$ 30 degrees, respectively. The largest ratio display transparency provides a maneuvering volume of 22,500 by 22,500 by 6,250 feet high. For near-ground flight, another transparency, which provides a maneuvering volume of 2,250 by 2,250 by 625 feet high, is utilized.

The motion base kinesthetic cues are designed for general-purpose maneuvers rather than for maneuvers throughout the complete flight envelope. The normal capabilities of the motion system are allowed to be the limit of maneuverability when this provides essential general-purpose maneuverability. The simulation is best suited to operation below 70 knots, where the rotational motion base cues are realistic, and where the absent or reduced linear cues do not greatly affect the

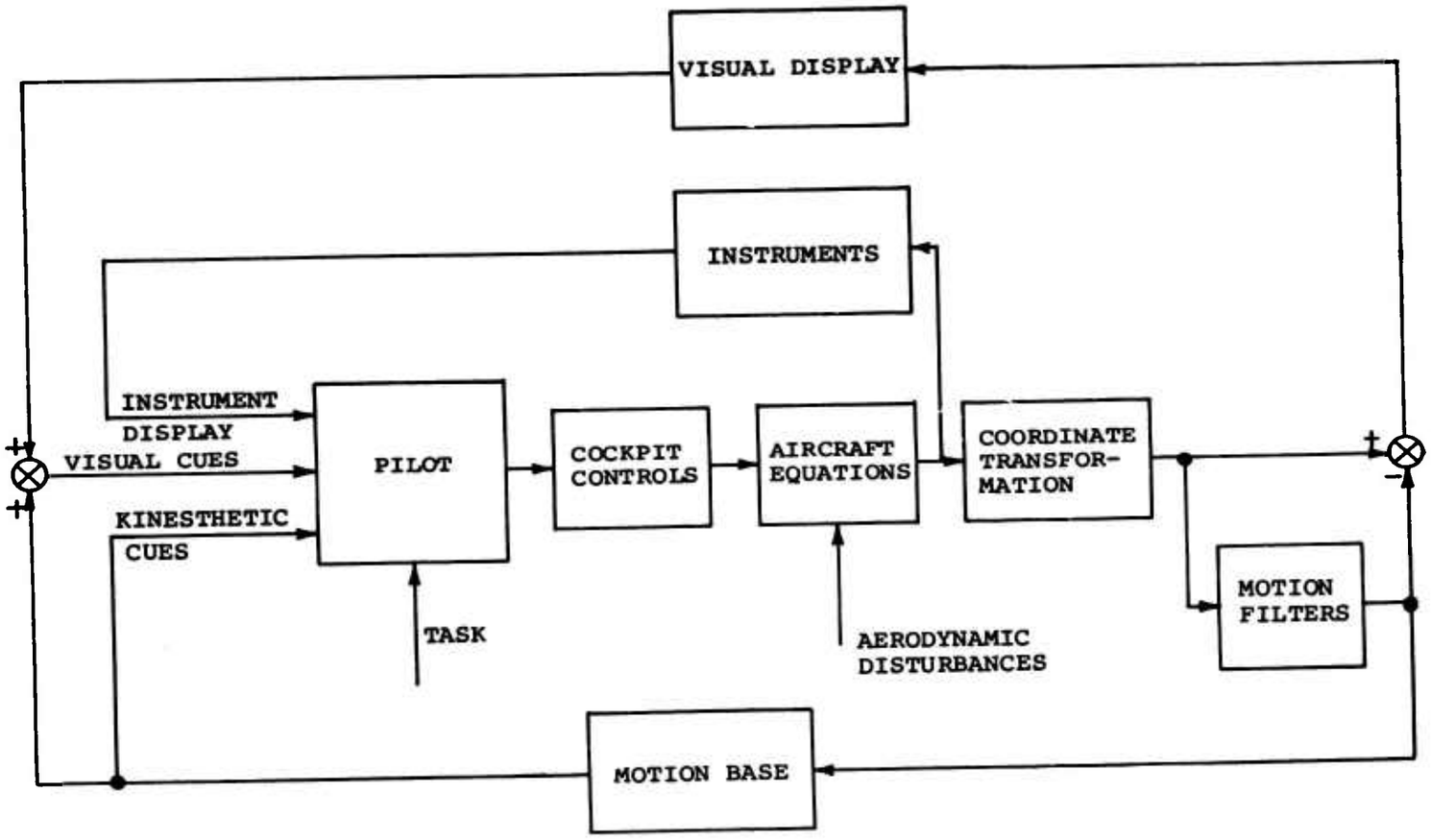

Figure 4. Ground-Based Simulation Block Diagram.

pilot. The resulting configuration allows maneuvers large enough to evaluate the basic handling qualities resulting from changes in the augmentation system, but it is not suitable for the maximum maneuvers allowable in the CH-47C.

Six 8-channel Brush recorders are provided for flight monitoring and data acquisition.

DEFINITION OF MATHEMATICAL MODEL

Basic Equations of Motion

A block diagram showing the information flow in the mathematical model is presented in Figure 5. The helicopter was modeled as having a rigid fuselage with symmetry about the x-z plane. The following equations of motion were written using body axes.[4] (Figure 6 shows the body axis system defining the linear and angular velocity components.)

$$\dot{u} = \frac{X}{m} - g \sin\theta + Rv - Qw \tag{1}$$

$$\dot{v} = \frac{Y}{m} + g \cos\theta \sin\phi + Pw - Ru \tag{2}$$

$$\dot{w} = \frac{Z}{m} + g \cos\theta \cos\phi + Qu - Pv \tag{3}$$

$$\dot{P} = \frac{L}{I_{xx}} + \frac{I_{xz}}{I_{xx}} \dot{R} + \frac{(I_{yy} - I_{zz})}{I_{xx}} QR + \frac{I_{xz}}{I_{xx}} PQ \tag{4}$$

$$\dot{Q} = \frac{M}{I_{yy}} + \frac{I_{xz}(R^2 - P^2)}{I_{yy}} + \frac{I_{zz} - I_{xx}}{I_{yy}} PR \tag{5}$$

$$\dot{R} = \frac{N}{I_{zz}} + \frac{I_{xz}}{I_{zz}} \dot{P} + \frac{I_{xx} - I_{yy}}{I_{zz}} PQ - \frac{I_{xz}}{I_{zz}} QR \tag{6}$$

Several assumptions were made to minimize the algebraic operations which the analog computers had to perform. Lateral velocity and angular rates were assumed to be small compared to the longitudinal rates. The resulting equations of motion are

$$\dot{u} = \frac{X}{m} - g \sin\theta - Qw \tag{7}$$

$$\dot{v} = \frac{Y}{m} + g \cos\theta \sin\phi - Ru \tag{8}$$

$$\dot{w} = \frac{Z}{m} + g \cos\theta \cos\phi + Qu \tag{9}$$

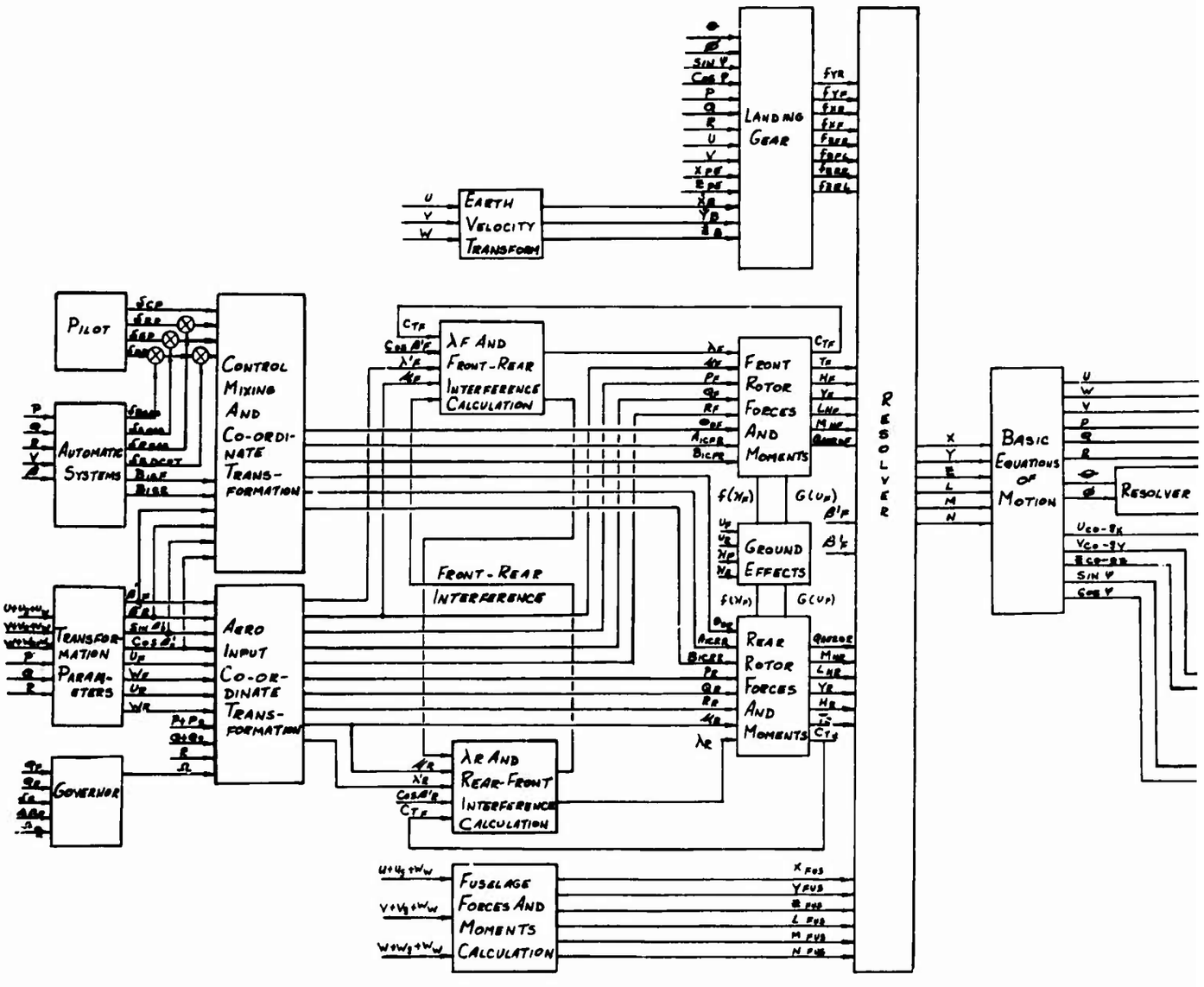

Figure 5. Equation Block Diagram.

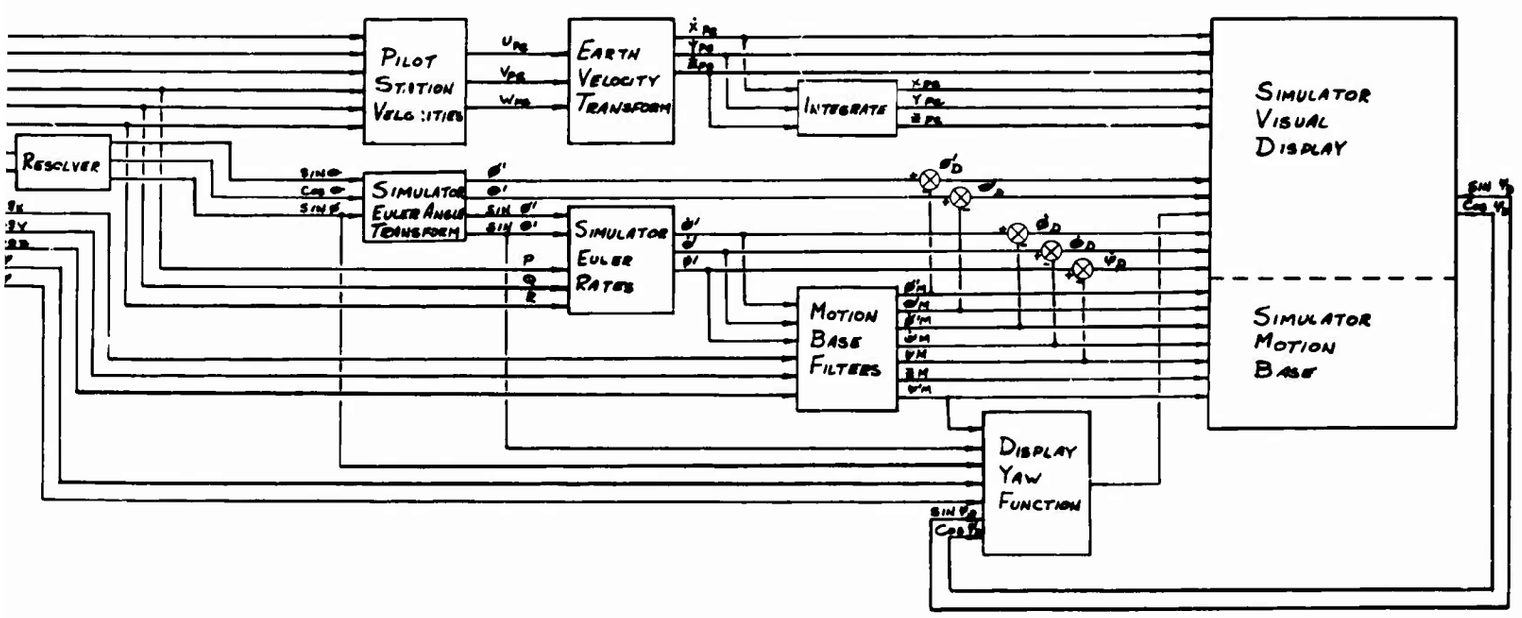
PILOT STATION VELOCITIES
EARTH VELOCITY TRANSFORM
INTEGRATE
SIMULATOR VISUAL DISPLAY
RESOLVER
SIMULATOR EULER ANGLE TRANSFORM
SIMULATOR EULER RATES
MOTION BASE FILTERS
SIMULATOR MOTION BASE
DISPLAY YAW FUNCTION

B

BLANK PAGE

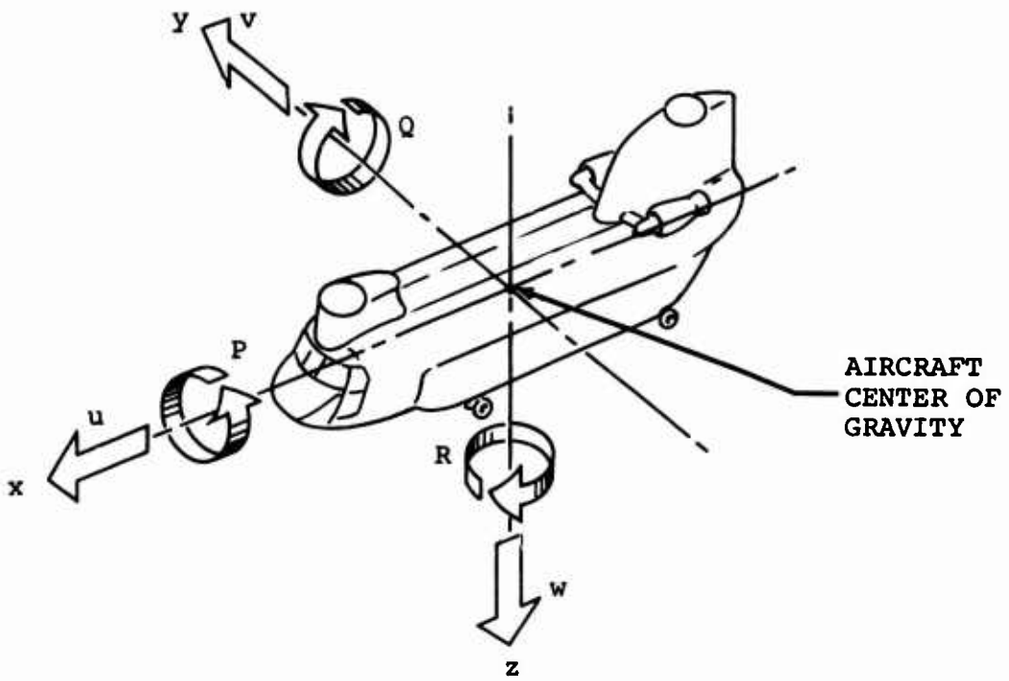

Figure 6. Aircraft Body Axis System.

$$\dot{P} = \frac{L}{I_{xx}} + \frac{I_{xz}}{I_{xx}} \dot{R} + \frac{I_{xz}}{I_{xx}} PQ \tag{10}$$

$$\dot{Q} = \frac{M}{I_{yy}} + \frac{(I_{zz} - I_{xx})}{I_{yy}} PR \tag{11}$$

$$\dot{R} = \frac{N}{I_{zz}} + \frac{I_{xz}}{I_{zz}} \dot{P} + \frac{I_{xx} - I_{yy}}{I_{zz}} PQ - \frac{I_{xz}}{I_{zz}} QR \tag{12}$$

The yaw, pitch, roll Euler axis system was used to describe the orientation of the airframe in inertial-earth coordinates. The equation for Euler angles in terms of the body axes angular rates[5] is

$$\begin{Bmatrix} \dot{\phi} \\ \dot{\theta} \\ \dot{\psi} \end{Bmatrix} = \begin{bmatrix} 1 & \sin\phi \tan\theta & \cos\phi \tan\theta \\ 0 & \cos\phi & -\sin\phi \\ 0 & \sin\phi \sec\theta & \cos\phi \sec\theta \end{bmatrix} \begin{Bmatrix} P \\ Q \\ R \end{Bmatrix} \tag{13}$$

A continuous resolver was used to provide unlimited rotational freedom in heading.

Rotor Equations

The rotor forces and moments were computed in rotor wind axes and then resolved into aircraft body axes for summation with the fuselage and landing gear forces and moments. The wind velocity components were transformed from aircraft body axes to rotor wind axes. Rotor inflow and advance ratios were formed as the ratio of the rotor wind axes vertical and longitudinal velocity components, respectively, to the rotor tip speed. The inflow ratio was composed of terms due to both free stream and induced velocity. The induced velocity input to the inflow ratio, resulting from thrust production and interference, was lagged to simulate the physical characteristics of the actual air mass movement. Interference factors between the front and rear rotors were programmed as functions of the quotient of the inflow ratio to the product of advance ratio and cosine of rotor sideslip angle. For rearward flight, these interference factors were interchanged between the front and rear rotor. Rotor-fuselage interference was neglected, since its effect on aircraft trim and dynamics is small.

Equations for the rotor forces and moments were derived from classical steady-state blade-element aerodynamics. Expressions were developed for coning and first-order longitudinal and lateral flapping coefficients. Second and higher order flapping

coefficients were neglected. Nondimensional rotor force and moment coefficients were computed from the flapping coefficients, inflow and advance ratios, and control inputs. Force and moment coefficients, which were similar for the front and rear rotor, were multiplied by the appropriate dimensional parameters to obtain the force and moment components. Since no provisions were made for continuous changes in air density with variation in altitude, air density had to be set for a specific flight altitude.

Rotor Limits

To simulate stall and increased drag due to compressibility, correction terms were added to the thrust and torque equations. Thrust correction was a function of both thrust and airspeed.

Governor and Engine Dynamics

Governor and engine dynamics were programmed as lagged torque feedback to the rotors proportional to the error in rotor speed. The torque anticipation from the collective control was included in the governor, and the engine beep switch was also included to allow the pilot to change the rotor speed. The governor was limited to the maximum power available from the engines (Lycoming T55-L-11). Maximum available power was not varied continuously with altitude, but it was set for the initial flight altitude. Single and dual engine failures could be simulated.

Ground Effect

Ground effect was simulated as a direct increase in the thrust coefficient for each rotor and was programmed as a function of rotor hub ground speed and distance from the ground. Aircraft pitch attitude was included in the calculation of the altitude for each rotor hub. Ground effects could be switched into and out of the system as desired to evaluate the ground effect model.

Fuselage Aerodynamic Force and Moment

Equations for the fuselage force and moment components were derived from wind tunnel data obtained at the University of Maryland with a one-eighth scale model of the CH-47.[6] These data have been incorporated in several digital computer programs which produce results that closely match flight test data. The data show that the effects of angle of attack on side force and of sideslip angle on vertical force and pitching moment are negligible. Variations of the force and moment components with fuselage angle of attack and sideslip angle, as presented in the wind tunnel data, were approximated by functions of the sine and cosine of these angles.

Conventional Controls

The conventional flight control system consisted of inputs from the longitudinal, collective, lateral, and directional controls. The longitudinal control was formed by inputs from the pilot's stick, the stability augmentation system, and differential collective pitch trim. The collective control consisted only of the pilot input. The lateral and directional controls were each formed by pilot and SAS inputs. These controls were mixed to produce collective pitch and longitudinal cyclic angles for each rotor. For calculating rotor force and moment components, lateral and longitudinal cyclic pitch were transformed to rotor wind axes.

Stability Augmentation System

The CH-47B SAS was used. This system, rather than the CH-47C SAS, was selected because it was more familiar to the test pilot who evaluated the simulation. Also, more comprehensive flight test data were available for the CH-47B SAS. The SAS provided inputs to the longitudinal, lateral, and directional controls. The pitch and roll axes were driven by the respective aircraft angular rates. Roll rate and sideslip angle were fed into the yaw axis in combination with yaw rate. Provisions were made for switching the SAS off and simulating single SAS hardover failures.

Wind Model

Steady wind was assumed to be constant in direction but could be varied in magnitude during the flight. Wind shear was programmed according to the data source used.[7] Body axes components of the steady wind were obtained by transforming from inertial earth axes using small-angle approximations for the pitch and roll angles.

Wind gusts were simulated by a method[8] similar to one previously used at the University of Toronto. The gusts were assumed to be homogeneous, isotropic, and frozen in space. The gust velocity of the three components was obtained by passing signals from three uncorrelated white noise generators through identical low-pass filters. It was determined from the pilot's comments that the break frequency of these filters should be a function of the advancing rotor blade tip speed. Because of insufficient analog capacity, the break frequency could not be varied during flight and had to be set for the initial advancing blade tip speed. During flight, the level of turbulence could be varied from zero to heavy.

Effective angular velocities due to gusts were computed for each rotor. Since the rotor shaft incidence angle is small, the contribution of the yawing component was discounted. The

gust inputs to the rear rotor were the same as those for the front rotor but were delayed to represent the passage of the aircraft through the frozen gust pattern. A second-order Pade approximation was used to simulate the delay. This provided a satisfactory approximation, since the gusts were of low frequency. When the wind was from the rear of the aircraft, the inputs to the front and rear rotor were interchanged. The gust inputs to the fuselage were taken to be the same as those to the front rotor. The effective angular gust velocities were introduced into the rotor flapping expressions.

Landing Gear

A landing gear model was developed to simulate vertical ground contact and all modes of taxiing. All of the landing gear force contributions to pitching and rolling moment were included. However, the contribution of differential braking to yawing moment was omitted. This simplification was consistent with the rigid-body approach used throughout the simulation. Ground contact on sloped terrain was represented with the terrain sloped upward toward north. The landing gear was defined to take account of this ground slope for all headings. The slope could be set to initial angles of from 0 to 15 degrees.

The vertical gear forces were calculated by computing the heights and rates of height change for each of the four wheels and applying them to the appropriate landing gear dynamic equations. The vertical forces were controlled by computer logic to be equal to zero when the respective wheel height was positive.

Longitudinal and lateral gear forces were computed for static, rolling, and sliding conditions. The condition of the longitudinal and lateral force equations was determined by comparing these forces to the applied brake force and force required to overcome static friction. The longitudinal and lateral forces were set in the sliding condition for touchdown.

Difficulty was encountered in mechanizing the landing gear equations. These difficulties were basically a result of excessive computer noise levels, extreme sensitivity of the gear equation logic control, and the degree of accuracy of the simulation at very low translational rates and altitudes.

Resolution and Summation of Forces and Moments

To obtain the total aerodynamic force and moment acting on the aircraft, rotor force and moment components were transformed from rotor wind axes into aircraft body axes and added to the contributions from the fuselage. The forces and moments due to the landing gear were added to the aerodynamic forces and moments to obtain the total external forces and moments acting

on the aircraft. The forces and moments due to gravity were applied directly to the basic equations of motion.

GROUND-BASED SIMULATOR CONFIGURATION

Cockpit Panel Instruments

Figures 7 and 8 show the layout of the cockpit panel instruments, which are listed in Table I. Although the panel layout was not an exact replica of the CH-47C, it was representative in that all of the normal flight instruments were included.

Eleven additional instruments were used for special purposes. A radar altimeter was included to assist the pilot in accurately determining his altitude above the terrain when in hover or low speed transition flight. This was required to compensate for the lower fidelity in visual cues near the ground. Four trim indicators were added to enable the pilot to trim the cockpit controls to the required initial condition before going to operate. Three of these were driven by the out-of-balance accelerations in pitch, roll, and yaw, while the fourth was driven by initial rate of climb. A lateral velocity indicator was used in lieu of a sideslip indicator. The remaining three special instruments were used with the AFCC.[1]

Pilot Controls

Except for the collective and the power steering knob, the controls already fitted from previous programs were used in the simulator cockpit. The controls had the same configuration and positioning as those of the aircraft. Table II compares the control travels provided in the simulator with the actual travels. Detailed differences between the simulator and the aircraft controls existed in the force feel and dead zone characteristics of the longitudinal and collective sticks. Magnetic brakes were used for collective and directional trimming; only beep trim was provided for the longitudinal and directional controls.

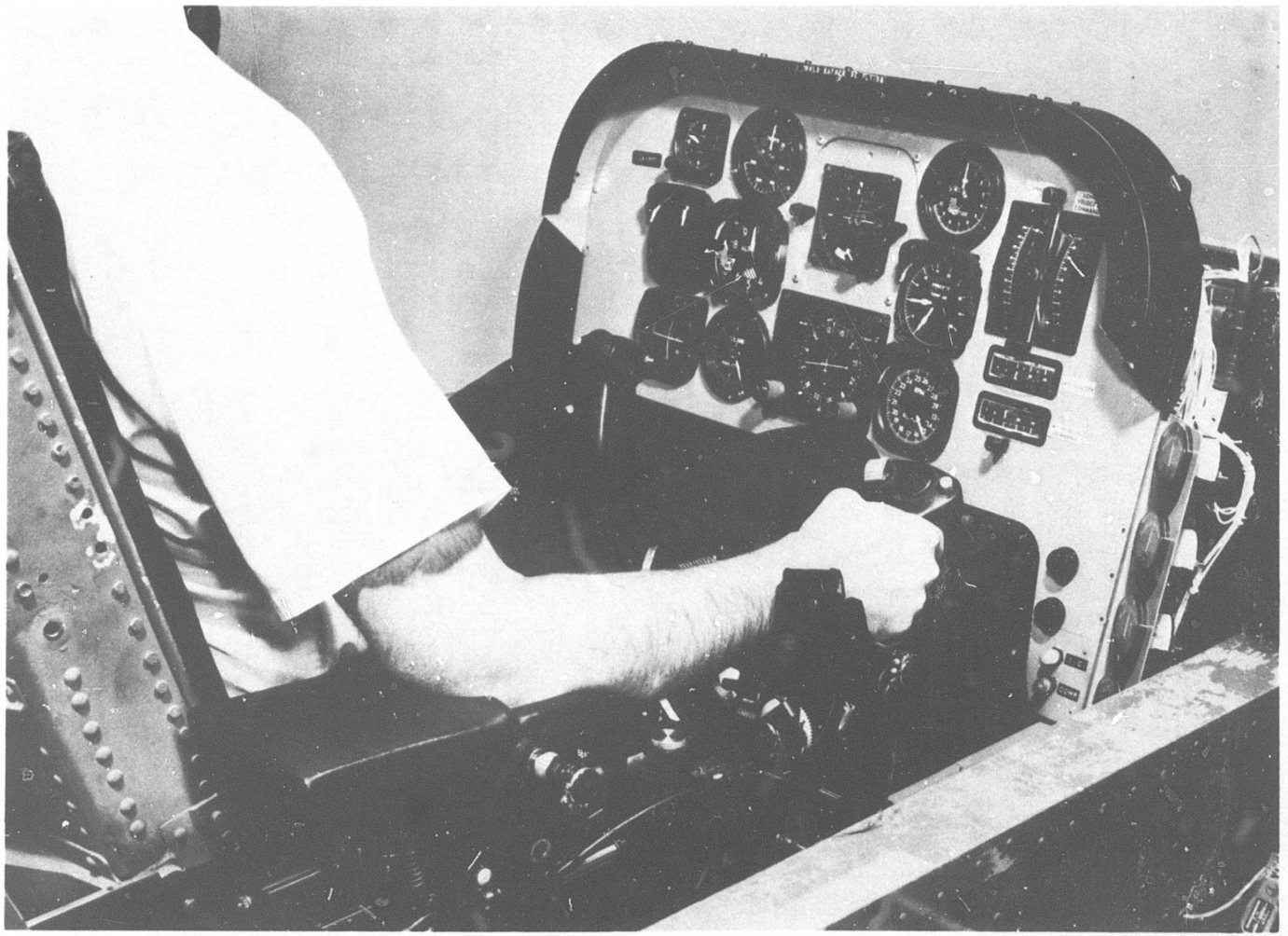

Figure 7. Instrument Display.

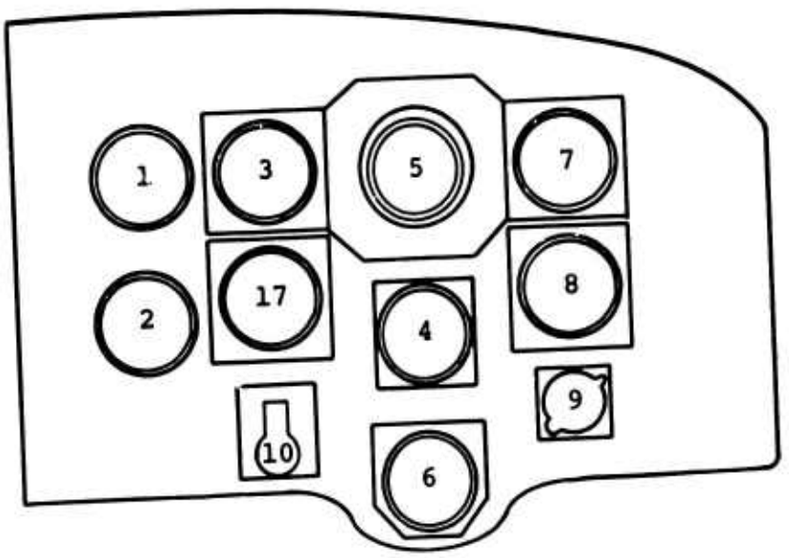

AIRCRAFT PILOT PANEL

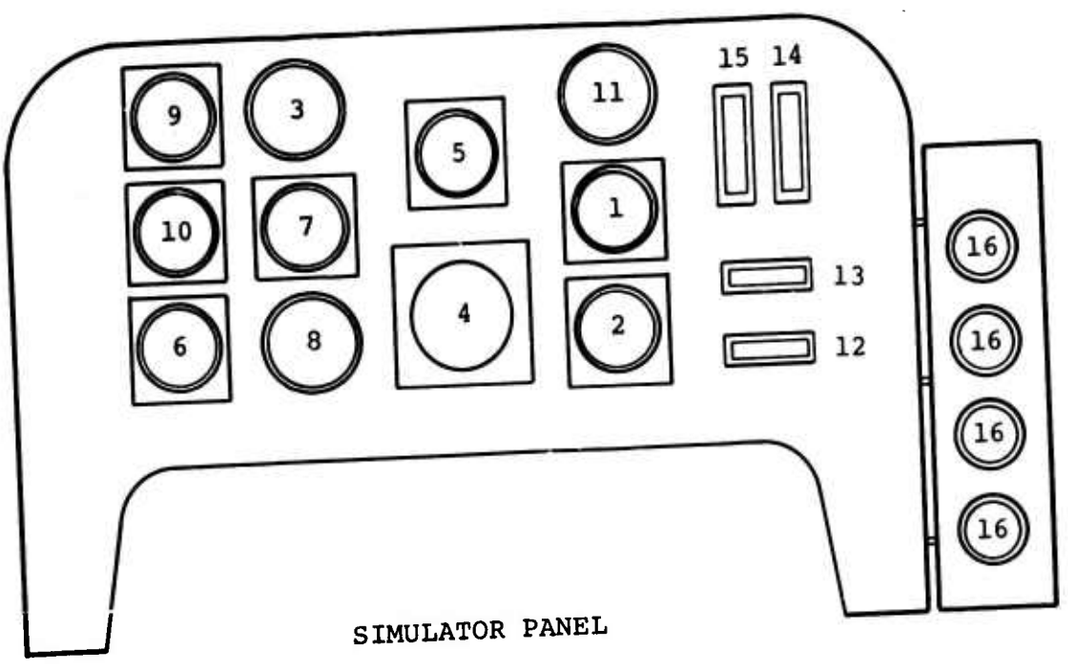

SIMULATOR PANEL

Figure 8. Cockpit Instrument Panel.

TABLE I. COCKPIT INSTRUMENTS

Position Number*	Instrument	Actual Scale Range	Simulator Scale Range
1	Torque Meter**	0-1300 ft-lb	0-100 pct
2	Rotor Tachometer**	0-290 rpm	0-290 rpm
3	Airspeed**	0-250 kn	0-250 kn
4	Gyrocompass**	0-360 deg	0-360 deg
5	Attitude Indicator**	±90 deg	±90 deg
6	Course Indicator**	0-360 deg	0-360 deg
7	Altimeter**	0-99,000 ft	0-99,000 ft
8	Vertical Velocity Indicator**	±3000 ft/min	±3000 ft/min
9	Clock**		
10	Turn and Slip Indicator**+		
11	Radar Altimeter		0-1000 ft
12	Lateral Velocity Command		±40 kn
13	Lateral Velocity		±40 kn
14	Longitudinal Velocity Command		+200 to -40 kn
15	Longitudinal Velocity		+200 to -40 kn
16	Trim Meters		
17	Blank Panel**		

*Refer to Figure 7.

**Existing aircraft equipment.

+Slip indicator blanked out on simulator.

TABLE II. COCKPIT CONTROL TRAVEL		
Control	Actual Travel (in.)	Simulator Travel (in.)
Longitudinal	±6.50	±5.25
Collective	9.12	8.75
Lateral	±4.18	±4.70
Directional	±3.60	±2.75

Cockpit Motion System

The motion system incorporated five degrees of freedom: pitch, roll, yaw, longitudinal, and vertical. The system was capable of ±15 degrees angular and ±9 inches linear travel. The motion drive equations were derived from the accelerations at the pilot's station and from the simulator Euler rates. The motion and visual display systems used the yaw, roll, pitch Euler axes system. The drives, therefore, had to be transformed to this axes system from the aircraft's yaw, pitch, roll Euler axes system. At the same time, redundant integration had to be avoided to prevent drift. This was accomplished, using trigonometric relationships, by transforming the angular components directly from the yaw, pitch, roll system to the yaw, roll, pitch system. Normal acceleration cues were provided using the vertical capability of the motion base. Slow tilting of the cockpit with respect to the gravitational vertical provided steady-state and low-frequency longitudinal and lateral acceleration cues. Since the accelerations perceived by the pilot in the simulator included gravity, the aircraft gravity terms were subtracted from the cockpit accelerations to give perturbation accelerations.

The linear and rotational motion filter characteristics were determined by a method described in a recent American Helicopter Society paper.[9] The normal acceleration was high-pass filtered; the longitudinal and lateral accelerations were low-pass filtered. The rotational cues were based on the dynamic sensitivity of the ear canals. The simulator Euler rates were low-pass filtered using a first-order washout to give the motion base rotations.

The performance level of the servos in the motion and visual display systems was high enough not to influence the fidelity of the simulation. Frequency responses of the motion and display systems are shown in Figures 9 through 14.

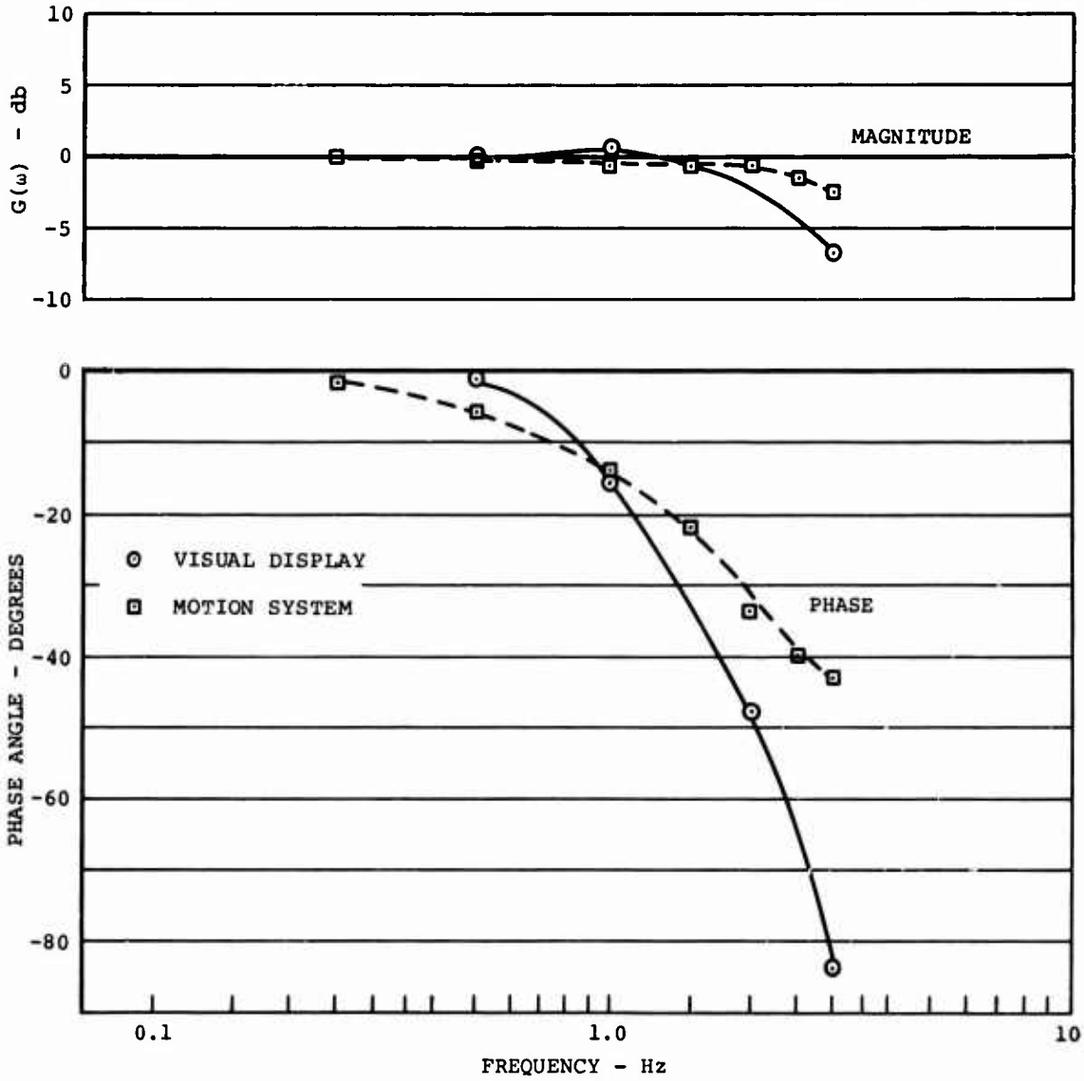

Figure 9. Simulator X-Axis Frequency Response.

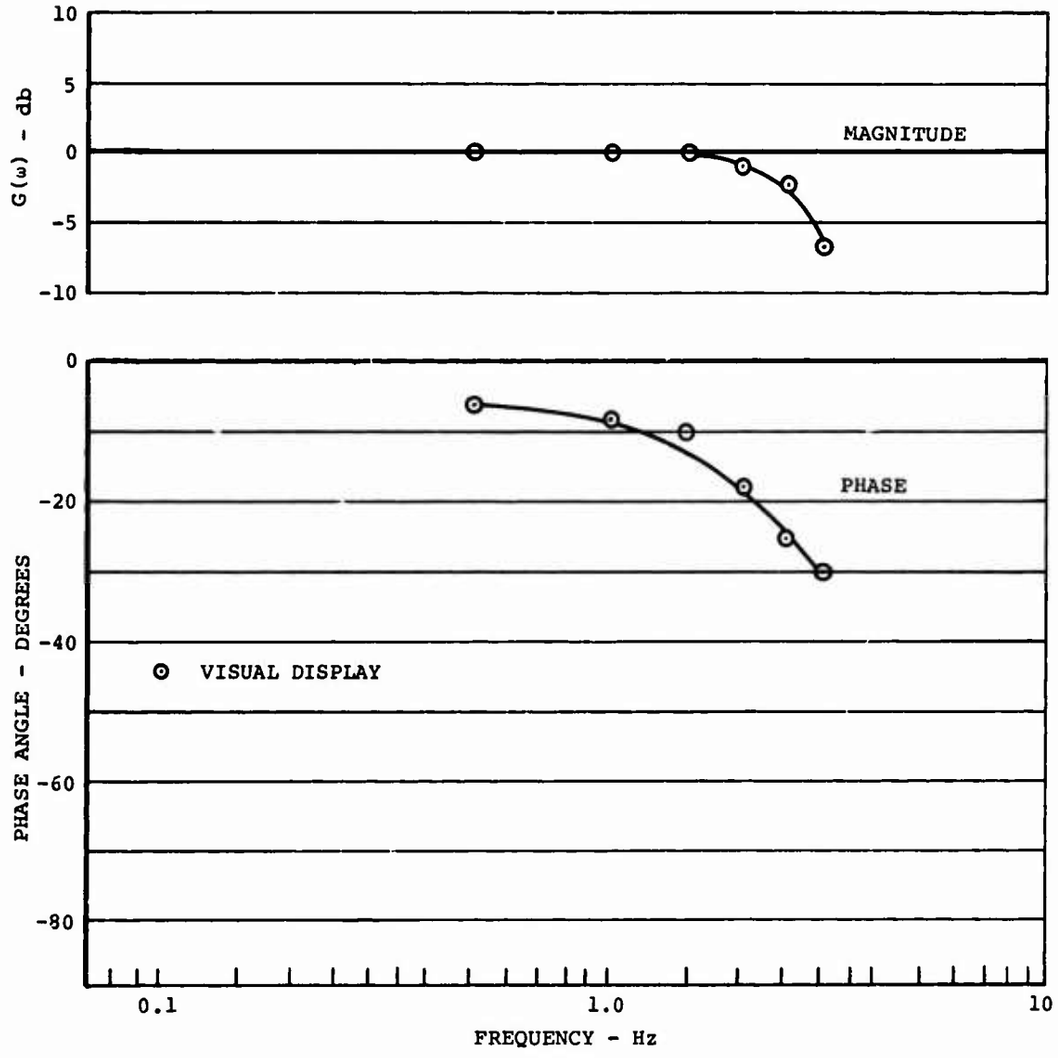

Figure 10. Simulator Y-Axis Frequency Response.

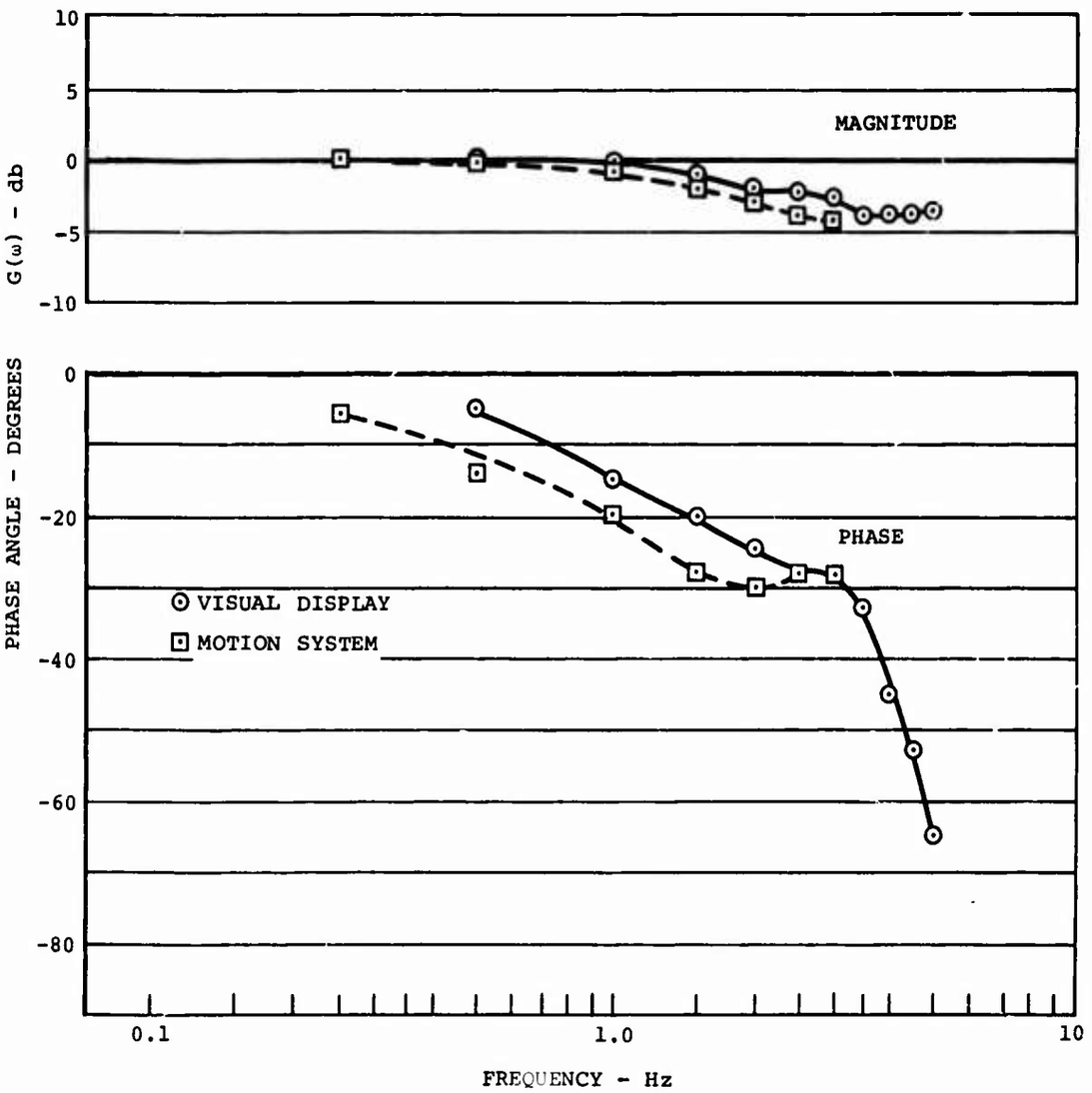

Figure 11. Simulator Z-Axis Frequency Response.

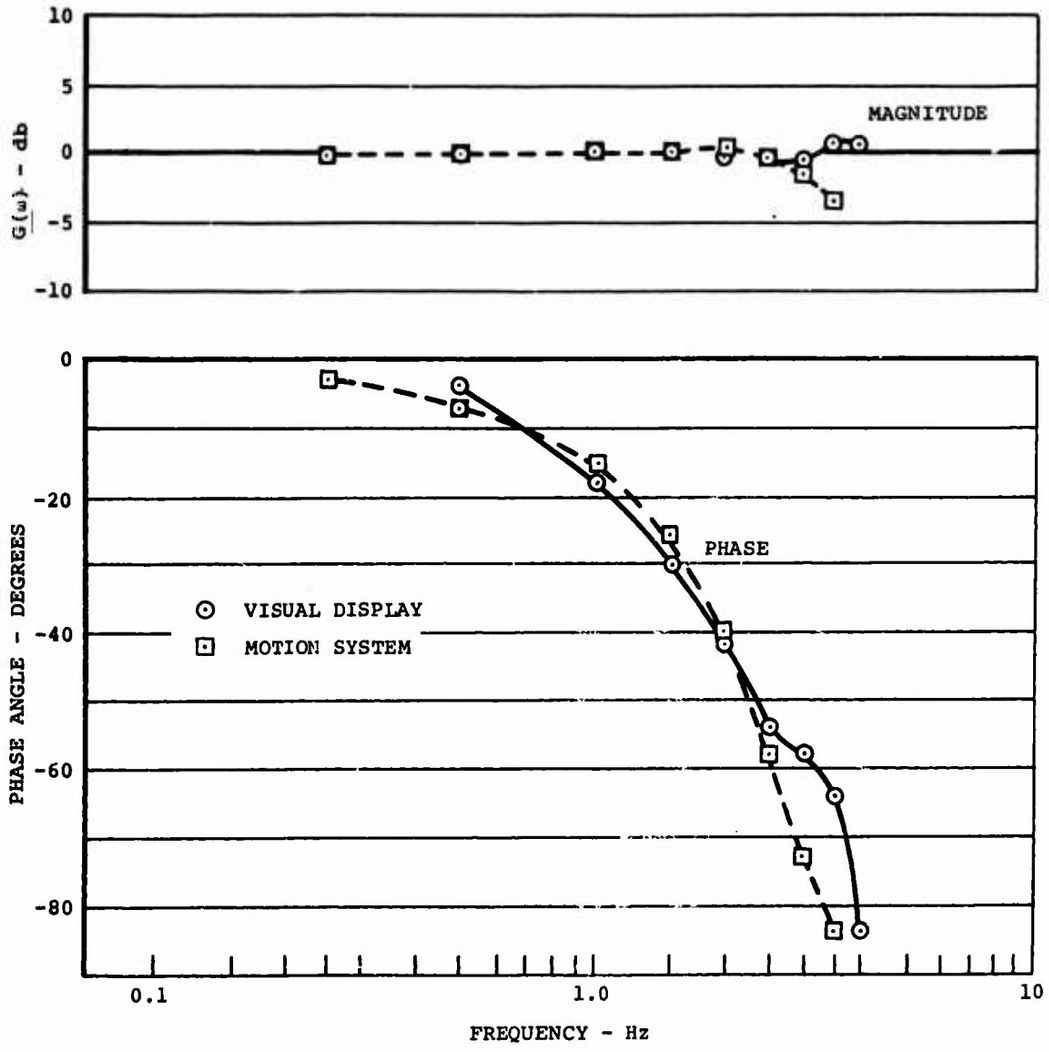

Figure 12. Simulator Pitching Frequency Response.

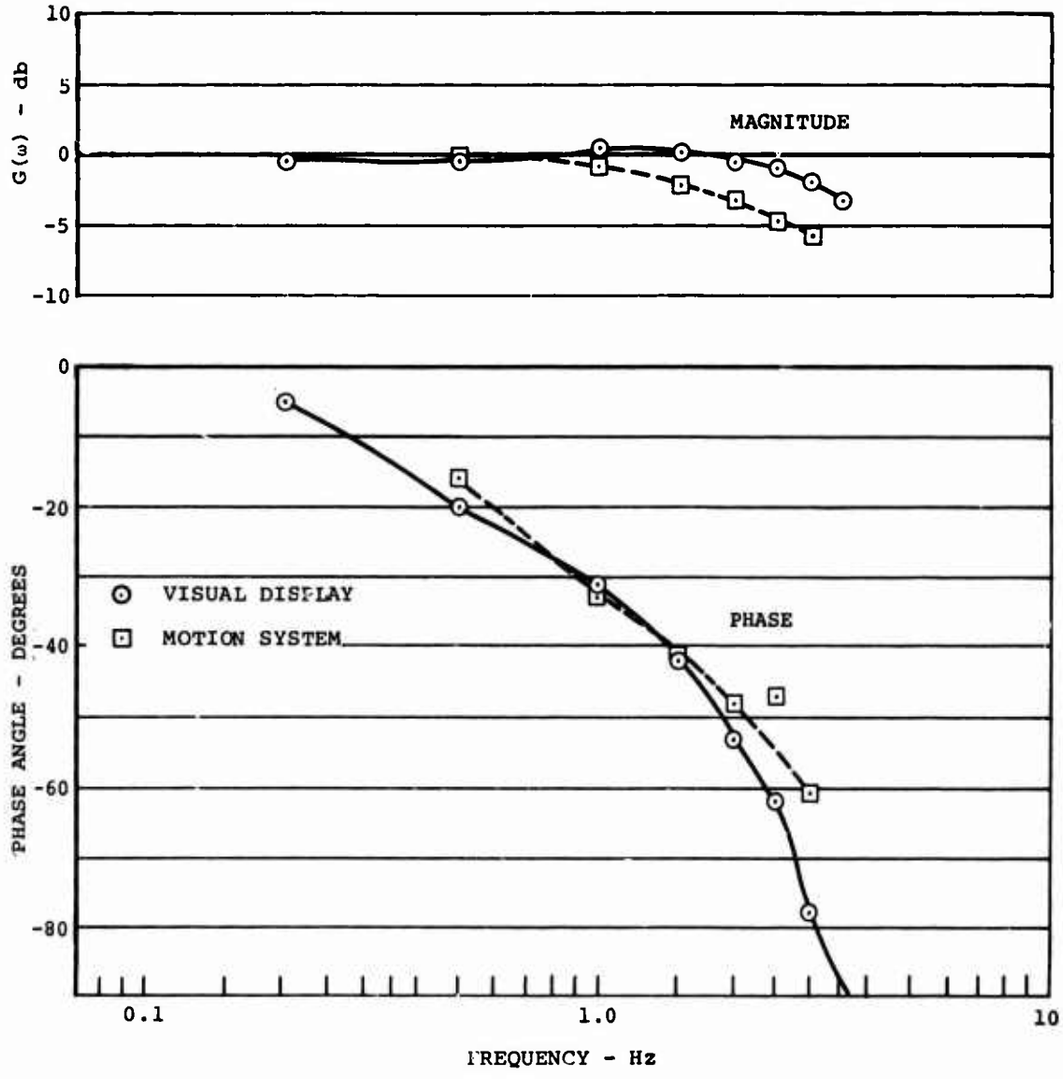

Figure 13. Simulator Rolling Frequency Response.

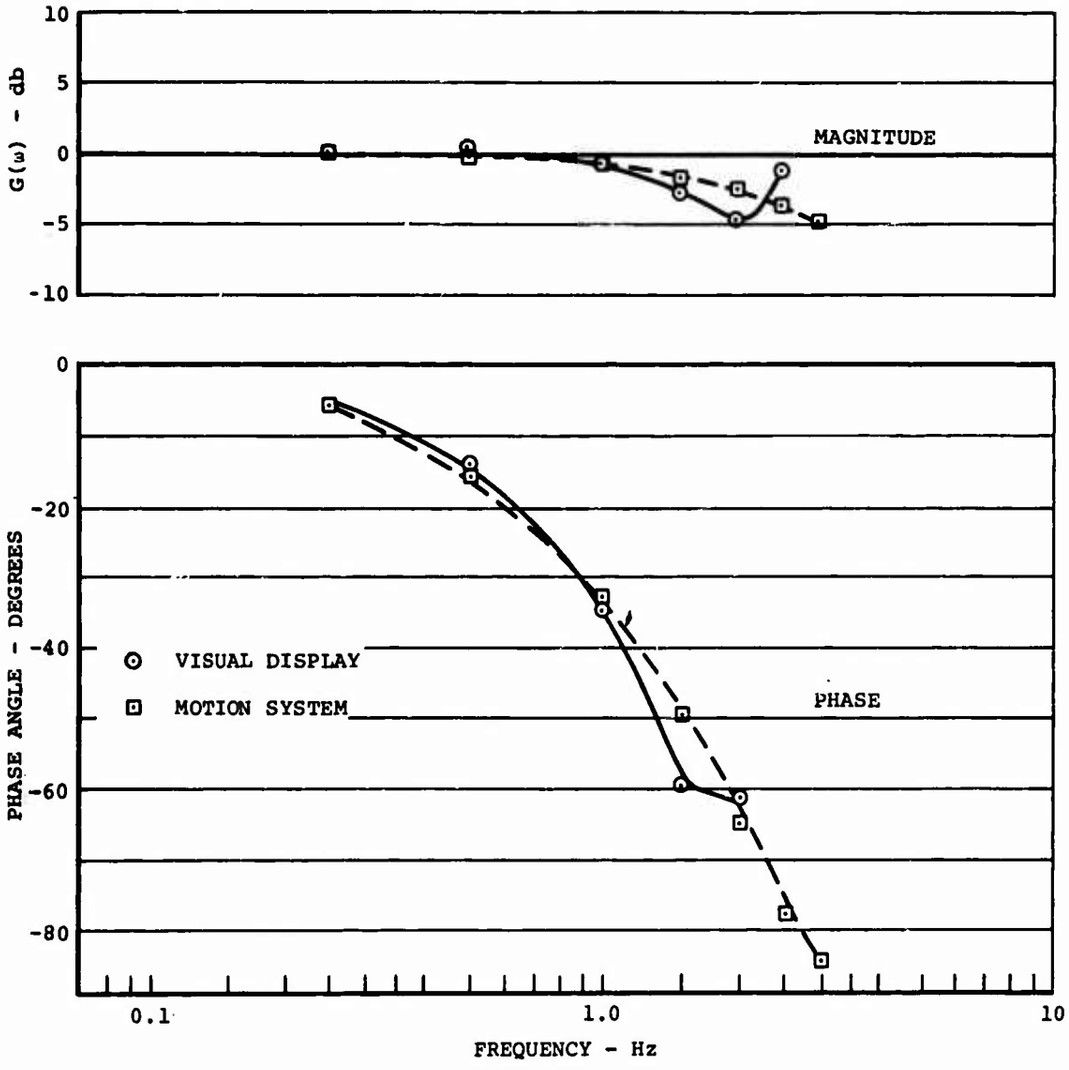

Figure 14. Simulator Yawing Frequency Response.

Visual Display System

A de Florez point light source projection system was used to produce a wide-angle visual display driven in six degrees of freedom. The display provided 80 and 200 degrees in pitch and azimuth, respectively. Two transparencies with scales of 750:1 and 7500:1 were used to project three-dimensional objects in color and to show terrain texture on a 12-foot-radius hemispherical screen. The display presented to the pilot appropriate perspective, size, and positon. The maximum angular capability was ±25 degrees pitch, ±30 degrees roll, and continuous yaw. (See Figure 15.)

Components of the vehicle velocity at the pilot's eye position were used to derive the visual display drive equations. The equations were generated in aircraft body axes and transformed into earth axes using conventional yaw, pitch, roll Euler angles. Position in earth axes was found by integrating the vehicle velocity at the pilot's eye position.

Rotations of the visual scene were calculated as the difference between the calculated airframe rotations and the motion base rotations in yaw, roll, pitch Euler axes. Thus, changes could be made in the motion drive equations without affecting the visual scene observed by the pilot.

The frequency responses of the visual display system were shown in Figures 9 through 14.

Cockpit Vibration

Two voltage-controlled oscillators (one sine wave and the other triangular wave) were used to simulate cockpit vibration. The outputs of these oscillators were summed and multiplied by a function of aircraft velocity and front rotor thrust and torque. The resulting signal was added to the vertical motion base drive. The basic frequency of the sine wave was set at 11.6 Hz, which is three times the rotor speed of 230 rpm. A basic frequency of 27 Hz for the triangular wave was determined experimentally. Figure 16 presents a flow diagram of the vibration simulation.

Cockpit Audio Environment

The cockpit audio simulation was designed to represent front rotor system transmission noise. A triangular-wave, voltage-controlled oscillator was frequency modulated by the rotor speed. Its nominal frequency was 11.6 Hz (three per rev for 230 rpm). It was used to frequency modulate a sine wave oscillator which had a basic frequency of 966 Hz. The output of this oscillator was input to the cockpit earphones. A flow diagram for the audio simulation is shown in Figure 17.

Figure 15. Visual Display.

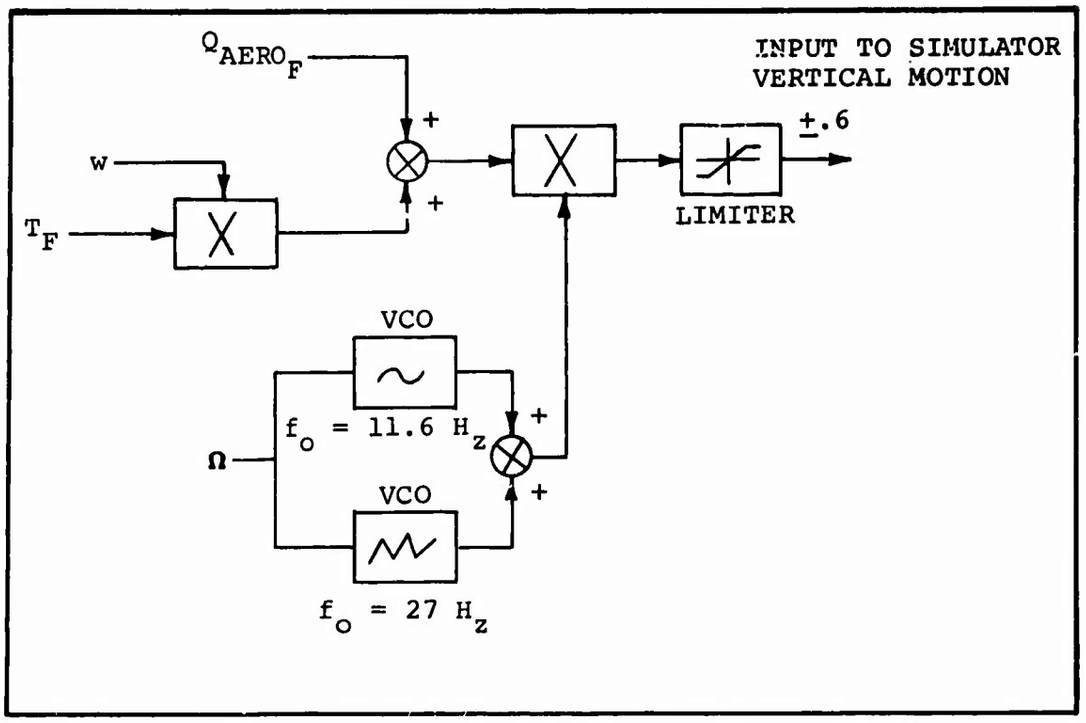

Figure 16. Vibration Simulation.

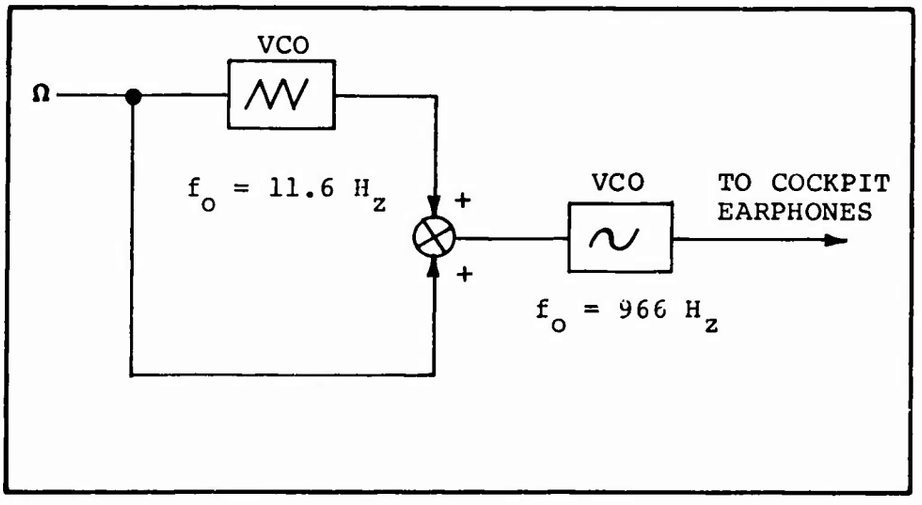

Figure 17. Audio Simulation.

Simulator Interface With Computers

Trunking was provided between the simulator and analog computers to input the cockpit controls to the mathematical model and to send the motion, visual display, and cockpit instrument drives to the simulator. The operation of the computers and simulator was coordinated by transferring mode control from the master computer console to the simulator cockpit.

ANALOG COMPUTER PROGRAMMING

The first step in the procedure for programming the analog computers was amplitude scaling of the mathematical model equations using the maximum range of the variables. Then the number of analog components required to mechanize each major part of the model was estimated. Considering the components and trunking available for each computer, a layout of what was to be mechanized on each of the seven computers was drawn. Detailed analog schematics were prepared for each computer. The logic required for switching and mode control was developed. Computer patchboards and logic boards were patched in accordance with the analog and logic diagrams. Mathematical expressions were developed for each potentiometer, and setting values were computed. Diode function generators were set up to represent each nonlinear function. Finally, values for limiters were determined and set. A list of the analog components employed in the simulation is given in Table III.

TABLE III. EQUIPMENT LIST

Component	No.
Amplifiers	700
Multipliers	200
Pots	465
Trunks	500
DFG's	30
Limiters	20
Switches	45
Relays	15
Comparators	15

The programming was checked, and necessary correlations were made. To accomplish this, static voltage, isolated rotor, static trim, and dynamic checks were performed. The static voltage check included selecting initial conditions, placing the computers in the static test mode, and comparing the voltage outputs of the computer components with precalculated values from the scaled equations. In addition, the output of each component was checked to be correct for its inputs. The static voltage check provided a good evaluation of the programming. However, it did have a shortcoming in that voltages for some of the selected initial conditions were negligibly small.

A more complete check on the simulation setup was obtained by rotor map, static trim, and dynamic checks. The results of these checks are discussed in subsequent sections of this report.

OPERATING PROCEDURES

For each session of the simulation operation, the potentiometers and limiters had to be set. Most of the potentiometers were set by digital tapes. After completion of computer setup, a check was performed on the program and hardware. Both static voltage and dynamic checks were performed. For the static check, the system was set for a gross weight of 46,000 pounds, a nominal center of gravity of zero inches, and a density altitude of sea level. These same conditions were used for the initial static check described previously. The initial conditions for the velocity components were input to the integrators. With the computers in the static test mode, the voltage outputs of key amplifiers and multipliers were compared with the calculated values. This provided a check on the potentiometer settings, trunking, and the operation of amplifiers, multipliers, and diode function generators.

After the static check, a more thorough evaluation of the system was obtained through a dynamic check. The simulated aircraft was trimmed by the trim loop integrators, which were operated by switching logic. The trim loops set the initial values of the control inputs and the aircraft attitude required to zero the aircraft linear and angular accelerations. With the trimming loops held, the computer was put in the operating mode, allowing all other integrators to operate. Control pulses and steps were introduced, and selected flight variables were recorded. The dynamic check was completed by comparing these recordings with the inital validation recordings, which closely matched flight test data (presented in succeeding sections of this report).

After the system check had been successfully completed, the computers were set for the conditions under which the pilot was to fly the simulation. Initial conditions for gross

weight, center of gravity, altitude, rotor speed, airspeed, steady wind, and atmospheric turbulence were set for each flight. Since the density altitude could not be varied during the flight, the air density remained constant at its initial value. The magnitude of steady wind and rms level of turbulence could be varied during the flight. However, the break frequency of the gust filters could not be varied with speed during the flight.

To conduct a simulated flight test, the simulator motion and display systems were activated and the cockpit controls were coupled into the computers. All computers were slaved to the simulator cockpit to give the pilot simulation mode control. The pilot could place the simulation in the initial condition mode to trim the aircraft. Trim meters in the simulator cockpit allowed the pilot to trim the controls while in the initial condition mode. After the aircraft was satisfactorily trimmed, the pilot was free to switch the simulation into the operate mode to commence simulated flight. The pilot terminated flight by switching into reset.

Maneuvering volume was limited by the visual display system, and, to increase it, the point light was masked when the valid range of the display system was exceeded during flight. This allowed the flight to be continued under instrument flight conditions with an artificial horizon. When the aircraft returned to the valid range of the display system, the point light was unmasked.

Switching was provided to simulate SAS hardover failures and single and dual engine failures during flight. It was also possible to simulate single SAS operation and SAS-off flight. Ground effect could be switched into and out of the system as desired.

Six 8-channel Brush recorders were used to record the flight variables and simulator drives. These recorders were slaved to a master switch so they could be operated simultaneously. Flights were monitored at a slow recorder speed of 2 mm/sec. A higher recorder speed (20 mm/sec) was used for unpiloted dynamic validation and for piloted flight maneuvers of short duration.

SIMULATION VALIDATION WITH CONVENTIONAL FLIGHT CONTROL SYSTEM STATIC CHECKOUT

Isolated rotor characteristics were checked by comparing carpet plots obtained from the simulation with theoretical plots, as in Figure 18. (Additional plots can be found in Appendix I.) These plots show rotor thrust, H force, and torque as functions of rotor angle of attack and collective pitch. The rear rotor longitudinal cyclic pitch schedule, which does not vary with altitude, was used. The effects of variations in airspeed, altitude, and rotor speed were evaluated.

A Boeing digital computer program for isolated rotors was used to generate the theoretical plots. This program computes the steady-state aerodynamic forces acting on an isolated rotor throughout the range of possible collective pitch settings for rotor angles of attack through 360 degrees. The rotor is modeled as having fully articulated, inelastic blades and uniform induced velocity distribution. Mach number effects are included, but unsteady aerodynamic and spanwise flow effects are neglected.

The thrust match between simulation and theory was good. The use of a constant lift curve slope in the mathematical model resulted in some degradation of the match, both at the onset of stall and for airspeeds near the maximum. In the stall regime, the discrepancy was as large as 10 percent.

The simulated rotor torque was quite acceptable for tip speeds below Mach 0.80, except for negative thrust when the torque was considerably larger than the theoretical values. This exception was of little consequence, since it occurred in a region beyond the normal operating range of the CH-47. When the rotor tip speed was large enough for compressibility effects to occur, the simulated torque became less satisfactory. The necessary torque corrections were programmed to simulate increased torque due to compressibility. The resulting steady-state torque compared closely to theoretical values, as shown in Figure 18. However, the dynamic characteristics of the torque near the power limit were not entirely correct. Further study in this area is recommended.

In hover, the simulated H force increased with collective pitch significantly more than the theoretical value. However, the match was good at an airspeed of 100 knots. For airspeeds near the maximum, the simulated H force was too large for both negative angles of attack and large collective pitch values.

The dynamic response of an isolated rotor to a step input in collective pitch was recorded (Appendix I). When the value of $\theta_{.75}$ was stepped from 6 to 8 degrees at several rotor airspeeds,

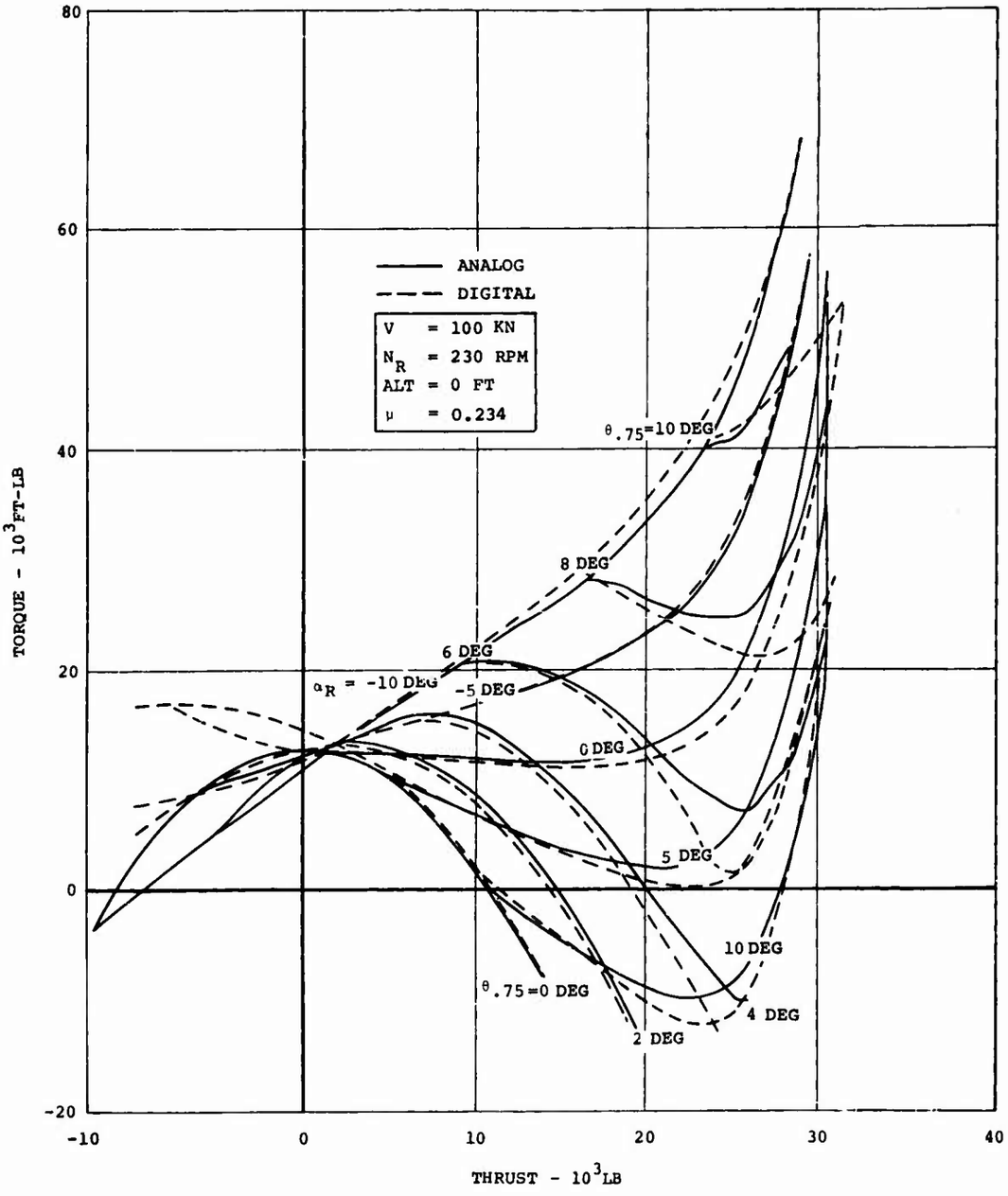

Figure 18. Torque Versus Thrust for CH-47C.

the desired lag (time constant of one-third of a second) in the inflow ratio response resulted.

The static trim was checked by comparing the simulation trim values with theoretical and flight test values. Trim values for the control inputs, rotor torque and forces, and helicopter attitude were compared, as shown in Figures 19 through 26. (Additional trim data can be found in Appendix I.) Several configurations and flight conditions were used. The center of gravity was located at 0, 7, and 18 inches aft for gross weights of 46,000, 33,000 and 22,000 pounds, respectively. The rotor speed was 230 rpm for all conditions, except that at a gross weight of 46,000 pounds with an altitude of 10,000 feet it was 245 rpm.

Theoretical trim values were obtained from a Boeing digital computer program for the complete aircraft. This program computes the helicopter trim parameters through an iterative solution to the six steady-state equations of motion developed by a force and moment balance along and about a fixed body axes system. Blade stall, reverse flow, and compressibility effects are included. The induced velocity distribution is assumed to be uniform over the rotors. Blade lead-lag, non-steady aerodynamic and spanwise flow effects, and all elastic degrees of freedom are neglected.

The match between the simulation and theoretical trim values was generally very good. The simulated aircraft attitude, forces, power requirement, and control positions were nearly identical to the digital trim values for all gross weights and airspeeds from -35 to 120 knots. For airspeeds above 120 knots, the largest discrepancy was a pitch attitude which was too nose down. This was attributed to the fact that the simulated H force was too large at high airspeeds. Some appreciable discrepancies were also present at high altitudes. Again, these discrepancies resulted from the limitations of simulated rotor H force.

The theoretical comparison for sideslip trims was also good. Discrepancies in the parameters were small for lateral velocities between ± 35 knots and for airspeeds up to 120 knots. Above 120 knots, the discrepancy was the same as that which occurred in zero sideslip trim.

A singularity occurred in hover due to a limitation in the analog mechanization. This limitation caused $\sin \beta$ and $\cos \beta$ to become small together, which reduced the lateral control power. The result was that a large lateral control input was required for trim in a 2-knot band around hover. The singularity was moved to -5 knots to allow correct trim in hover. Further investigation is necessary to reduce the effect of or eliminate this singularity.

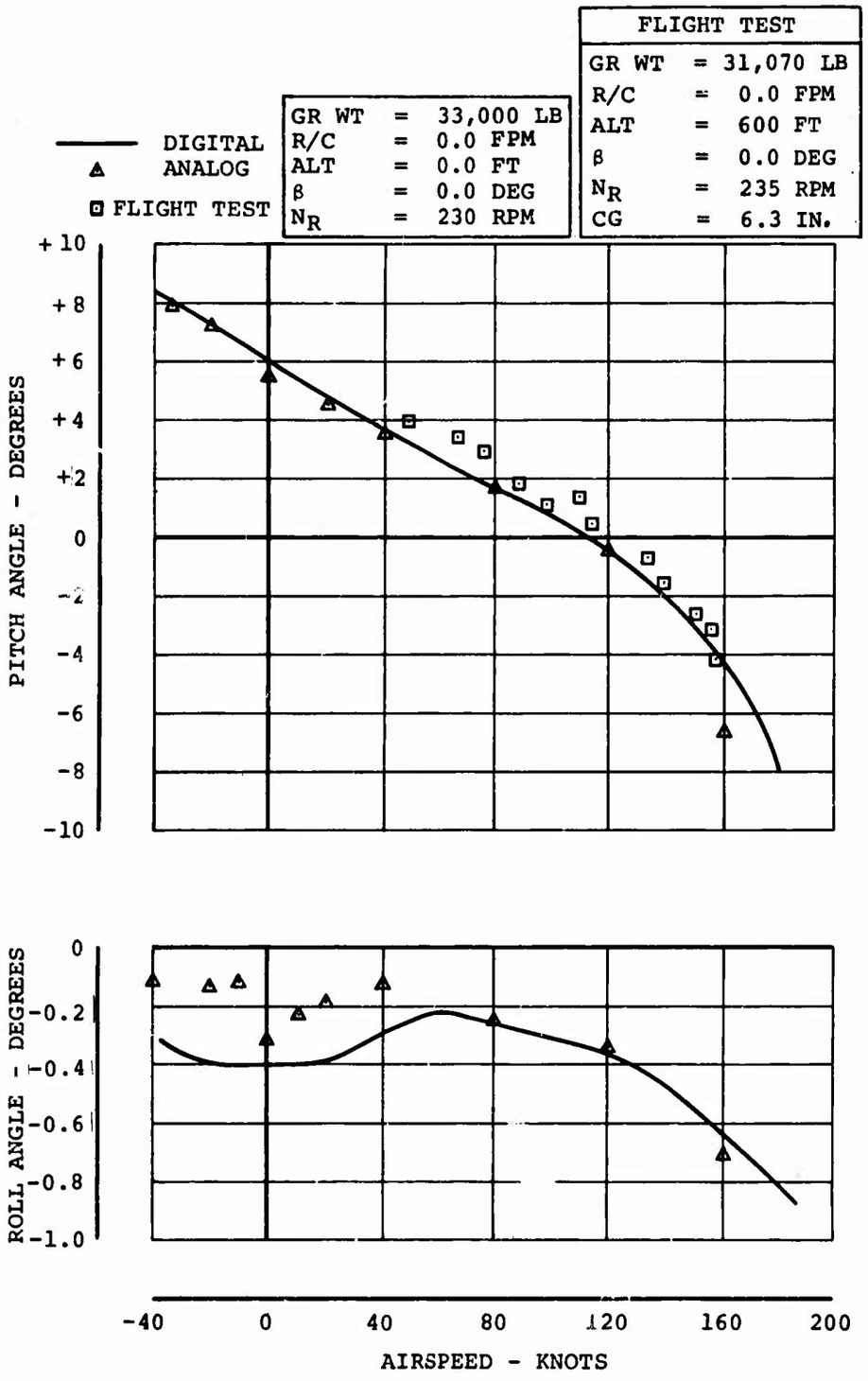

Figure 19. Forward Flight Trim.

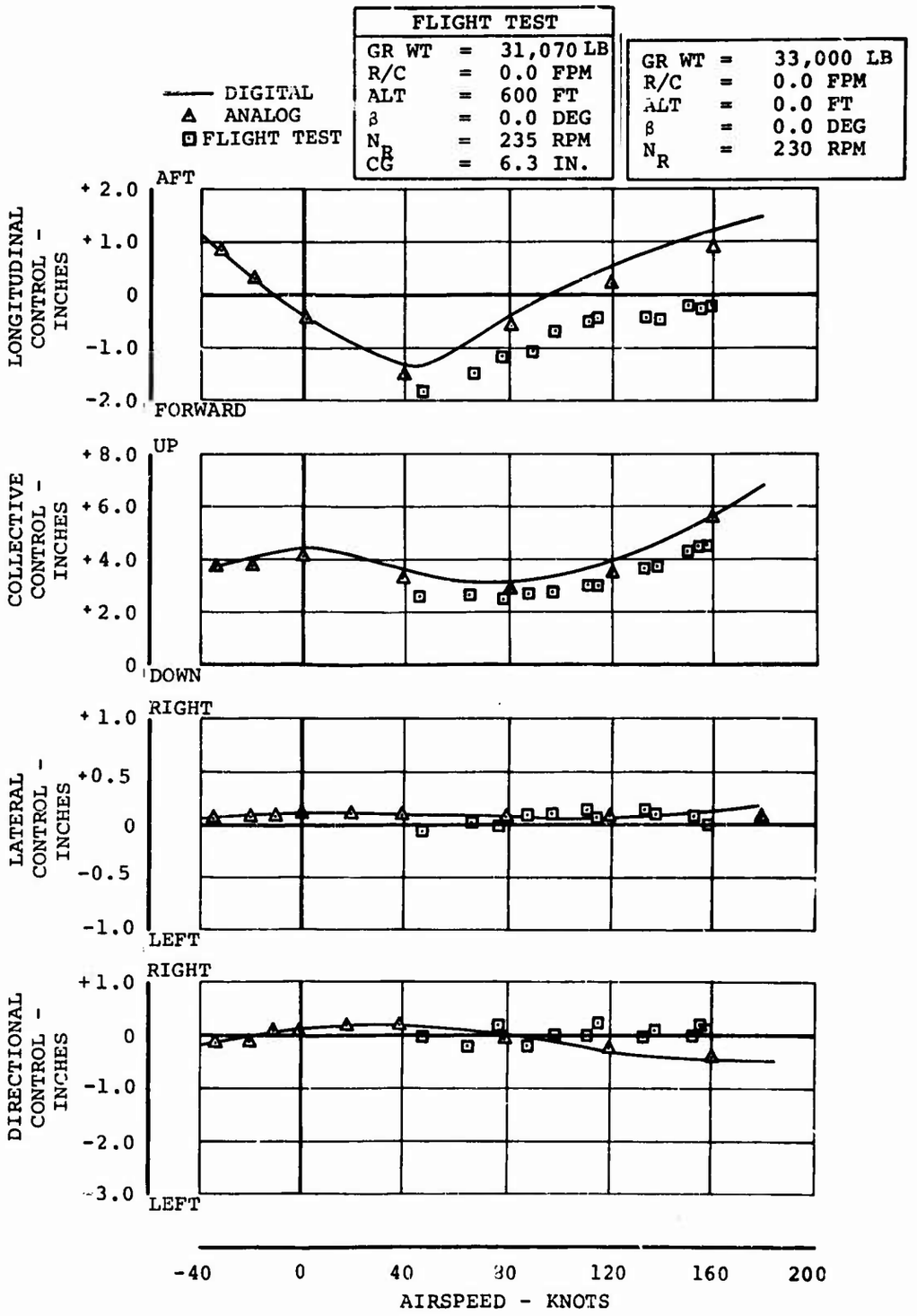

Figure 20. Forward Flight Trim.

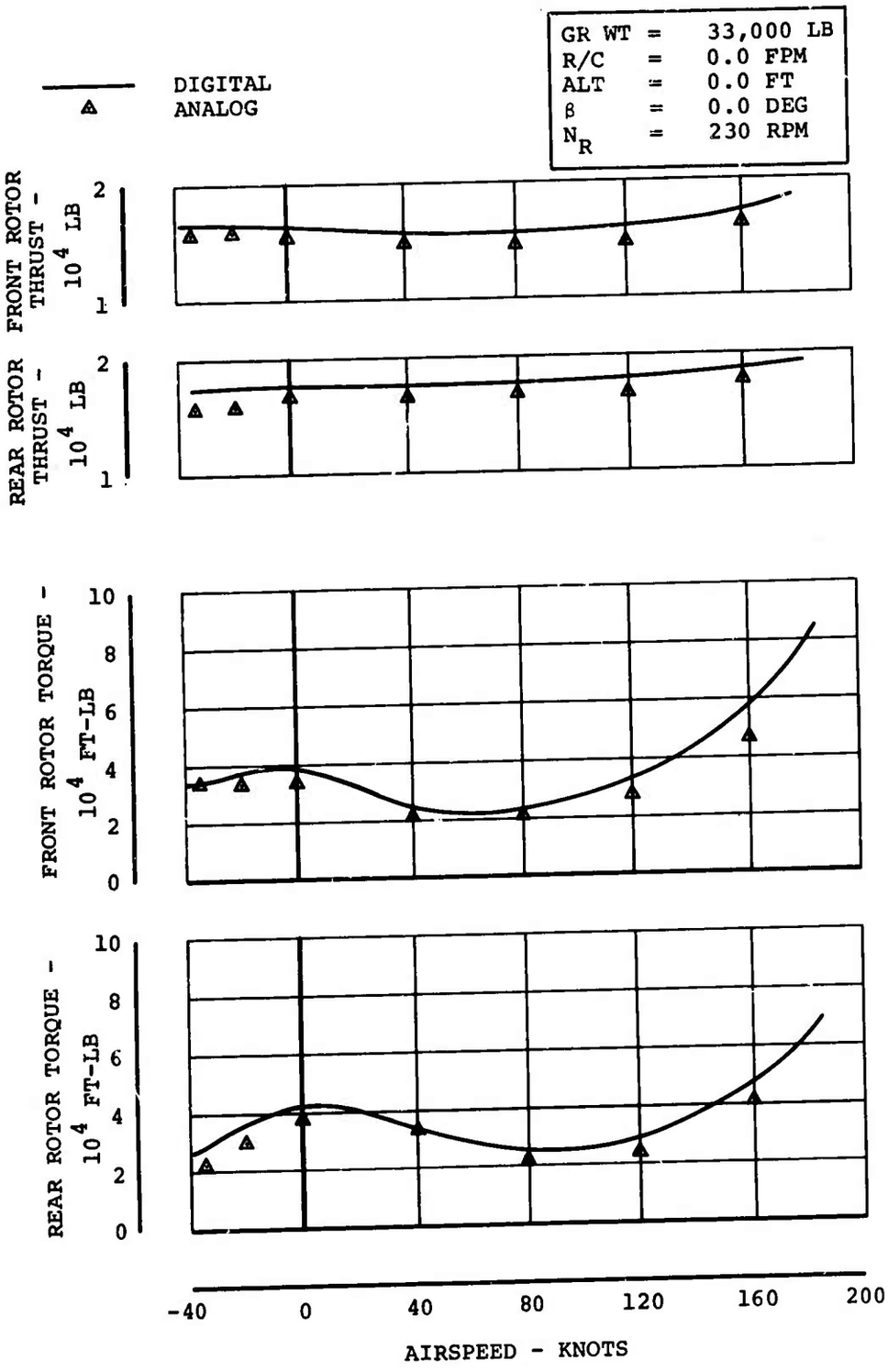

Figure 21. Forward Flight Trim.

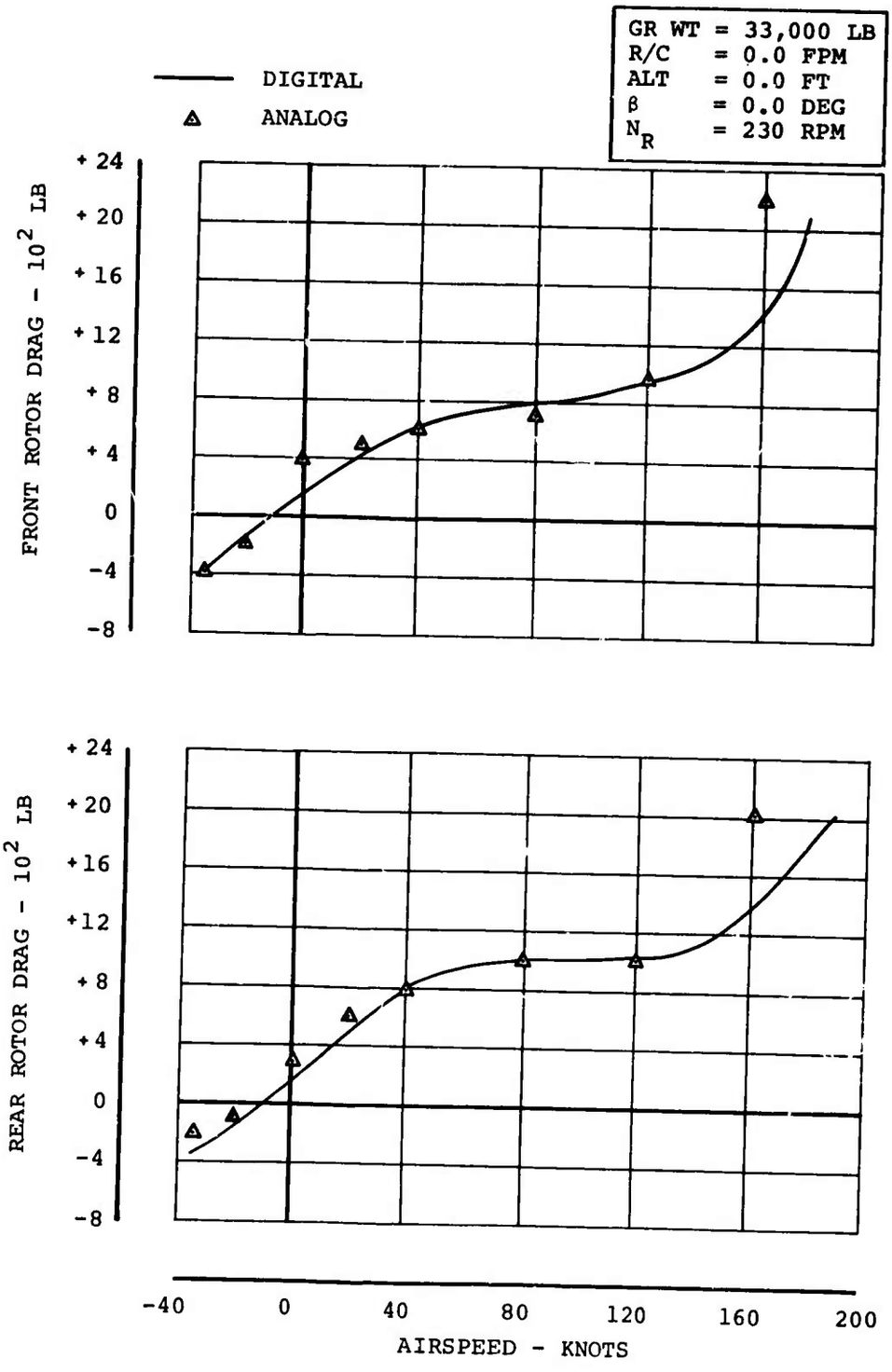

Figure 22. Forward Flight Trim.

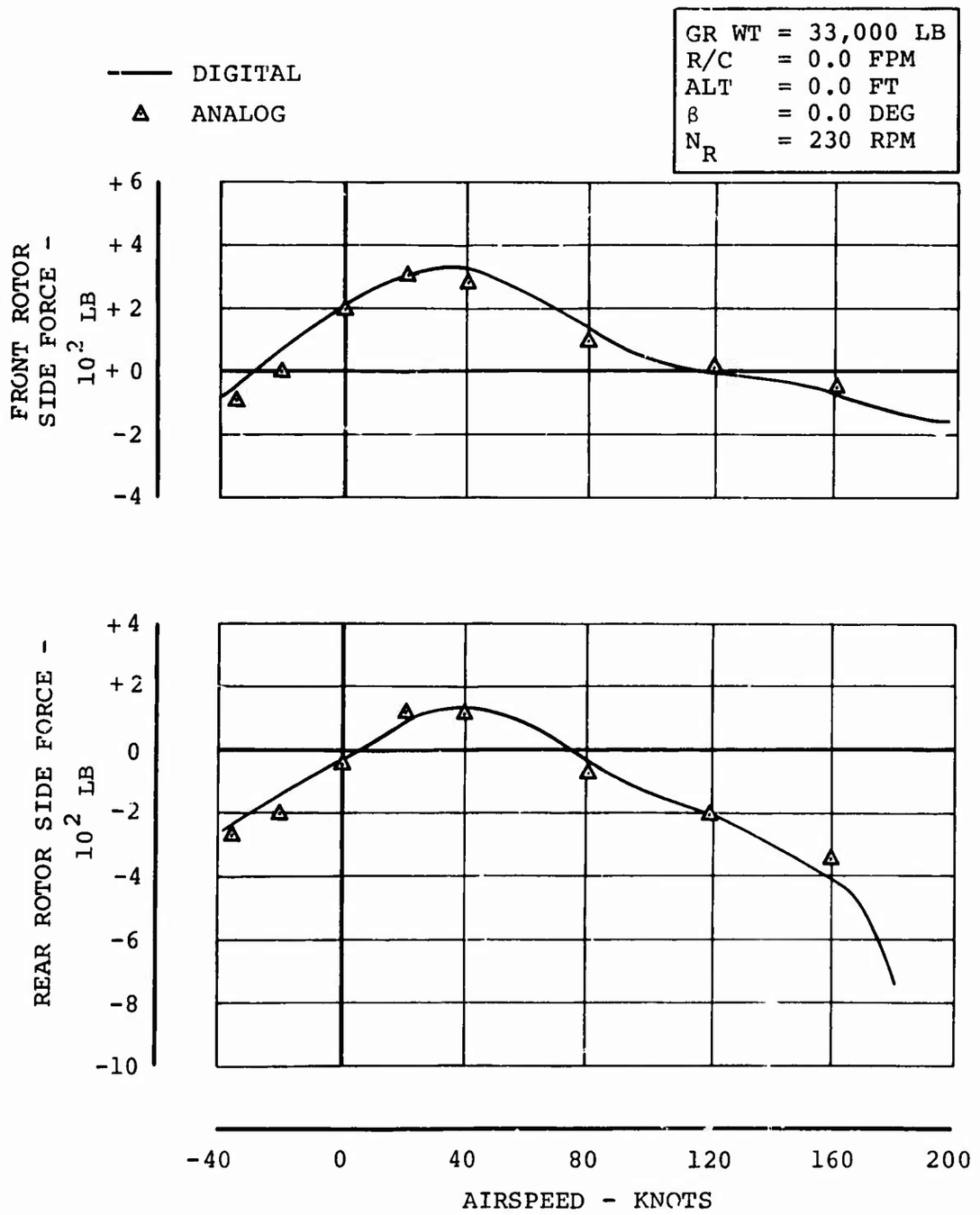

Figure 23. Forward Flight Trim.

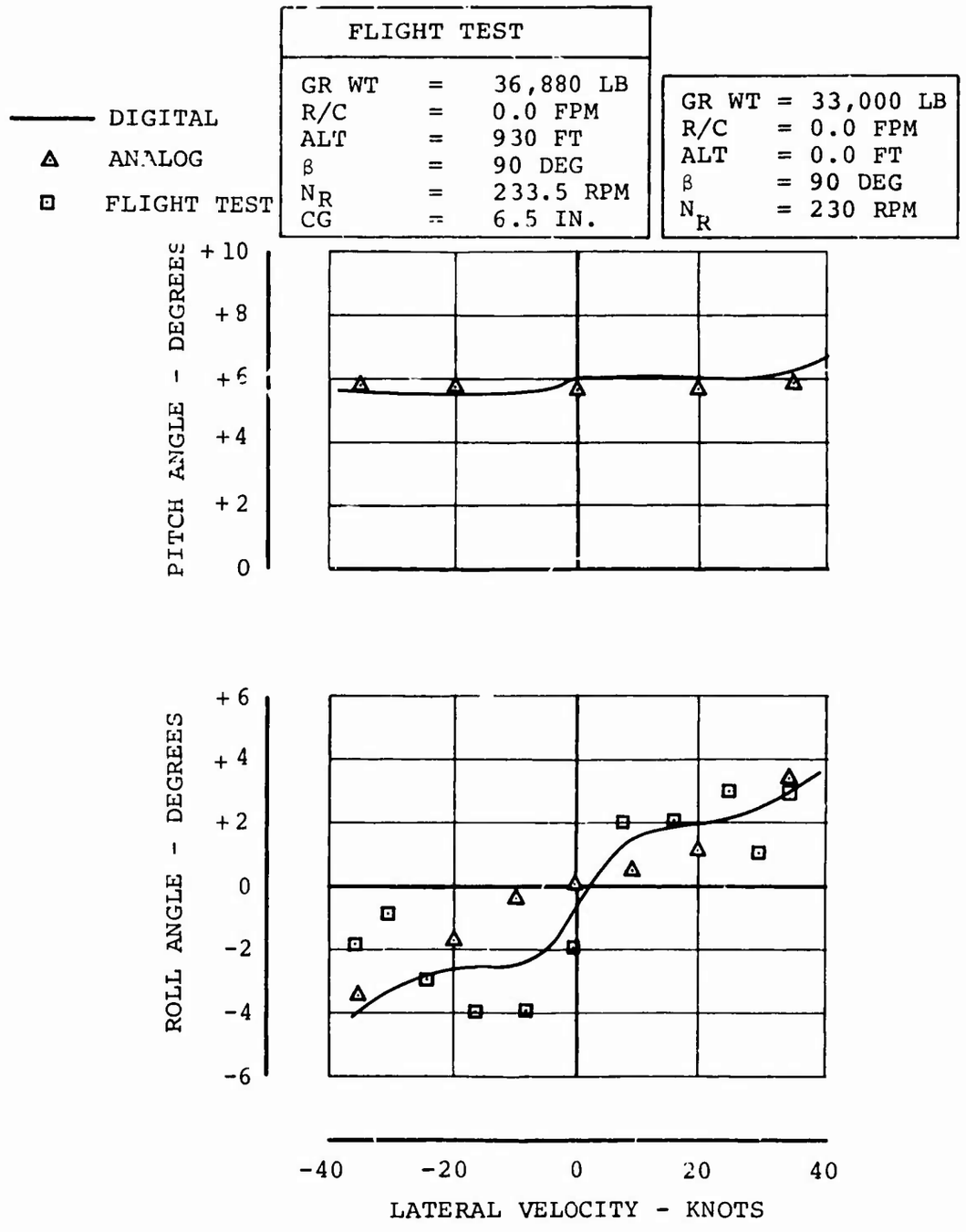

Figure 24. Sideward Flight Trim.

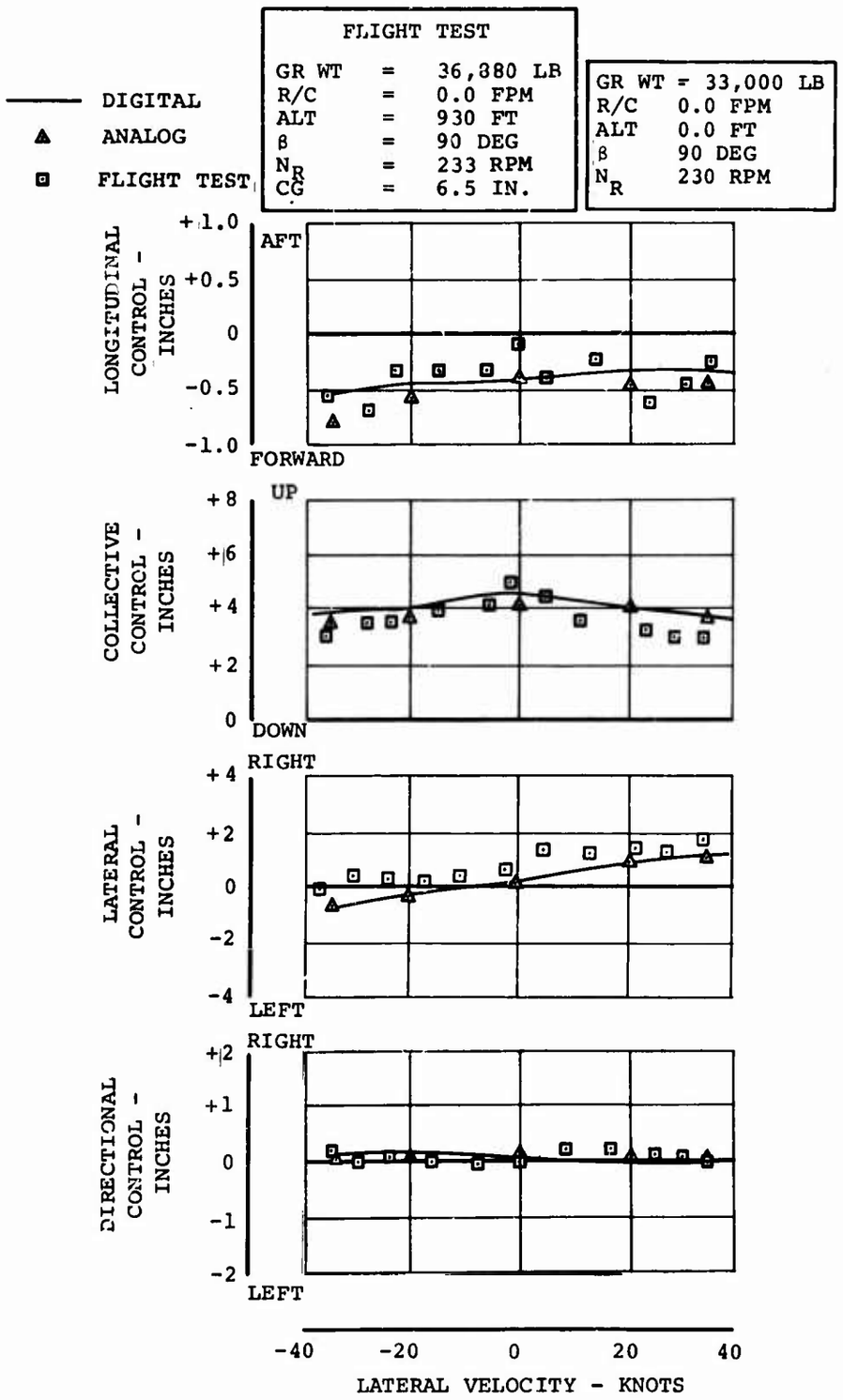

Figure 25. Sideward Flight Trim.

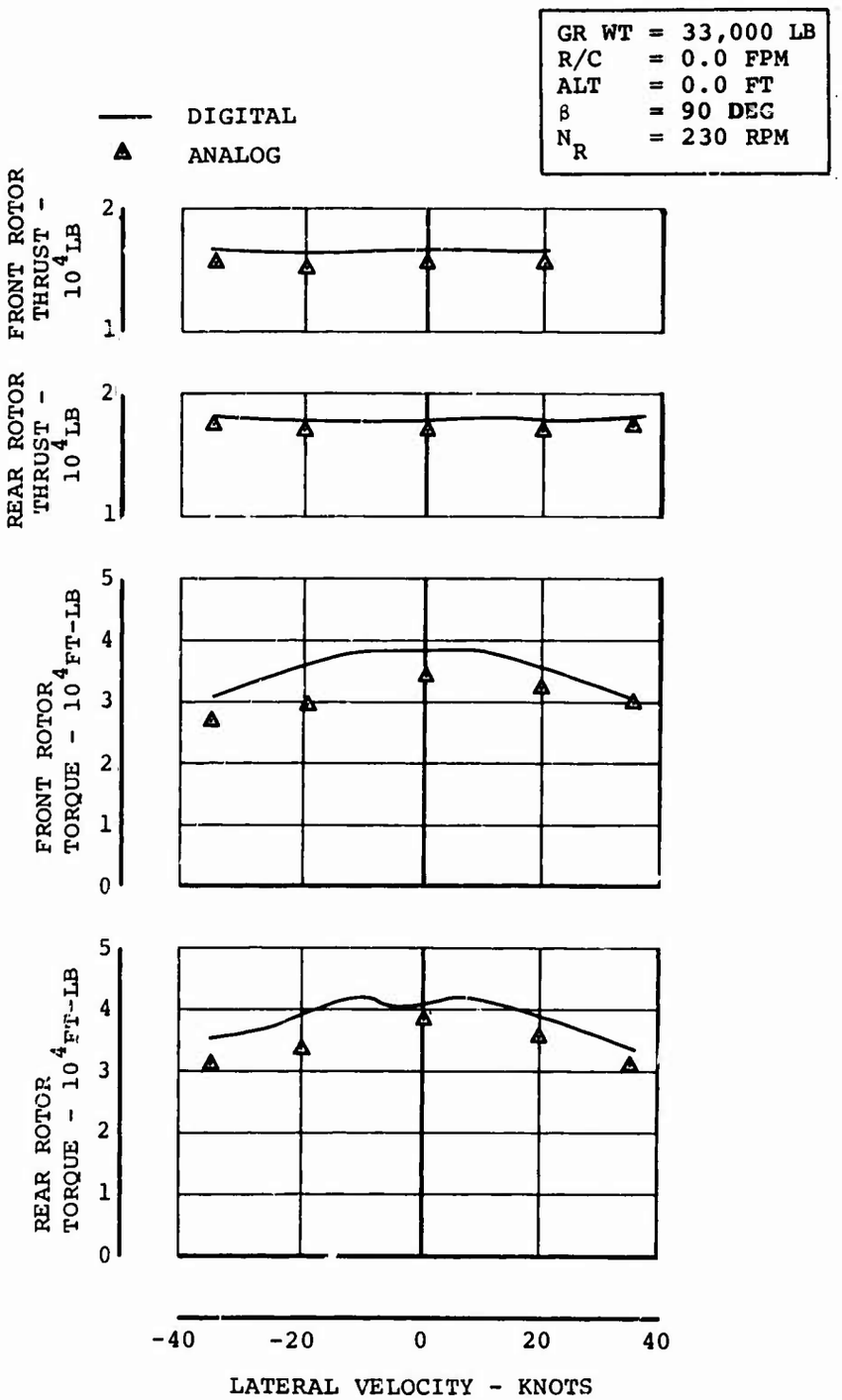

Figure 26. Sideward Flight Trim.

Flight test trim data were available for comparison with the 33,000-pound cases at sea level and at an altitude of 10,000 feet. These data, obtained in the U.S. Army APE flight test program, Contract No. DA23-204-AMC-04366(Y), with aircraft No. USA S/N 66-19121, will be presented in a subsequent Army report. The flight test data provided trim values for pitch and roll angle and control positions. The pitch angle and collective control required for trim were in close agreement. At sea level, the simulation longitudinal control was 0.5 inch more aft than in flight test throughout the airspeed sweep. This axis is by far the most sensitive to rigging tolerances, and 0.5 inch is within production tolerances. The simulation lateral and directional control positions were each approximately 0.4 inch left of the flight test values. Also, the change in lateral and directional control with airspeed was somewhat different between the simulation and flight test. A more accurate simulation of fuselage rolling and yawing moments could have reduced these discrepancies. All of the discrepancies were in the order of 0.5 inch, of which a considerable amount can be attributed to rigging tolerances.

Simulated aircraft rate of descent in autorotation was recorded as a function of airspeed. In Figure 27 these results are compared with flight test and other theoretical values. This comparison indicates that the simulation rates of descent were shifted in airspeed by approximately 10 knots.

Several simulation control power and stability derivatives were measured and compared to theoretical values (Table IV). The control power derivatives were in particularly close agreement.

The static and steady-state check results proved the mathematical model to be inertially and quasi-statically correct. The results were very good for flight up to an airspeed of 120 knots and quite satisfactory to 140 knots. Although the steady-state characteristics deteriorated considerably above 140 knots, the small perturbation dynamic characteristics were accurate to the maximum airspeed.

DYNAMIC CHECK

The short-period dynamic responses of the simulation to control pulses, SAS failures, and single-engine failures were measured and compared to flight test data. A representative response is shown in Figure 28. (Additional dynamic response cases are presented in Appendix II.) The simulation results were obtained by producing a short-time duration step in one of the controls while the other controls remained fixed at the trim value. The configuration and flight conditions for the simulation and flight test responses are indicated for each case. Although simulation conditions were not identical to the flight test conditions, they were similar enough to provide a good comparison.

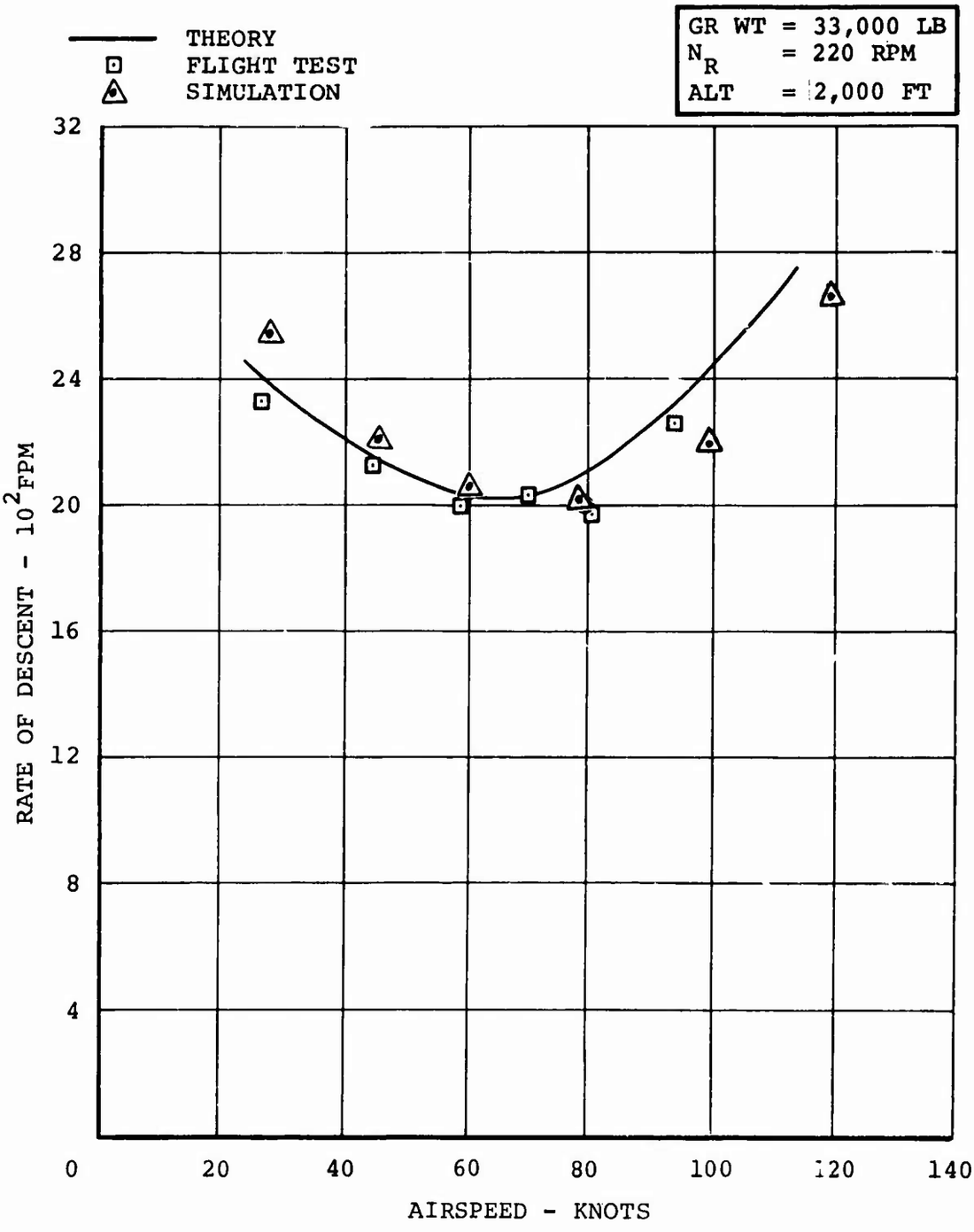

Figure 27. Autorotation Rate of Descent.

TABLE IV. CONTROL POWER AND STABILITY DERIVATIVES

CONTROL DERIVATIVE	SIMULATION	DIGITAL
M_{δ_B}	0.494 1/IN./SEC^2	0.459 1/IN./SEC^2
L_{δ_S}	0.444 1/IN./SEC^2	0.448 1/IN./SEC^2
N_{δ_R}	0.202 1/IN./SEC^2	0.200 1/IN./SEC^2
Z_{δ_C}	-11.60 FT/IN./SEC^2	-11.70 FT/IN./SEC^2
STABILITY DERIVATIVES		
M_Q	-1.93 1/SEC	-1.67 1/SEC
L_P	-0.876 1/SEC	-0.818 1/SEC
N_R	-0.057 1/SEC	-0.068 1/SEC
Z_W	-0.705 1/SEC	-0.704 1/SEC

GR WT = 33,000 LB

AIRSPEED = 100 KN

ALT = SEA LEVEL

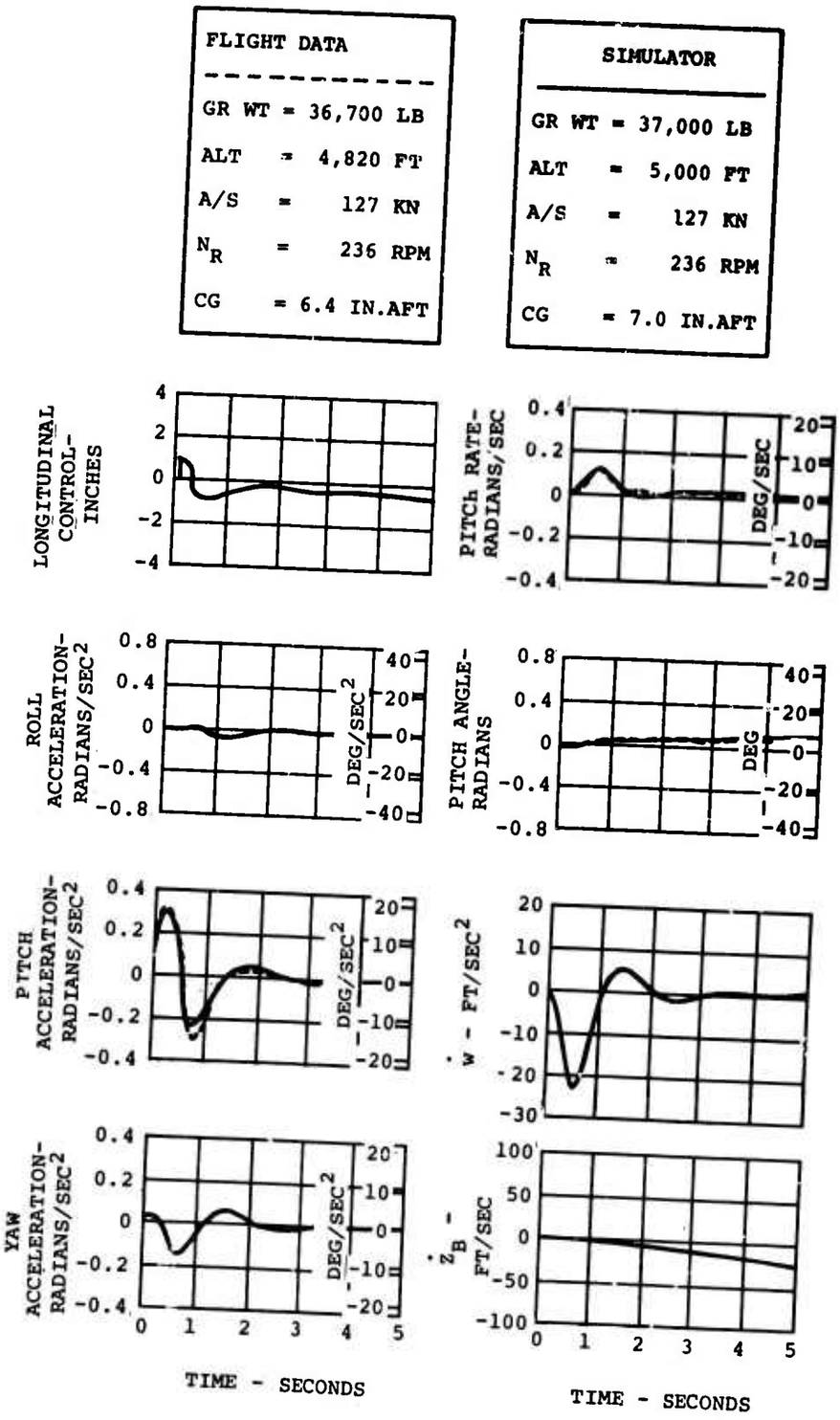

Figure 28. Dynamic Responses - Longitudinal Pulse.

The flight test data were taken from data obtained by the U.S. Army with their APE flight test program for the CH-47B. These data will be published in a forthcoming Army report.

Longitudinal control pulses, both forward and aft, were performed for several gross weights, airspeeds, and density altitudes. Most of the pulses were 1 inch in magnitude and of 0.5 second duration. Flight test response time histories for pitch acceleration, velocity, and angle were superimposed on the corresponding simulator response traces. Amplitude, frequency (approximately 0.6 Hz), and damping were nearly identical for all flight conditions. The flight test results showed more delay than the simulation between the input and response. This was attributed to the omission of rotor high frequency flapping dynamics in the simulation and to filtering employed to reduce the level of high-frequency vibration present in the flight test data.

The response to a step increase in collective control was recorded for the simulation. Flight test data were not available for collective steps. Steps of 1.0 inch and 0.5 inch were used for gross weights of 33,000 and 46,000 pounds, respectively. For 33,000 pounds, the vertical acceleration was initially 4.6 ft/sec^2, and then it decreased slowly such that the rate of climb was 1,800 ft/min after ten seconds. At 46,000 pounds, the resulting vertical acceleration was nearly constant at 2.2 ft/sec^2 during the first ten seconds.

The responses to lateral and directional control pulses were very similar for the simulation and flight test. Again, the amplitude, frequency, and damping were nearly identical. The pulses were performed for various flight conditions, magnitudes, and time durations.

Single SAS failures were introduced for each axis separately. The responses of the respective SAS, angular velocity components, and attitude were particularly close to flight test results for failures in all axes. The simulation rolling response to a yaw SAS failure was somewhat less in magnitude than the flight test rolling response.

The decrease in rotor speed for the simulation as a result of a single-engine failure was 60 percent greater than for flight test. This indicates that the simulation governor gain was too small. The pitching response to the engine failure compared closely to flight test results.

PILOT EVALUATION

A CH-47 test pilot flew the simulated aircraft to determine the degree of realism achieved in the illusion of flight and to evaluate the accuracy with which the CH-47 was represented. The

simulation characteristics were evaluated throughout the complete flight envelope, including the responses to gusts and failures in the engine and augmentation systems. Due to limitations of the visual display, much of the evaluation at high airspeeds was done under instrument flight conditions. Subsequent sections of this report contain a discussion of the pilot's comments resulting from this evaluation. The pilot's comments appear in Appendix I.

Hover and Low-Speed Flight

Overall fidelity of the simulation was high in hover and in low-speed flight. The responses of the simulated aircraft to control pulses in all three axes appeared to be identical to those of the aircraft. Control positions, power requirements, and engine characteristics were normal both in and out of ground effect, except that torque splitting due to engine mismatch was not simulated. Engine beep trim operation speed and static and transient rotor speed droop characteristics were realistically reproduced.

The behavior in spot turns and low-speed sideward and rearward flight had a fair correspondence to the actual aircraft. The pilot felt that the 2 degrees required to sustain 25 knots of lateral velocity was approximately half of what it should have been. However, the 2-degree value is consistent with flight test results (Figure 24). The reason for this discrepancy is not definitely known. It may have been due to nonlinear CH-47C lateral stability derivatives, reduced motion cues, incorrect horizon placement, or some combination of these.

An altitude control problem existed in hover and throughout the flight envelope. This problem was caused by the absence of the normal acceleration cues associated with center-of-gravity accelerations, difficulty in height perception at low altitude, absence of lag on the simulator rate-of-climb indicator, and mechanical dead space in the simulator collective lever. The motion base amplitude available for normal acceleration was ± 9 inches, which was insufficient to provide the normal acceleration cues associated with the motion of the center of gravity. However, it was possible to provide a normal acceleration cue associated with pitching acceleration, since this acceleration is of shorter duration, and since the CH-47C cockpit is 22 feet forward of the center of gravity.

The absence of secondary cross-coupling effects resulted in a ride smoother than normal. These effects are chiefly observed as lateral accelerations in the CH-47C due to lead-lag motion of the blades. These observed lateral accelerations are also characteristic of the response to gusts and of the jerk associated with SAS failures in roll and yaw. Since the five degrees of freedom in the motion base did not include lateral

acceleration, a representation of blade lead-lag was not included in the rotor mathematical model.

From out-of-ground-effect (OGE) hover, the aircraft sank gently to an accurate in-ground-effect (IGE) hover when the appropriate IGE hover torque setting was selected. This demonstrated a very realistic simulation of the ground effect phenomenon.

When the gross weight was increased from 33,000 to 46,000 pounds, the translational and rotational inertia effects of the increased weight were realistically presented. The response to control pulses revealed behavior very similar to that of the actual aircraft. Spot turn and lateral flight characteristics were fairly realistic for the increased gross weight.

Acceleration and Deceleration Through Transition

Ground effect was accurately represented for airspeed in low-altitude transition. The simulation of static and transient rotor speed droop was very good. The overall realism was reduced by a lack of realistic noise, vibration, and control cross-coupling effects. This was true not only for transition but also throughout the flight envelope.

In transition turns, yaw control was more difficult than normal, due to the absence of lateral motion in the motion base. Above 50 knots the yaw SAS sideslip control became operative, greatly reducing the yaw control problem. As the result of thrust-pitch coupling, the simulation was only fair during rapid transitions and quick stops. It was difficult to maintain the correct pitch attitude required to provide the desired combination of linear acceleration and vertical rate of climb. This thrust-pitch coupling was attributable to the interference effects of low values of λ/μ. Experimentation with the interference coefficient factors should lead to elimination of this coupling.

Level Flight

The simulated aircraft response to control pulses corresponded closely to that of the aircraft at all airspeeds. The level-flight pitch control required slightly more than normal attention, while directional and roll control required somewhat less. During acceleration and deceleration, significant difficulty was encountered in adjusting the pitch attitude with changing airspeed to maintain level flight. This difficulty can be attributed to a number of causes. In addition to thrust-pitch coupling, no instrument lag was included other than that inherent in the simulator instruments. Pitch dead zone in the motion base gave a noticeable jerking effect and thus an apparently excessive longitudinal stick sensitivity shown by

the dynamic correlation tests not to be in the mathematical model. Detailed differences in the force feel and dead zone characteristics of the longitudinal stick were noted. A change in the location of the stick's dead zone improved the sensitivity effect.

With an increase in gross weight from 33,000 to 46,000 pounds, the control and stability characteristics remained very close to those of the actual aircraft. The simulated aircraft responded correctly to control pulses at an airspeed of 70 knots. At the maximum velocity, an aft longitudinal pulse of 1.5 inches resulted in an abrupt and increasing pitch-up rate which could not be recovered. The aft rotor had apparently stalled without any prior notice. At this large gross weight, the rotor limit representation provided good steady state trim, but there was not sufficient margin for representative maneuverability. The rotor representation was not able to provide the shaking and vibration which act as a warning of rotor stall. The rotor thrust limits were generally too abrupt. Further development of the mathematical model is necessary to improve the rotor limit representation.

Climbs and Descents

Control characteristics appeared to be accurately simulated for hovering and steep climbing takeoffs. Steep approaches, however, were surprisingly difficult to coordinate smoothly. A crab angle of 30 degrees was used during steep approaches to permit an unobstructed view of the landing area. The absence of lateral motion aggravated the required control coordination for this maneuver.

During autorotation entry, the visual cues were realistic, although the acceleration forces in all axes were low. For this reason, pitch and yaw control was slightly oversensitive during entry. In stabilized autorotation and in autorotative turns, the simulated aircraft control and rotor speed responses corresponded closely to those of the aircraft. In all axes it was difficult to avoid overcontrolling during flare. This was probably due to thrust-pitch coupling, a low level of realistic motion cues, and the low level of visual cues below 150 feet above ground level.

Sideslips and Coordinated Turns

In high-speed sideslips and coordinated turns, fully stable characteristics were exhibited. No marked discontinuities were evident, and the behavior was very similar to that of the actual aircraft. Due to reduced visual and motion cues, total reliance was placed on the aircraft instrument indications for sideslip control.

The long-term lateral accelerations due to sideslip were produced by slowly tilting the motion base in roll. The pilot consistently commented on the absence of the high-frequency lateral acceleration term, known to be an important cue for sideslip control.

Response to Atmospheric Turbulence

The simulation of steady wind was very convincing. Aircraft attitude changes were of the correct order, and the sequence of control actions was nearly normal for spot turns in steady wind.

Gust simulation and aircraft response to gusts in hover with a rotor speed of 235 rpm were very realistic in terms of aircraft attitude and altitude excursions. Pitch excursions were particularly good from the pilot feel point of view. Attitude control was somewhat more difficult than for the actual aircraft.

When either the airspeed or the rotor speed was increased, the gusts produced a ride which was noticeably too smooth. The pitch attitude excursions were significantly lower than would have occurred in actual flight. In all cases the secondary gust responses of shaking, cross coupling, and changes in noise and vibration were not reproduced.

The development of the gust model was based on existing data and design information.[7,8] It was found that the gust spectrum was more realistic when based on advancing rotor blade tip speed rather than on aircraft forward speed alone. Account was taken of forward speed in applying the gusts to the aircraft. The smoothness of ride was to be expected, since a quasi-static representation of the rotor was used.

Engine Failures

An overall close correspondence existed between the simulated and actual aircraft for single engine failures. However, the rotor speed droop and altitude loss were greater than could be expected in the actual aircraft. The noise simulation was of help in warning that failure had occurred, but further development is necessary to provide a realistic representation of the cockpit audio environment.

SAS-Off Flight and Single SAS Failures

SAS-off characteristics in hover were very similar to those of the true aircraft. Due to the previously discussed control difficulties in yaw and pitch, the aircraft with SAS off was uncontrollable in yaw above 70 knots and in pitch above 130 knots. Consequently, the investigation of single SAS failures was limited to those airspeeds. Due to reduced acceleration

cues, the failures were generally too mild. Failures in pitch were the most realistic in terms of motion cues, pitch rate, excursion amplitude, and required recovery technique. In all cases, instrument indications of aircraft behavior following failure and before initiating recovery were normal.

IMPLEMENTATION OF SIMULATION WITH ADVANCED FLIGHT CONTROL CONCEPT

MODELING OF AFCC

The control concept incorporated in the simulation is described in detail in Reference 10. Adjustments were made to the control gains and time constants to suit the characteristics of the CH-47C.[1] The pilot's conventional controls were set up so that each mode could be used in conjunction with the AFCC.

ANALOG COMPUTER PROGRAMMING FOR AFCC

Analog diagrams were drawn for mechanization of the AFCC, and the computer was patched according to the diagrams. Diode function generators were set up for the variable gains. Function switches were patched to interchange the AFCC with the conventional control system.

SIMULATOR COCKPIT CONFIGURATION FOR AFCC

The conventional pilot controls were available for coupling into the advanced flight control system. In addition, a sidearm controller was installed in the right side of the cockpit. This controller, which subsequently replaced the conventional cyclic and collective sticks, was evaluated by Northrop-Norair under a separate USAAVLABS contract.

The conventional cockpit instruments were augmented by longitudinal and lateral velocity indicators. Figure 29 shows the cockpit configuration for the AFCC.

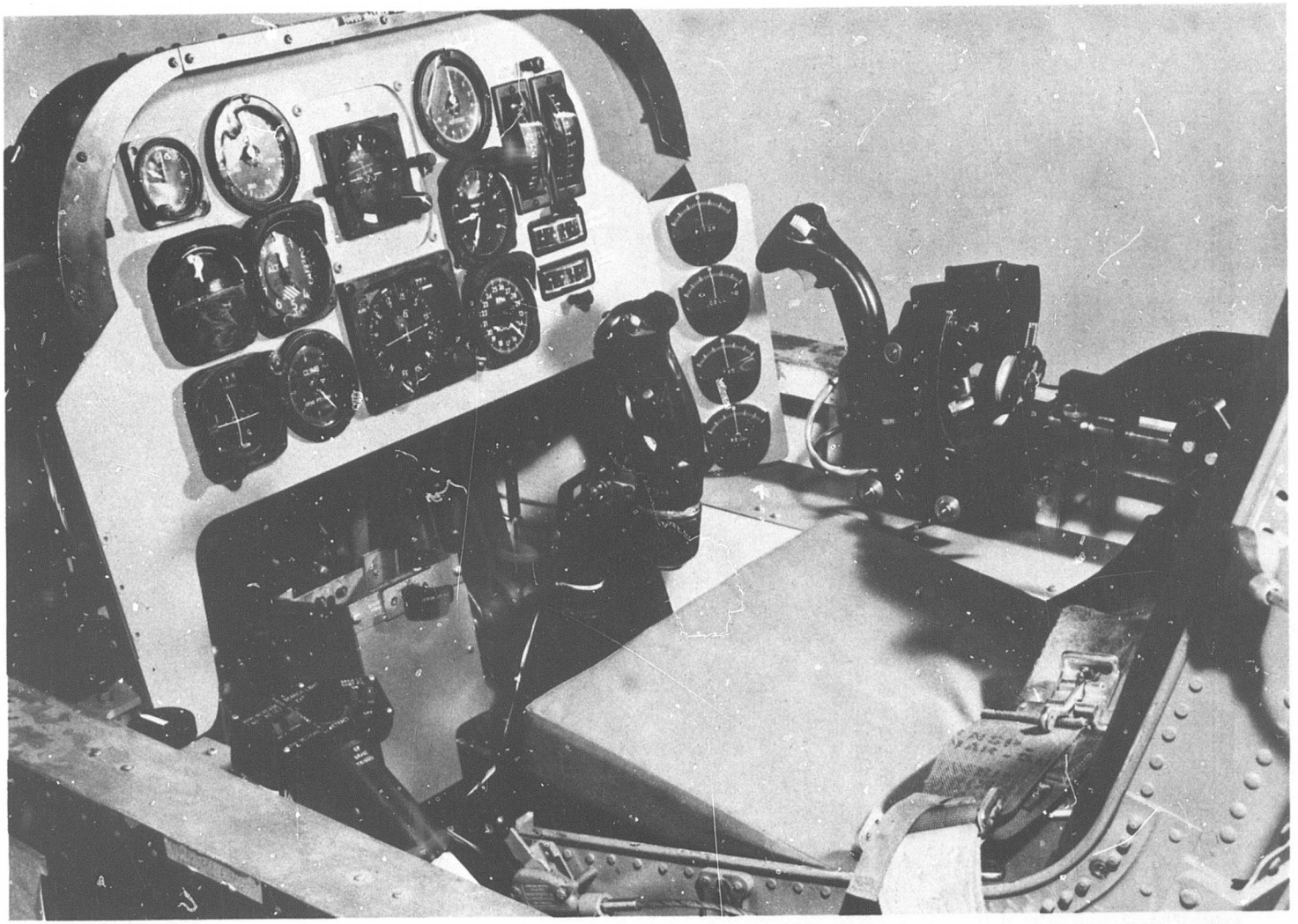

Figure 29. Simulator Cockpit.

ADVANCED FLIGHT CONTROL CONCEPT VALIDATION

The AFCC was mechanized[10] and modified as described in Reference 1. The modifications consisted of tailoring the short-period feedback loops of the AFCC to be compatible with the flight characteristics of the CH-47B/C helicopter.

The AFCC system was evaluated only at a gross weight of 33,000 pounds and a center-of-gravity location 7 inches aft. The evaluation covered the full flight envelope at these conditions and showed the AFCC system to be stable at all airspeeds including climbs and autorotation. However, oscillations were observed at bank angles approaching 30 degrees. These were attributed to the use of Euler rate feedback, as opposed to body rate feedback in the AFCC system.

CONCLUSIONS

The unpiloted validation showed that the simulated mathematical model provides a satisfactory representation of the actual aircraft. This validation was based primarily on comparison with flight test and digital computer data. Static trim comparison was very good for straight and level flight and steady sideslips. The match with flight test data for unpiloted control pulses and SAS failures was generally close in the short period. Amplitude, frequency, and damping of the responses were nearly identical. More delay between the input and response was present in the flight test data than in the mathematical model. The difference in delay, 0.2 second, produced a minor effect in the stability and control characteristics. This discrepancy was attributed to the omission of rotor flapping dynamics in the mathematical model and to filtering present in the flight test data.

Test pilot evaluation demonstrated that the mathematical model provides a realistic representation of the actual helicopter. Response to pulsed control inputs in all axes and throughout the flight envelope closely resembled that of the aircraft. Simulated spot turns, sideward and rearward flight, sideslips, and coordinated turns corresponded fairly well to the actual aircraft. Simulation of and response to atmospheric turbulence, ground effect, and gross weight changes were quite realistic. Behavior with SAS off and in SAS failures was similar to the actual aircraft for hover through medium-speed flight. SAS failures were somewhat too mild, due to a lack of jerking and cross-coupling effects. However, instrument indications of aircraft behavior following failure were normal. Pronounced thrust-pitch coupling reduced the performance of the mathematical model in flares.

The simulator motion and visual display systems provided overall high fidelity. The illusion of actual flight was quite convincing in hover and in low-speed flight. Both angular and translational movement of the simulated aircraft were limited by the visual display. For high-speed maneuvers, inadequacy of the visual cues caused the pilot to rely on his instruments. Under these conditions the behavior of the simulated aircraft was nearly normal for the CH-47C. Pitch control required slightly more than normal attention, while lateral and directional control required slightly less. The difficulties in pitch control were attributed to a dead zone in the motion base which produced confusing cues, and to insufficient instrument lag. The motion base travel was insufficient to provide normal acceleration cues associated with motion of the center of gravity, which resulted in an altitude control problem. The simulation of cockpit vibration and noise was not realistic

enough to aid in the illusion of flight. However, the vibration and noise provided some warning of rotor speed change.

The conclusions reached in this investigation may be summarized as follows. The simulation possessed sufficient fidelity and realism to be used for investigating control system concepts and handling qualities of the CH-47C. The mathematical model proved to be satisfactory for the complete flight envelope. However, the motion and visual display systems limited the envelope somewhat. The simulation was best suited for operation below 70 knots, where the motion and visual cues were most realistic.

RECOMMENDATIONS

The following changes and areas of additional investigation are recommended to further improve the accuracy of the simulation mathematical model:

- In the basic equations of motion, the effect of neglecting the terms which are products of lateral velocity and angular rate should be investigated. It is quite possible that these terms are significant during lateral maneuvers in hover.

- The problems encountered in flaring and in thrust-pitch coupling are attributable to rotor-rotor interference effects. Research should be performed in this area to provide a better understanding of the interference effects when the inflow ratio of the rotors approaches zero.

- The rotor horizontal force equations should be further developed to provide better results at high airspeeds. This force was too large at high airspeeds, causing an excessive nose-down pitch attitude.

- Continuous change in gust frequency and delay between the front and rear rotor, as a function of advancing blade tip speed and airspeed, should be provided by the addition of multipliers.

- In future studies of ground contact, the simulation envelope limits should be substantially reduced. Angular rates should be voltage scaled to a maximum value of approximately 15 degrees per second. Translational rates should be voltage scaled to a maximum value of 25 feet per second. Maximum simulation altitude should be scaled to 25 feet above ground level. Also, a simpler helicopter model should be employed in order to reduce the amount of equipment used and to minimize interconsole trunking.

- The rotor thrust limit should allow a transient and thrust above the steady-state limit. Some investigation is necessary to provide satisfactory transient characteristics.

To increase the effectiveness of visual and kinesthetic cues and to improve the simulation illusion of flight, the following changes are recommended:

- To make the simulated altitude control problem more closely resemble that of the actual helicopter, motion base vertical travel should be increased to provide realistic vertical acceleration cues.

- Lack of lateral movement capability in the motion base created a control problem for high-speed yaw maneuvers. Lateral motion base freedom and blade lead-lag should be included to permit precise evaluation and optimization of control concepts.

- To allow maneuvering throughout the complete flight envelope, the angular displacement limits of the visual display should be ±50 degrees. The display translational volume should be made more versatile to allow high-speed maneuvers. The representation of ground and runway texture should be improved to provide better height cues.

- To provide the instrument flight reference characteristics, appropriate instrument lags should be included.

- Further development is needed to improve the simulation of noise and vibration. The power spectrum of the noise simulation should be improved to produce the proper level of noise from the different frequency sources. Vibration should be improved by making the wave forms transmitted through the motion base more repeatable. More data should be obtained to improve the vibration drive equation.

LITERATURE CITED

1. SIMULATION OF THE ADVANCED FLIGHT CONTROL CONCEPT FOR THE CH-47C: Boeing Vertol Report D8-2420-1, February 1969, (Confidential).

2. OPERATOR'S MANUAL - ARMY MODEL CH-47B AND CH-47C HELICOPTERS, TM 55-1520-227-10, Department of the Army, Washington, D.C., 1968.

3. CH-47C EQUATIONS OF MOTION AND SIMULATION DATA: Boeing Vertol Report D8-2419-1, February 1969.

4. Etkin, B., DYNAMICS OF FLIGHT, Wiley, New York, 1965.

5. Thelander, J.A., AIRCRAFT MOTION ANALYSIS, FDL-TDR-64-70, 1965.

6. Davis, J.M., STABILITY AND CONTROL ANALYSIS, Boeing Vertol Report No. 114-AD-603, 1966.

7. Lappe, V.O., DESIGN OF A LOW ALTITUDE TURBULENCE MODEL FOR ESTIMATING GUST LOADS ON AIRCRAFT, TR AFFDL-TR-64-170, 1965.

8. Case, E.R., A STUDY OF THE EFFECTS OF C_L-COUPLING OF THE LATERAL STABILITY OF AIRCRAFT IN ATMOSPHERIC TURBULENCE, UTIAS TN118, 1967.

9. Blake, B.B., Albion, N., and Radford, R.C., FLIGHT SIMULATION OF THE CH-46 HELICOPTER, AHS Paper No. 361, Presented at the 25th Annual National Forum Proceedings, Washington, D.C., 1969.

10. ADVANCED FLIGHT CONTROL SYSTEM CONCEPTS FOR VTOL AIRCRAFT, Instrumentation Laboratory, Massachusetts Institute of Technology; USAAVLABS Technical Report 66-74, U.S. Army Aviation Materiel Laboratories, Fort Eustis, Virginia, May 1967, AD 381675L (Confidential).

GLOSSARY

Advance Ratio - Ratio of rotor wind axis longitudinal velocity component to rotor tip speed.

Autorotation - Descent in a helicopter with no engine power driving the rotors.

Control Pulse - A step change in control input which is removed after a short duration between 0.5 and 1.0 second.

Flapping - Vertical motion of rotor blades about a hinge (horizontal pin) which is perpendicular to the rotor shaft.

Heave and Lunge - Vertical and longitudinal components of linear acceleration motion cue, respectively.

Homogeneous - Independent of position in space at a given altitude.

Inflow Ratio - Ratio of rotor wind axis vertical velocity component to rotor tip speed.

Isotropic - Independent of axes orientation.

Kinesthetic - Human sensory perception of forces in motion by senses other than vision; an adjunct to what are considered the five normal human senses.

Lead-Lag - Horizontal motion of rotor blades about a hinge (vertical pin) which is parallel to the rotor shaft.

SAS - Stability augmentation system.

SAS Hardover or Failure - Condition in which SAS actuator moves rapidly to and stays at either of its extreme positions, producing a destabilizing control input.

Sidearm Controller - Device by which the pilot can provide all control commands with one arm; in a helicopter, replaces the cyclic stick, collective pitch lever, and directional pedals.

Three-Degree Detent - Collective control setting which provides a blade pitch of three degrees at the three-quarter span point. The pilot uses this to set the collective necessary for engine start/stop.

Thrust-Pitch Coupling - Aircraft pitch resulting from collective changes.

Uncorrelated - Statistically independent.

APPENDIX I
PILOT COMMENTS

HOVER AND LOW-SPEED MANEUVERS

Tests In Ground Effect at 33,000 Pounds and 7 Inches Aft CG

Hover With SAS On - Calm Air

Overall fidelity of the simulation was high when hovering in ground effect (IGE) with SAS on and under calm wind conditions. The response of the aircraft to the standard SAS check of pulsed control inputs in all three axes closely resembled that of the true aircraft. Pulsed collective inputs were unrealistic in that no vertical g was felt as a result. This feature also necessitated greater than normal altimeter reference in order to maintain accurate hover heights. Visual display cues, also, were not completely satisfactory at low altitudes, which further aggravated the height control problem. Power requirements and control positions were normal. Engine beep trim operating speed and the CH-47 characteristics of static and transient N_R droop were realistically reproduced. The marked tendency of the engines toward torque-splitting and load changeover between engines was not reproduced. The absence of secondary cross-coupling effects between roll, pitch, and yaw resulted in a smoother than normal ride.

Maneuvers In Ground Effect

Spot turns and sideward and rearward flight revealed a generally fair correspondence between simulation and aircraft. Lower than normal bank angles were necessary to achieve high lateral velocities, 2 degrees being required to sustain 25 knots. The conditions resulting from the absence of cross-coupling effects (noted above) also applied to these maneuvers. The limitations of the visual display dictated a minimum IGE maneuvering height of approximately 50 feet. At this altitude the visual height information was not precise and ground speeds also appeared to be lower than data revealed them to have been.

Hover With SAS Off

The SAS-off hover characteristics were very similar to those of the true aircraft. The general illusion was quite good, although the limitations indicated in the previous two paragraphs also applied here.

SAS Failures

SAS hardover failures were carried out in all three axes in both directions. Calm air conditions were used for the tests. The failures in pitch were the most realistic in terms of motion cues, required pilot recovery technique, pitch rates, and amplitude of the excursion. The simulation was inadequate on aircraft shaking and cross coupling with yaw. Failures in roll and yaw were too mild, due mainly to lack of jerk, shaking, and reaction in other axes.

Gust Effects and Steady Winds

The gust simulation in hover at 235 N_R was very realistic in terms of aircraft attitude and altitude excursions. Pitch excursions were particularly good from the pilot feel point of view. Attitude control was somewhat more difficult than with normal aircraft. At 250 N_R, little change in the simulated response to gusts could be detected. In an actual aircraft,the response is livelier at the higher rpm. The secondary gust responses of shaking, cross coupling between axes, and changes in noise and vibration were not reproduced.

The simulation of steady winds was very convincing. When hovering into, down, and cross wind, aircraft attitude changes were necessary to maintain the hover over a selected point. These attitude changes were of the correct order for the into-the-wind and downwind cases. In cross-wind hover, the attitude change of only 1 degree bank for 10 knots of wind was too low. Spot turns required almost the normal sequence of control actions for their accurate performance in quiet wind conditions and were quite convincing. The illusion would have been further improved by the provision of realistic noise and vibration. It was also found that the turns could be carried out at a fixed collective setting in spite of changes in the position of the other controls. This was unrealistic.

Hover Out of Ground Effect

Hovering was carried out at a radar altitude of 500 feet. The control techniques, positions, and aircraft attitudes were generally close to those of normal aircraft. Maintaining a constant height was rather difficult. The selection of the correct collective setting for a zero rate of climb was almost impossible, even under calm air conditions. This was believed to have been due to total absence of a vertical motion cue in response to collective inputs. Lateral flight at 500 feet again suggested that unrealistically low bank angles produced quite high lateral

velocities (2 degrees = 20 knots). Engine torque requirements for the stabilized hover were recorded as in the IGE hover condition. It was noted that slightly more torque was required when hovering IGE at 250 N_R. The reversal of this situation at 500 feet above ground level (AGL) was not understood.

From the out of ground effect (OGE) hover condition, the aircraft sank gently to an accurate IGE hover when the appropriate IGE hover torque setting was selected. This was a very realistic simulation of the ground effect phenomenon.

Tests at 46,000 Pounds and 4 Inches Aft CG With 250 N_R

The translational and rotational inertia effects of increased weight were realistically presented. The normal pulsed control input SAS check revealed behavior very similar to that of the true aircraft under the same conditions. At a height of 20 feet (in ground effect with wheel height of approximately 5 to 10 feet) 60 percent engine torque was necessary. At the dual-engine torque limit, the hover stabilized at 100 feet under calm air conditions. Spot turns and lateral flight were fairly realistic. The vibration simulation was unconvincing due to frequency fluctuations.

ACCELERATIONS AND DECELERATIONS THROUGH TRANSITION

Tests at 33,000 Pounds and 7 Inches Aft CG

Low-Speed Forward Flight Transition

During initial transition tests, it was found that forward flight at 50 knots could be obtained without change of the IGE hover collective pitch setting and without any detectable height due to loss of ground effect. This simulation fault was eventually traced to the unrealistically low value of the visual cue at the lower heights. The initial hovering had been conducted at an unrealistically high level of 50 feet. The sensitivity of the radar altimeter was changed from full-scale deflection of 1,000 feet to 100 feet. This altimeter then became, again somewhat unrealistically, the prime low-level source of height information. Under this new system when transitions were made from hover heights of 20 feet and below, the normal ground effects with forward velocity could be clearly detected. From the beginning of the test, the effects of translational lift became apparent at 25 knots indicated airspeed (IAS). Overall realism was reduced by the lack of realistic noise, vibration, and control cross-coupling effects.

Low-Speed Flight at Low Altitude

Flight below 50 knots IAS was fairly representative of the true aircraft. In turns, yaw control was harder than normal due to the absence of lateral motion cues. The prime source of yawing information then became the non-standard lateral velocity meter incorporated in the simulator instrument display. This provided reliable flight balancing information under zero wind conditions only. A general tendency to overcontrol in the yaw axis existed. Above an IAS of 50 knots the SAS sideslip system became operative, which greatly reduced the yaw control problem.

Rapid Transitions and Quick Stops

During rapid transitions, the simulation of the aircraft was only fair. It was difficult to accurately select and maintain the correct pitch attitude required to provide the desired combination of linear acceleration and vertical rate of climb at maximum power. A marked pitch overcontrol tendency resulted. This could have been caused by the absence of the vertical motion cue normally provided by the aircraft and the lower-than-normal visual cue provided by the display close to the ground. Perhaps due to the same cause, achievement of fine control was further aggravated by exaggerated thrust-pitch coupling. Vibration simulation was not entirely realistic. Static and transient rotor droop simulations were very convincing.

Control during quick stops at low level was very much more difficult than with the actual aircraft. Collective control for precise height corrections was almost impossible, due to a marked overcontrolling tendency. An unrealistically high level of thrust-pitch coupling existed, particularly at the lower end of the range below 5 degrees of pitch. During the final stages of the stop in the flare recovery, full forward longitudinal cyclic control was insufficient to prevent increasing pitch attitudes. Through practice, a technique for providing additional pitch control was developed. The extreme thrust-pitch coupling was used to apply collective at an early stage in the maneuver. During these tests it was noticed that the simulated 3-per-rev vibration totally disappeared at low collective pitch settings. Static and transient rotor droop simulation were again convincing.

Tests at 46,000 Pounds and 4 Inches Aft WG With 250 N_R

The runway takeoff flight path was very realistic. Stability and control seemed to be normal in transition and for climbs at 70 knots, however, the vibration was poor.

ENGINE FAILURES

Single-Engine Failures at Sea Level Air Density

Hover

Due to the lack of realistic cues at heights below 150 feet AGL, this investigation was carried out at that level and was, therefore, OGE. Torque reduction following engine failure was extremely rapid. A reduction of 10 N_R occurred before power increased on the live engine in compensation. The height losses, which were 50 to 60 feet (estimated), were greater than those to be expected in the CH-47C during practices in which one engine is set to ground idle. The noise simulation lacked impact.

Level Flight at 500 Feet AGL

Overall close correspondence existed between the simulation and the CH-47C at 500 feet and 100 knots IAS. Again the noise simulation was of very little help in warning that failure had occurred.

Dual Engine Failures at 150 Knots

Though the evaluating pilot had never experienced dual-engine failure in actual flight, its simulation was investigated. All failures were premeditated, and the noise simulation was relied on with extreme concentration as the failure warning. Of a number of tests run, in only 25 percent of the failures was the aircraft recovered. Following failure, immediate collective lowering to full down was vital in retaining N_R above 190. The aircraft became markedly less stable in pitch and particularly so in roll during the N_R decrease. Aft movement of the longitudinal cyclic control by an estimated 1 to 1-1/2 inches aided N_R recovery, which was otherwise very slow. When this technique was not used and operations at 190 N_R were prolonged beyond 1 or 2 seconds, control of the aircraft was lost in every case.

SAS-OFF FLIGHT AND SAS HARDOVER FAILURES

SAS-Off Speed Sweeps and Turns

From a stabilized straight and level flight condition at 40 knots IAS and at 2,000 feet, the aircraft was accelerated at constant altitude with SAS off. As a result of a progressively worse overcontrol tendency with airspeed, the aircraft was uncontrollable in yaw above 70 knots. Further acceleration was continued with yaw SAS on. The limit of controllability in level flight and turns was reached at 130 knots, due to overcontrolling in pitch and roll.

Single SAS Failures in Level Flight at 2,000 Feet

In view of the characteristics described above, single SAS failure recovery delay times were investigated only in pitch and roll to 130 knots and in yaw at 70 knots. It should be emphasized that these tests were conducted under conditions close to actual instrument flight due to the absence of visual attitude and heading information. Generally, the failures were too mild in the absence of normal heavy accelerations and shaking of the aircraft. In all cases, the instrument indications of aircraft behavior following the failure and before initiating recovery were normal for the CH-47. At 130 knots, recovery from a single SAS pitch-up hardover was impossible. Full forward cyclic control failed to stop the pitch rate generated by the failure. When recovery was initiated at an earlier pitch attitude and elapsed time stage following failure, the full cyclic control applied still remained ineffective.

EFFECTS OF TURBULENCE IN LEVEL FLIGHT AT 2,000 FEET

The simulation was initially investigated under conditions of light to moderate turbulence. At 70 knots the gusts were detectable as a smoothly undulating ride. They remained unrealistically smooth to 130 knots. Above this speed their character changed somewhat to a sharper, jarring effect more closely representing the true in-flight gust effect. During the test, variation of N_R was evaluated in relation to gust response, but little change could be detected. At the torque limit (78 percent) speeds, marked excursions in indicated torque and N_R occurred. An additional evaluation of 30 degrees banked level turn reversal was made with the main test. The aircraft control and stability characteristics had been faithfully reproduced.

When the turbulence level was raised from light through moderate to heavy at 155 knots IAS and 235 N_R, the excursions of N_R and indicated engine torque increased somewhat. It was noticeable that the pitch attitude excursions in the gusts were significantly lower than what would have occurred in flight. Above 140 knots rotor speed fluctuations of $\pm$ 3 at 235 N_R and $\pm$ 10 at 250 N_R occurred with sympathetic torque fluctuations of up to $\pm$ 5 percent.

SIDESLIPS AND COORDINATED TURNS

Steady Sideslip at 2,000 Feet

Sideslips were made at 80 and 150 knots IAS (ship's system only and not oriented to free stream) with 235 N_R, and at 155 knots with 250 N_R. In each case, fully stable characteristics were exhibited to sideslip angles equivalent to lateral velocities of 20 to 25 knots. No marked discontinuities were evident, and

the behavior was very similar to that of normal aircraft. Total reliance was placed on the aircraft instrument indications for sideslip control due to the absence of realistic visual and motion cues.

Turns at 150 Knots and 2,000 Feet

Turns under instrument flight only were evaluated. These were limited to 30 degrees of bank by the simulator limits. The behavior of the vehicle was fairly realistic, and the general comments contained in the preceding paragraph are applicable. The SAS sideslip system worked well under these conditions.

CLIMBS AND DESCENTS

Tests at 33,000 Pounds and 7 Inches Aft CG

Hovering Takeoffs and Steep Approaches

Hovering takeoffs and steep climbing takeoffs used in confined areas were carried out into wind. The CH-47 control characteristics were reproduced very satisfactorily. As noted for other conditions, lack of noise and vibration detracted from the overall realism.

Steep approaches were surprisingly difficult to smoothly coordinate. The approaches were made at approach angles of approximately 30 to 40 degrees using a constant sight picture. A crab angle of about 30 degrees was used to permit an unobstructed view of the chosen landing area. It was suspected that the previously reported low bank angle requirement for lateral velocity and absence of lateral motion cues may have aggravated the required control coordination for the maneuver.

Climb and Climbing Turns to 2,000 Feet

Control during the climb entry and in the climb at 70 knots IAS was fairly well represented. The lack of an accurate visual horizon reference required greater than normal instrument reference to retain the stabilized climb. It was impossible to maintain accurate speeds and rates of climb when normal attention division between visual and instrument reference was used. From the pure instrument flying point of view, the simulator seemed to be somewhat less stable in pitch but rather more stable directionally and in roll than the true aircraft. The overall ride quality of the vehicle was softer and smoother than the CH-47 when moderate gusts were used. When climbs at 100 knots IAS were made, little change in the aircraft behavior was detected. Climbing turns to 30 degrees bank revealed no significant behavioral changes.

Partial Power Descents

Partial power descents were investigated at 60 and 130 knots with 235 N_R. The illusion was reasonably convincing in straight flight and medium turns. Instrument reference greater than normal for the CH-47 was required for accurate and balanced flight.

Autorotation

Autorotation at 70 and 100 Knots

Autorotation was investigated at 70 and 100 knots IAS during entry while stabilized, in turns, and during flare. Collective reduction to zero torque produced a reduction in N_R from 235 to 225. The rotor speed recovered as full autorotation was established. When the autorotation was entered at 950 feet AGL, initial visual cues were realistic, though the acceleration forces in all axes were very low. For this reason, pitch and yaw control were slightly oversensitive during entry. During stabilized autorotation, the aircraft control and N_R responses closely corresponded to those of the true aircraft. This also applied to autorotative turns of up to 25 degrees bank. A presentation of noise was made for these tests. It approximated the standard aircraft only in being responsive to N_R. It lacked command and was therefore rather ineffective as an N_R control feedback. Overcontrolling in all axes during flare was extremely difficult to avoid. This was believed to be primarily due to a very low level of, and in some cases total absence of, realistic motion cues and the poor standard of visual cues below 150 feet AGL. Repeating the test with light-to-moderate turbulence failed to reveal new and significant features.

Autorotative Entries at 150 Knots

Autorotation was entered at 150 knots and at 950 feet AGL using both 235 and 250 N_R. The initial N_R response to collective reduction to zero torque was an unrealistic drop from 235 to 225. Subsequently, N_R was recovered as autorotation was established and behaved in a normal and convincing manner. Following power reduction, deceleration and cyclic climb characteristics required to obtain the optimum autorotative IAS were very similar to those of the CH-47C. This impression was gained primarily from instrument readings in the absence of motion cues of a sufficiently high order. Noise simulation was as indicated above. When entries were made from 250 N_R and at the same speed, the 10 N_R loss occurred as described above but caused less embarrassment. Behavior was otherwise indistinguishable from the 235 N_R case.

LEVEL FLIGHT

Tests at 33,000 Pounds and 7 Inches Aft CG

Level-Flight Speed Sweeps at 2000 Feet

Due to the previously reported visual display limitations, the investigation of the higher end of the speed range was somewhat unrealistically conducted under virtually full instrument condition. In comparison with the true aircraft, pitch control required slightly more than normal attention, while directional and roll control required somewhat less. Longitudinal cyclic control inputs primarily intended for IAS adjustment produced an immediate response on the vertical speed indicator which was followed, after a significant delay, by a change in airspeed indicator reading in the desired direction. This feature was disconcerting and is believed to be an exaggeration of the normal aircraft behavior. It adversely affected accurate IAS and altitude control. The response of the aircraft to pulsed control inputs of 1 inch for 1/2 second corresponded closely to the CH-47B at all speeds. The maximum obtainable IAS at the maximum dual-engine torque limit of 78 percent was 160 knots. When an accurate N_R setting of 235 was made at 70 knots, N_R increased with airspeed to become 243 at 160 knots. A simulated 3-per-rev vibration increased in a fairly realistic manner with airspeed.

Acceleration and Deceleration in Level Flight

Accelerations and decelerations were made under conditions of light turbulence between 40 and 150 knots IAS and at 2,000 feet. A rotor rpm of 235 was used. Accelerations were made at 78 percent torque, while decelerations were made with the collective at the 3 degrees detent position. Extreme difficulty was encountered in adjusting the pitch attitude with changing IAS to maintain a zero rate of climb or descent. Large-magnitude acceleration cues normally associated with these maneuvers in flight were noticeably absent.

Tests at 46,000 Pounds and 4 Inches Aft CG

The simulated aircraft was accelerated from the stabilized condition of 70 knots IAS in level flight at 2,000 feet using torque-limit power. The maximum velocity in level flight was found to be 130 knots IAS. Due to the absence of the normal sideslip cues, constant instrument reference was necessary to monitor sideslip and to retain balanced flight. The previously described visual display limitations effectively left the pilot free to perform the evaluation by sole reference to flight instruments. At

70 knots the aircraft responded to the standard SAS check in a manner very similar to the CH-47. Throughout the level flight acceleration, control and stability corresponded very well to that of the standard aircraft. The aircraft vibration simulation was much improved during these tests, although it was at a rather low amplitude. At all speeds it was noticed that small aft longitudinal cyclic inputs quickly applied reduced N_R by as much as 5 N_R at 70 knots and by 15 N_R at V_{max}. Forward inputs produced the reverse result. Small torque fluctuations in the opposite sense occurred in sympathy with the N_R changes. This behavior was the reverse of what occurs in the actual aircraft. At V_{max} an aft longitudinal cyclic pulse of 1-1/2 inches resulted in an abrupt and increasing pitch-up rate. Forward longitudinal cyclic control was ineffective. Evidently the aft rotor had stalled out without any prior warning whatsoever. This behavior frequently recurred during and at the beginning of medium turns at all speeds above 100 knots IAS. The situation became aggravated in light to moderate turbulence.

PILOT SUMMARY

The simulator has been programmed to represent the CH-47C aircraft, retaining the CH-47B SAS characteristics. The primary pilot reaction was that the system, as programmed, demonstrated an exciting principle which possesses significant development potential as a tool for research, development, and training.

A high standard of fidelity was achieved in the simulation of the CH-47C at speeds below 70 knots and in hovering flight. In flights at higher speeds and at heights greater than 1,000 feet above the ground, the illusion was somewhat less convincing. The simulation shortcomings were traceable primarily to the low motion capability of the base and to practical design problems resulting in detectable distortion in the visual display. Motion cues, particularly at high speed, were either totally absent or much too low, which caused the apparent aircraft characteristics to differ from those of the actual aircraft. The visual horizon was apparently located some 15° above the true horizon which reduced considerably the value of visual horizon, cues at higher altitudes and speeds. This problem was not nearly as pronounced at low altitudes and speeds. In this situation the main visual display problem was a difficulty in accurately judging height by visual reference alone. It is believed that this was due to a number of causes:

1) Slight distortion due to the optical arrangement.

2) Textural differences between the highly magnified picture and the real world.

3) Scale errors in buildings, runway sizes, and standard runway markings.

The basic maneuverability of the CH-47C could not be fully investigated due to the limitations of the simulation system. Bank angles and pitch attitudes exceeding 30 degrees and ± 25 degrees respectively resulted in a system "reset". A reset could also result from pitch and roll rates well within the true aircraft capability.

Recent tests carried out on this simulator indicated that realistic reproductions of noise, vibration, and cockpit layout and equipment are necessary for the production of a totally convincing illusion.

APPENDIX II
ISOLATED ROTOR AND STATIC TRIM DATA

Table V lists the isolated rotor and static trim data taken for the simulation. Theoretical data were generated and superimposed on the simulation data for comparison in all cases except the isolated rotor dynamic responses to collective pitch steps. Flight test trim data were obtained for the cases as indicated. The comparison of the simulation, flight test, and theoretical data was discussed in the body of this report. The cases presented in this appendix (Figures 30 through 52) are indicated. Static trim and isolated rotor dynamic data are summarized in Tables VI and VII. The complete data package can be found in a Vertol Division internal report.

TABLE V. ISOLATED ROTOR CHARACTERISTICS

Plot	Rotor Speed (rpm)	Airspeed (kn)	Altitude (ft)
Torque Versus Thrust	230*	0.0	Sea Level
	230	0.0	10,000
	230*	100	10,000
	230	170	Sea Level
	230	170	10,000
	245	0.0	Sea Level
	245	0.0	10,000
	245	170	Sea Level
	245	170	10,000
H Force Versus Thrust	230	0.0	Sea Level
	230	0.0	10,000
	230*	100	Sea Level
	230*	100	10,000
	230	170	Sea Level
	230	170	10,000
	245	0.0	Sea Level
	245	0.0	10,000
	245	170	Sea Level
	245	170	10,000
Y Force Versus Thrust	230	100	Sea Level
	230	170	Sea Level
	245	100	Sea Level
	245	170	Sea Level

* Included in this appendix

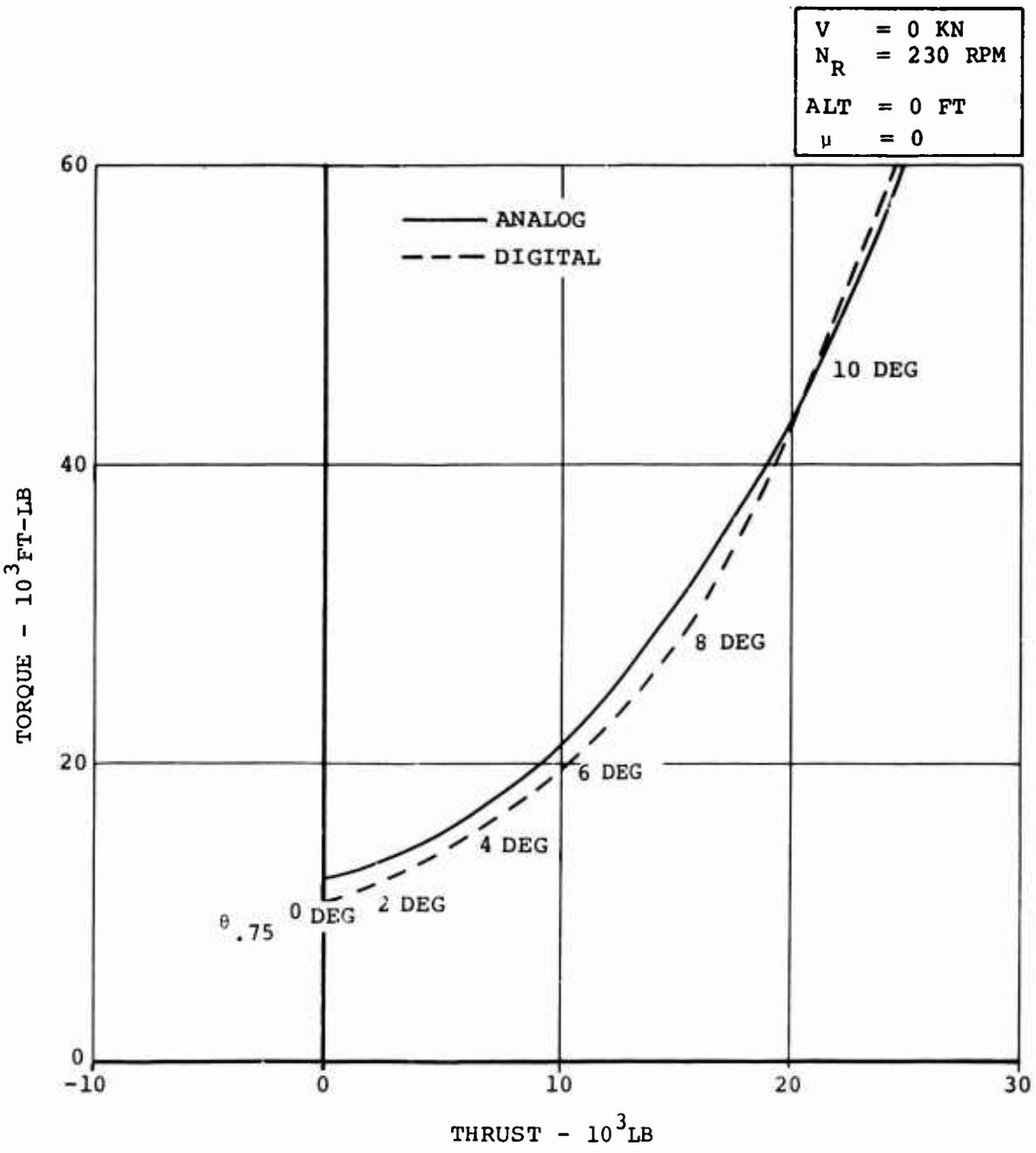

Figure 30. Torque Versus Thrust for CH-47C.

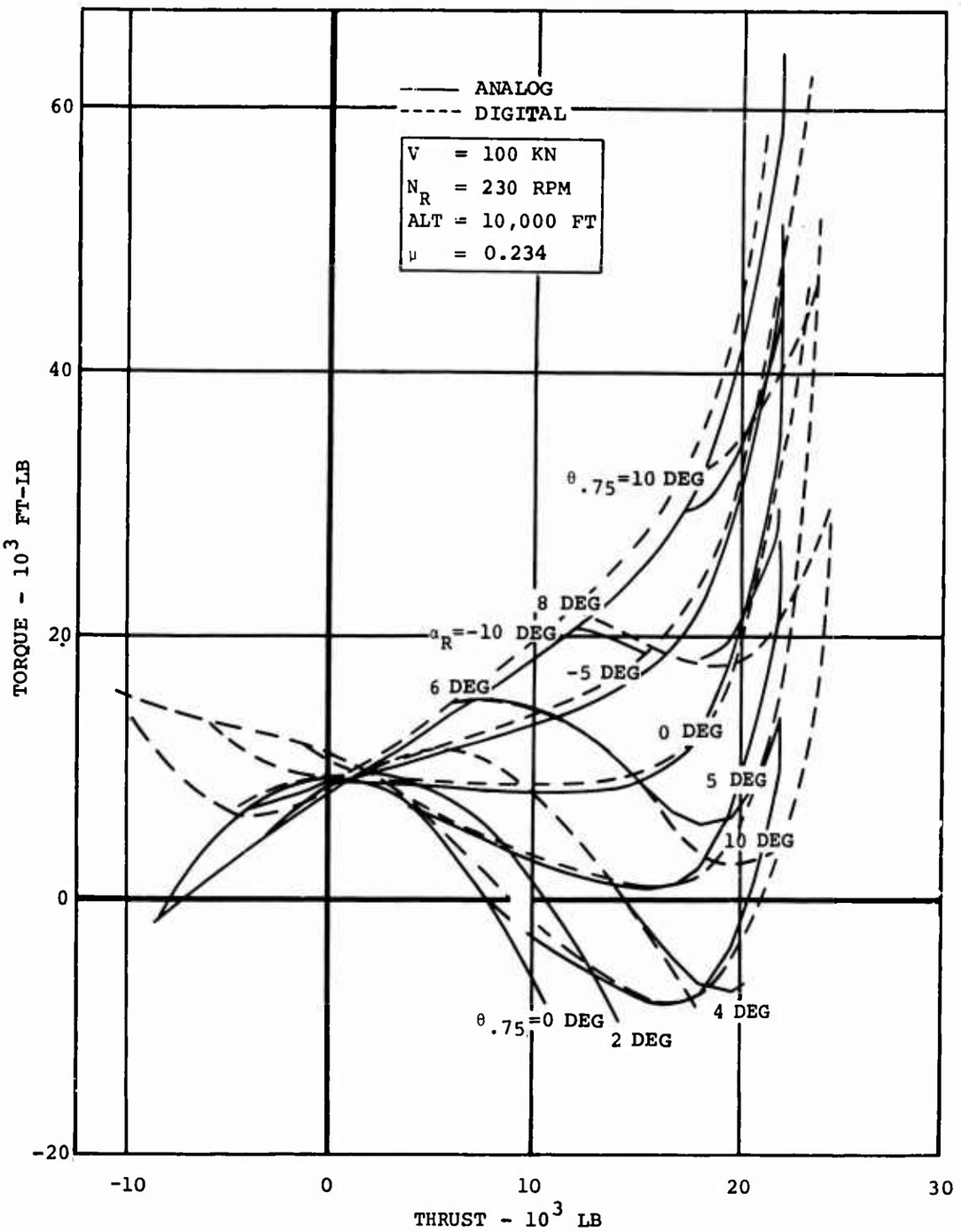

Figure 31. Torque Versus Thrust for CH-47C.

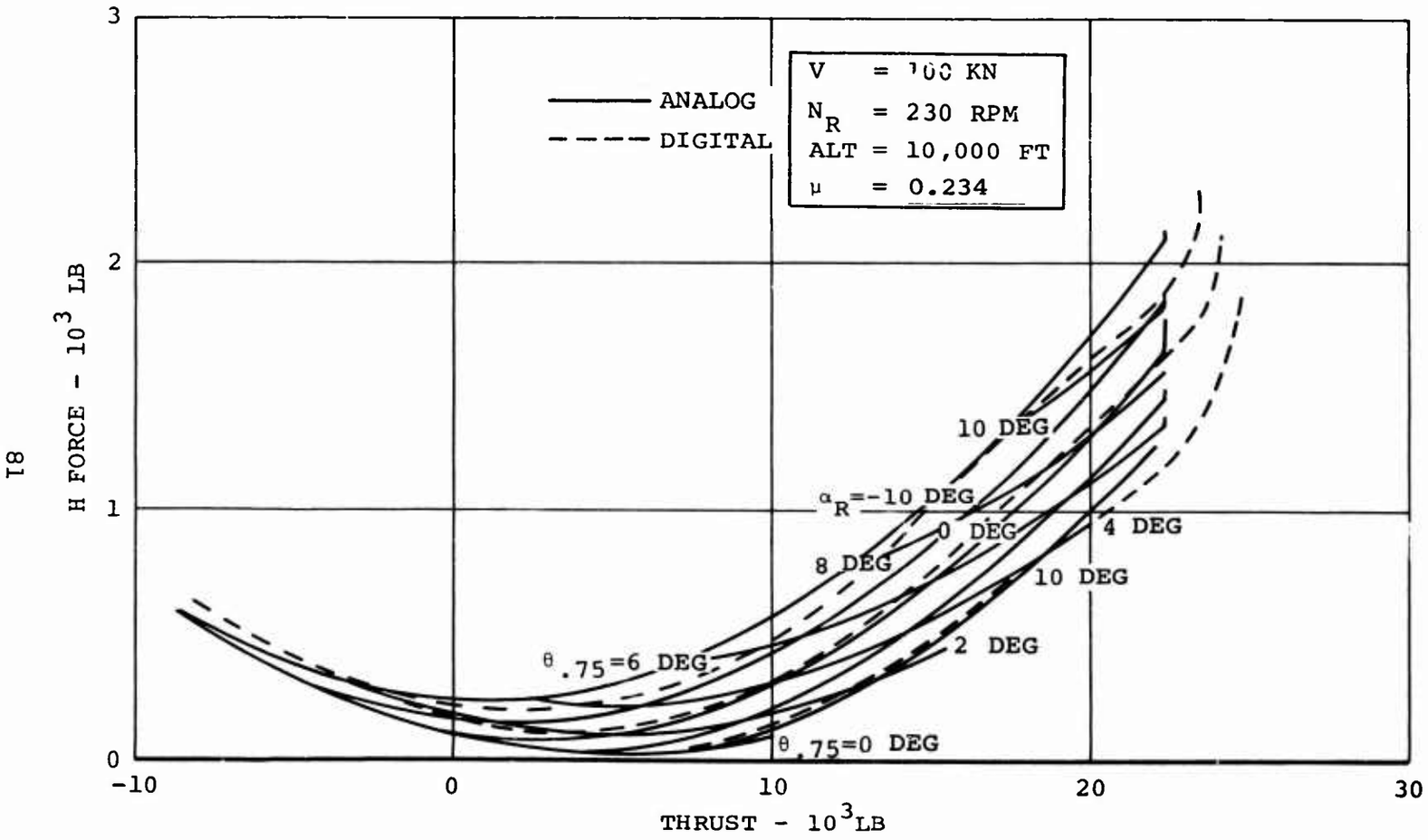

Figure 32. H Force Versus Thrust for CH-47C.

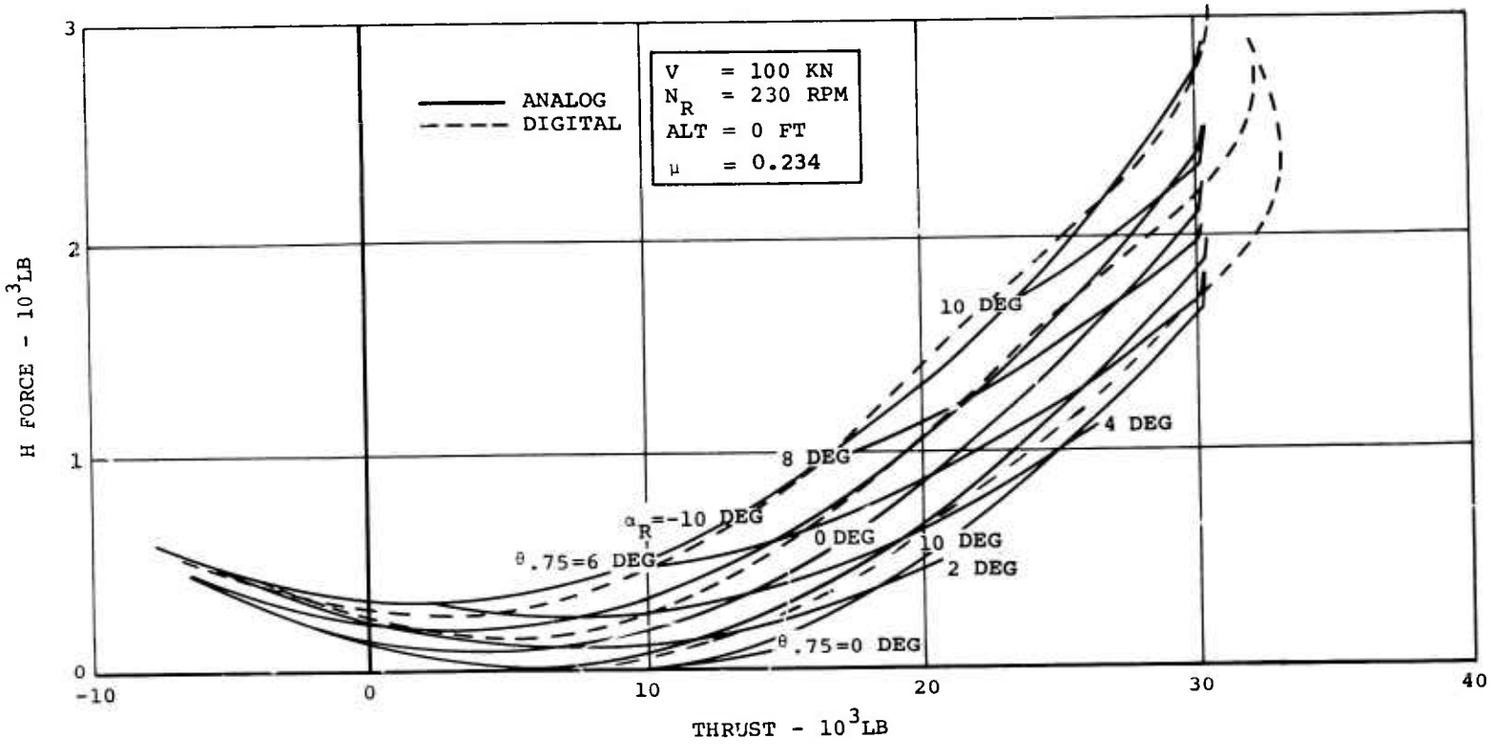

Figure 33. H Force Versus Torque for CH-47C.

TABLE VI. STATIC TRIM DATA

Sideslip Angle (deg)	Gross Weight (lb)	Airspeed (kn)	Altitude (ft)	Rotor Speed (rpm)
0.0*	22,000	Sweep	Sea Level	230
0.0	22,000	Sweep	10,000	230
0.0*+	33,000	Sweep	Sea Level	230
0.0*+	33,000	Sweep	10,000	230
0.0*	46,000	Sweep	Sea Level	230
0.0	46,000	Sweep	10,000	245
>0,<90*	33,000	100	Sea Level	230
>0,<90	33,000	150	Sea Level	230
±90*+	33,000	Sweep	Sea Level	230

* Included in this appendix

+ Flight test correlation

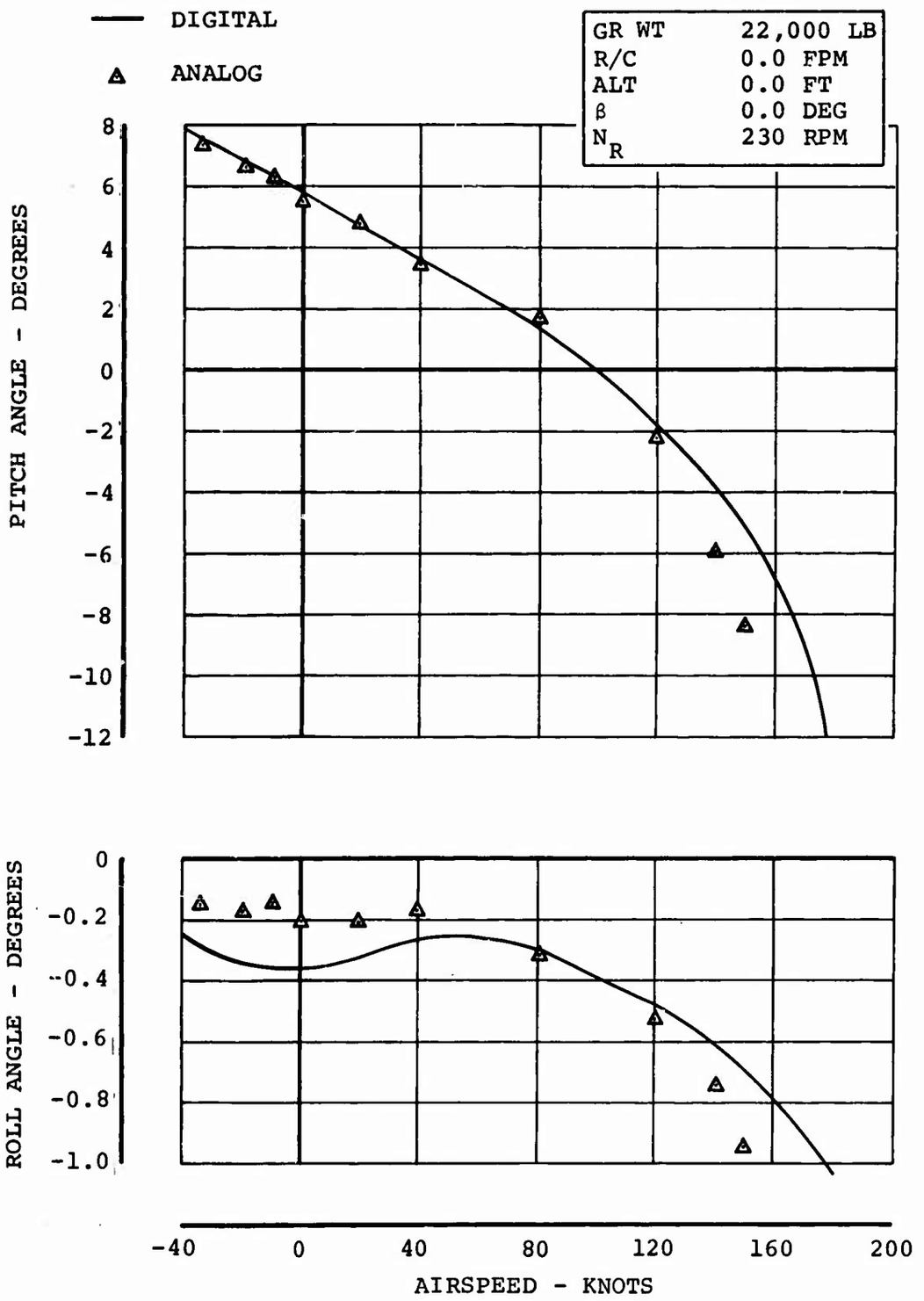

Figure 34. Static Trim Data.

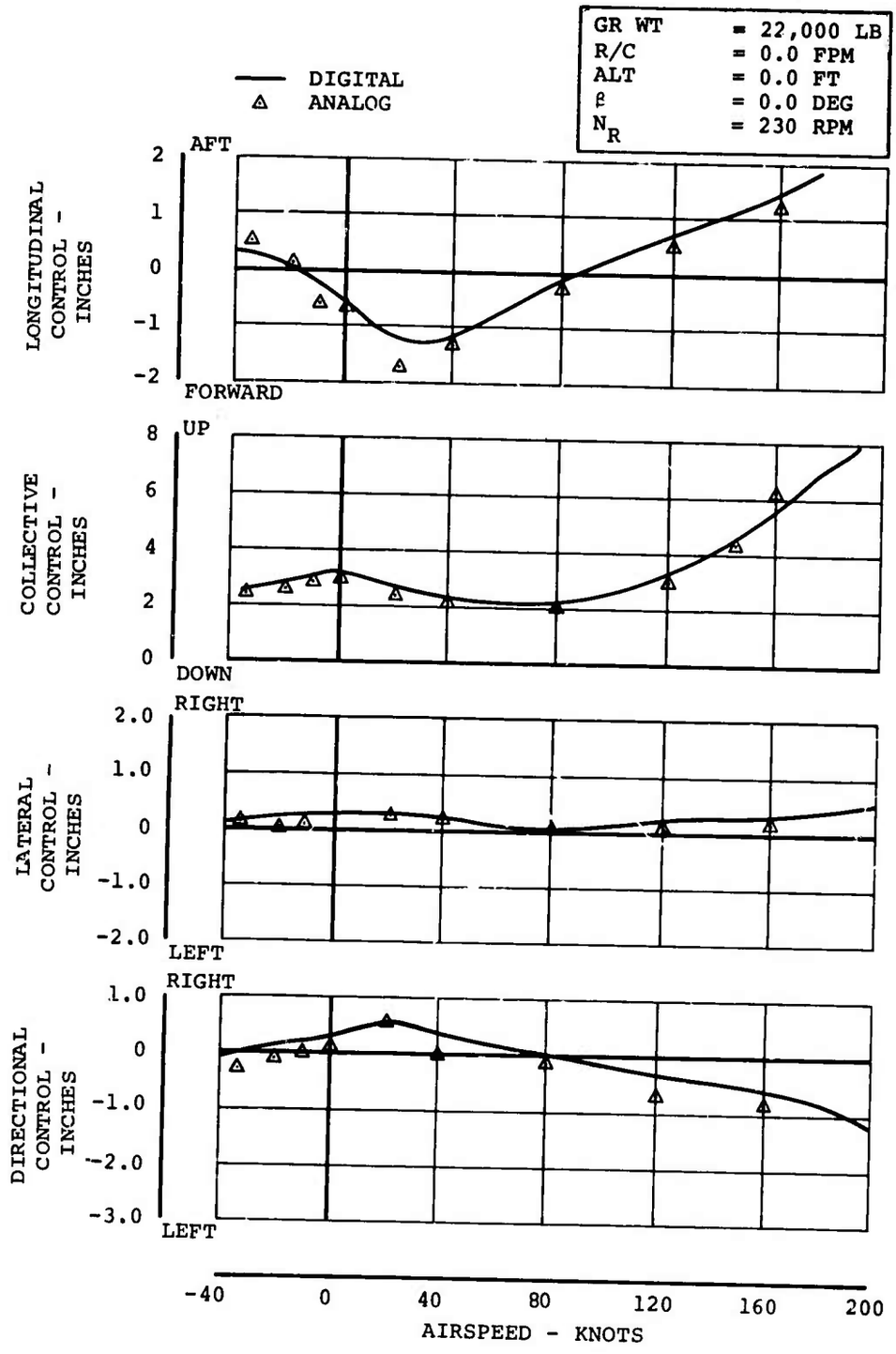

Figure 35. Static Trim Data.

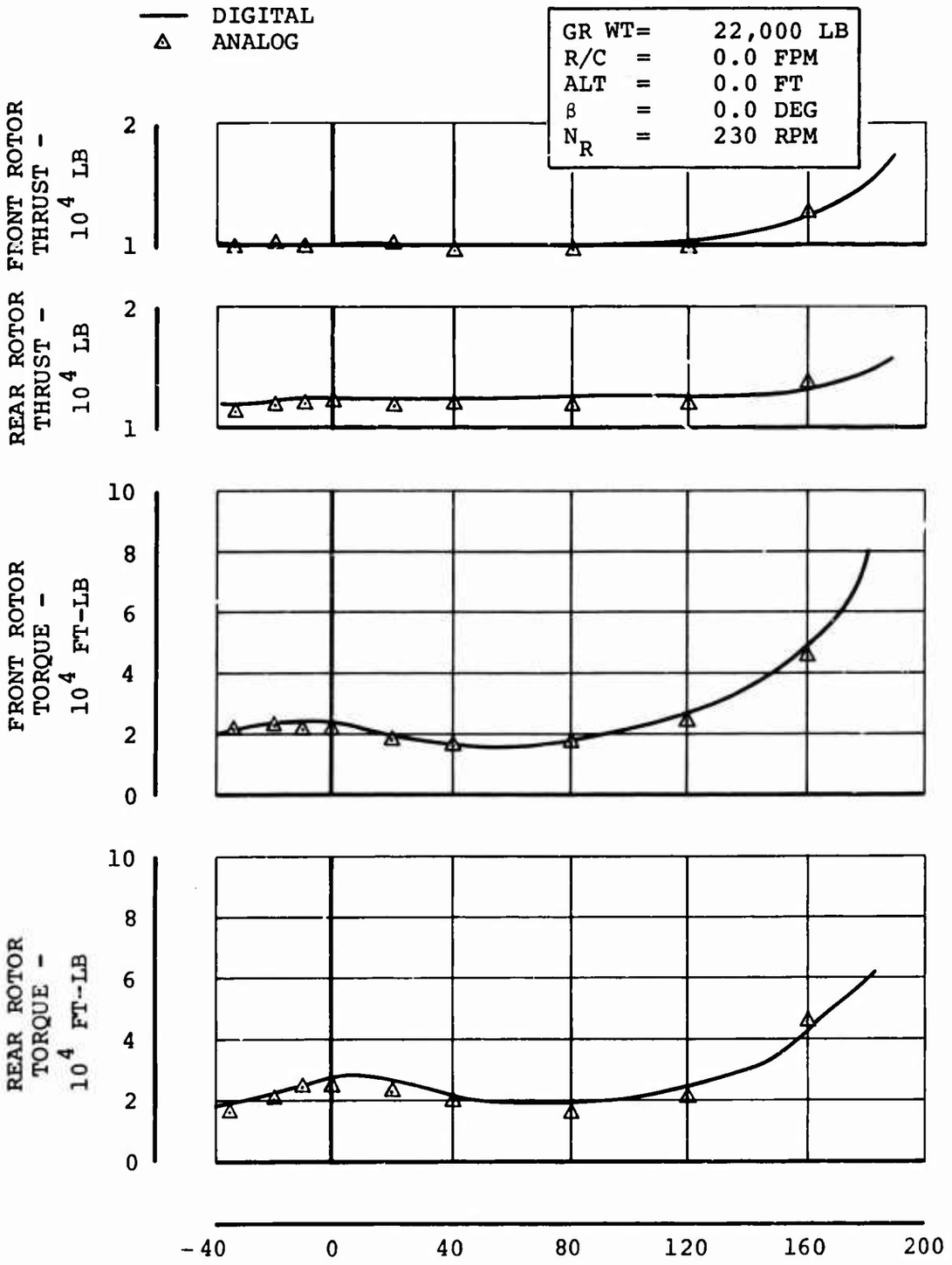

Figure 36. Static Trim Data.

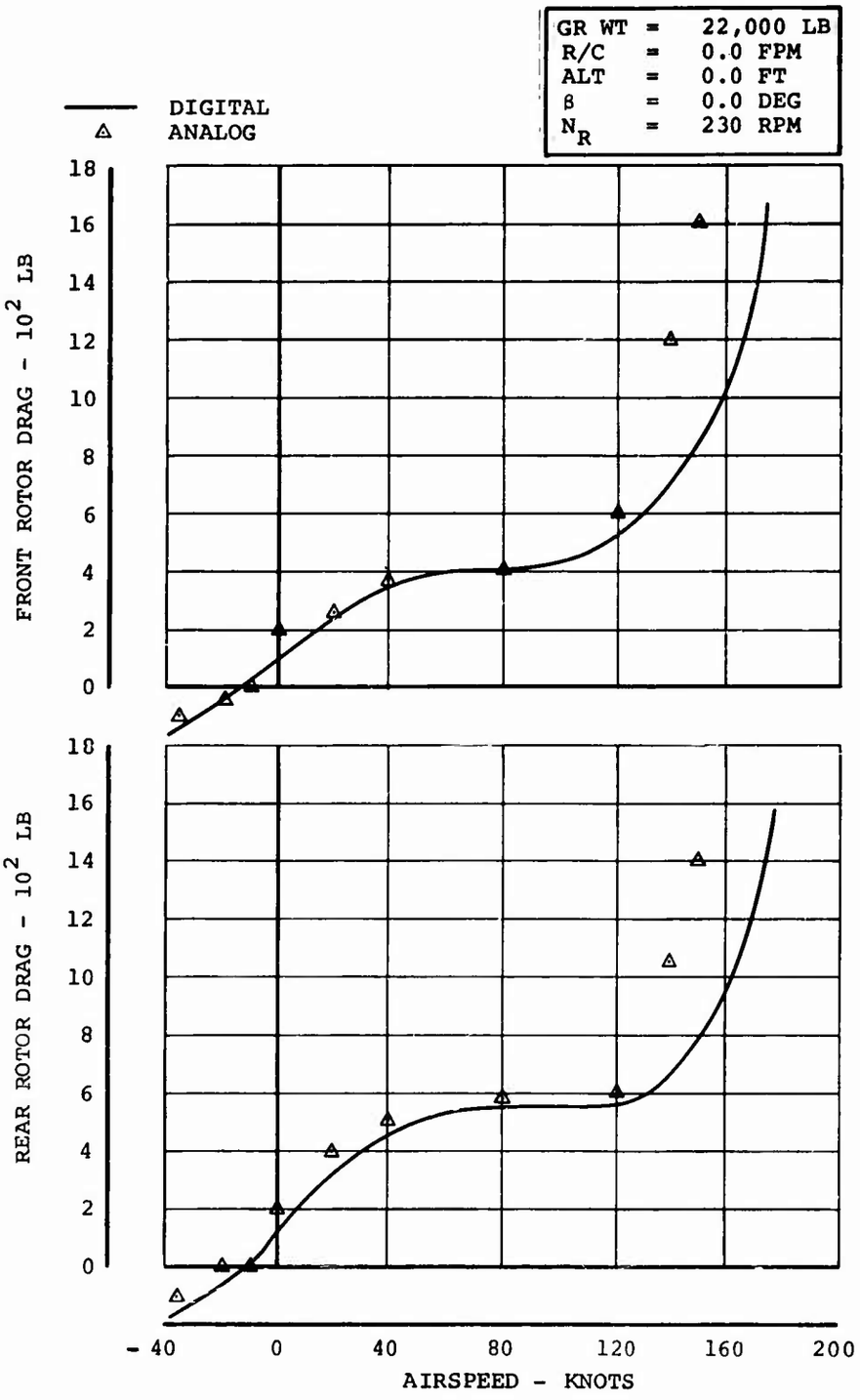

Figure 37. Static Trim Data.

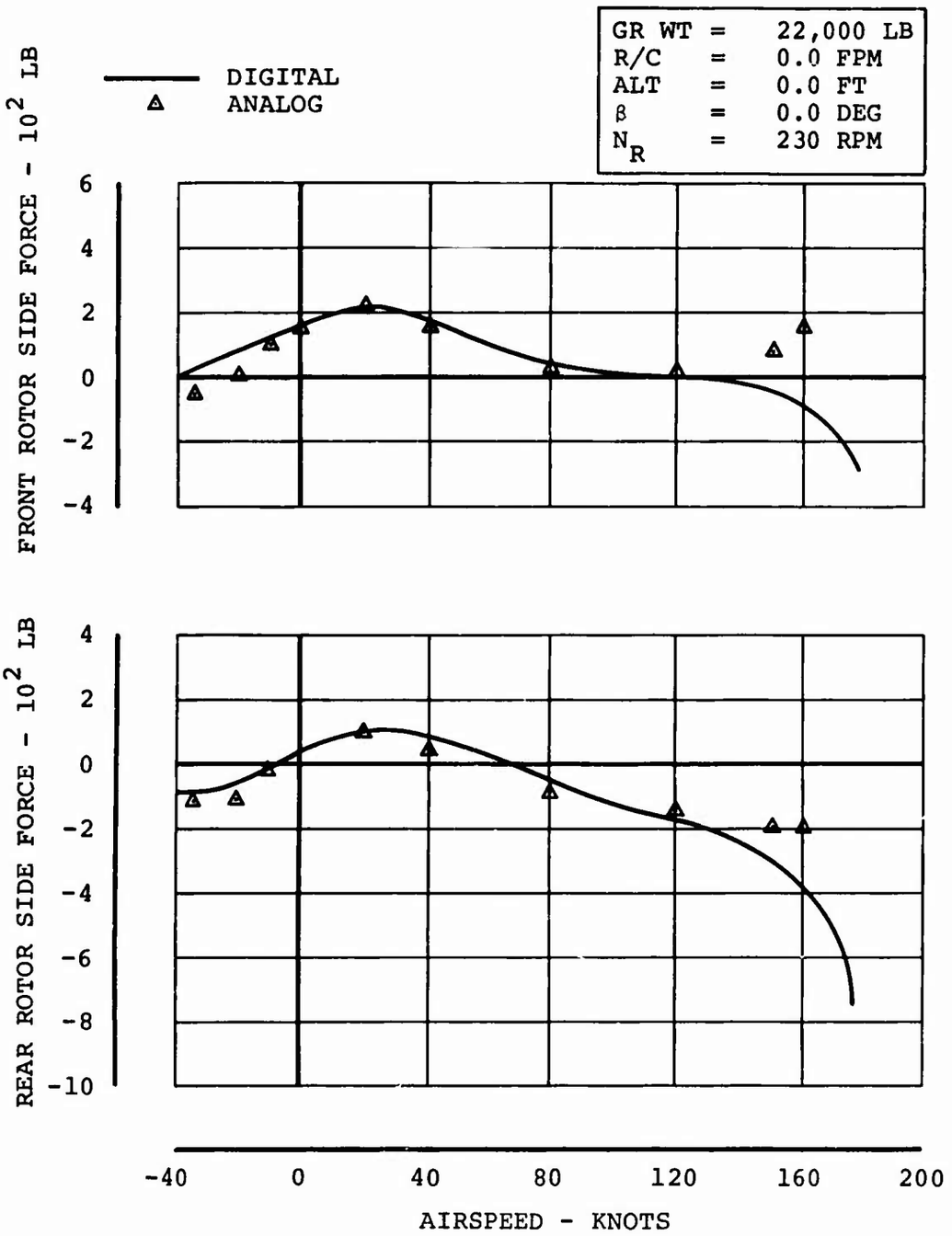

Figure 38. Static Trim Data.

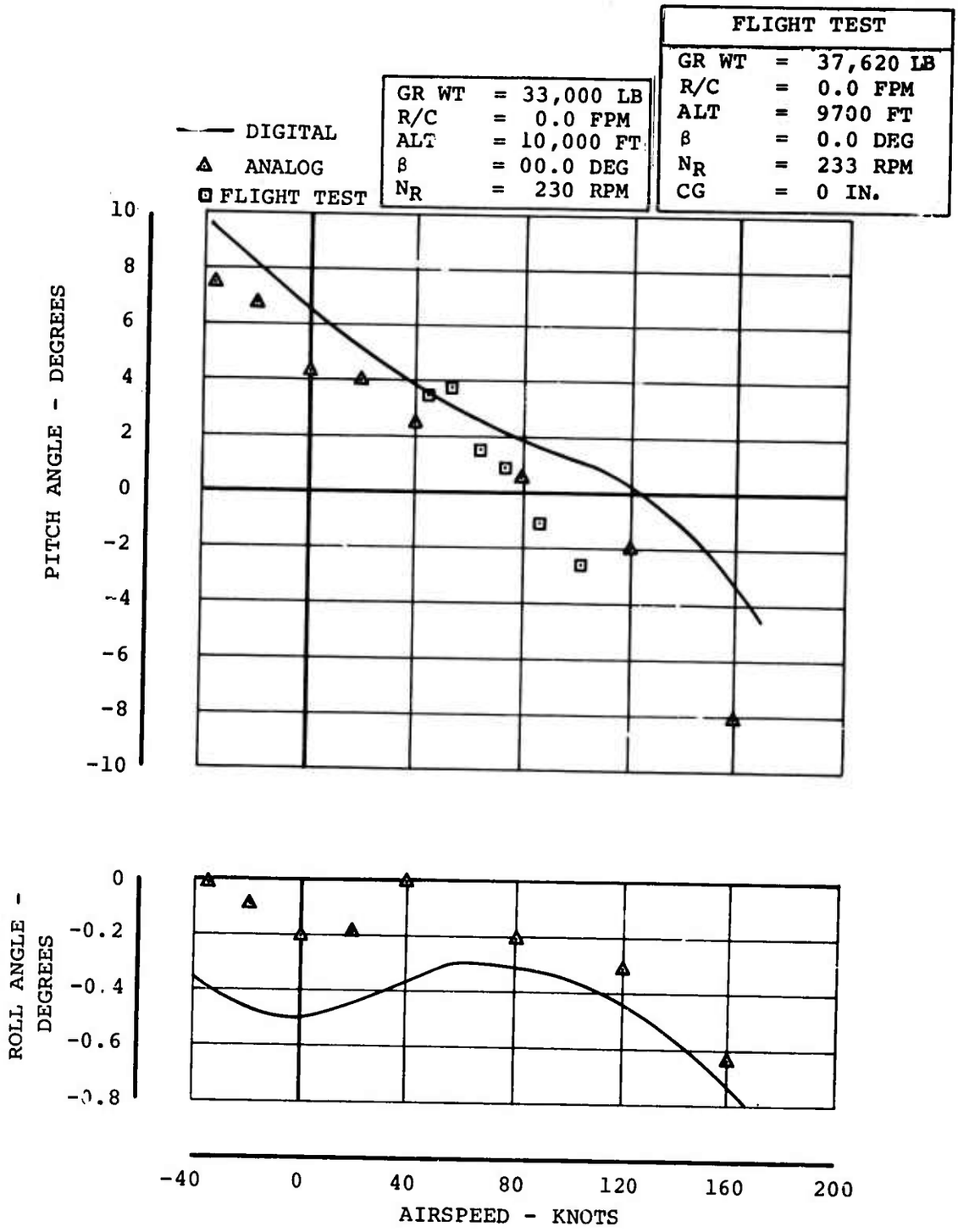

Figure 39. Static Trim Data.

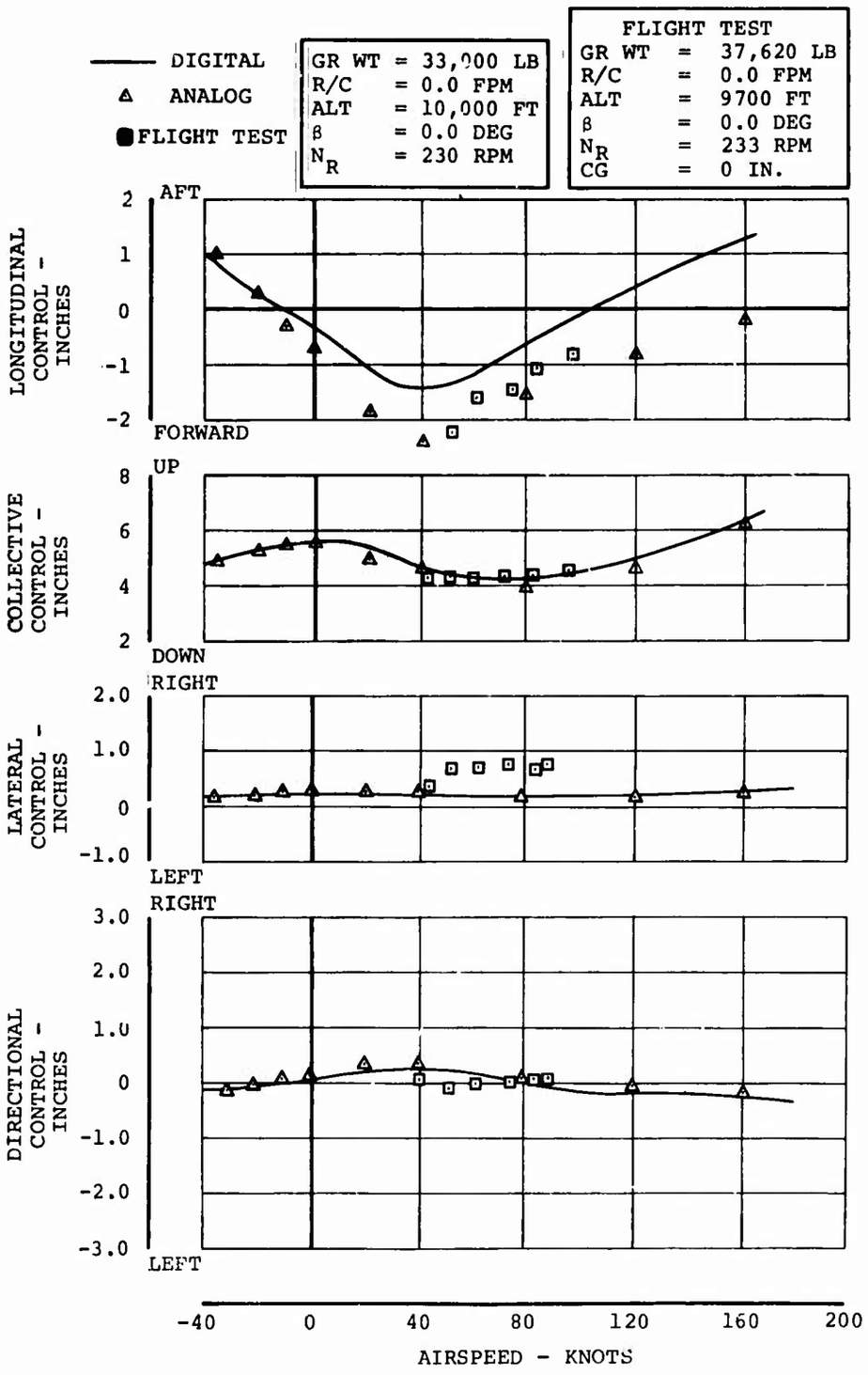

Figure 40. Static Trim Data.

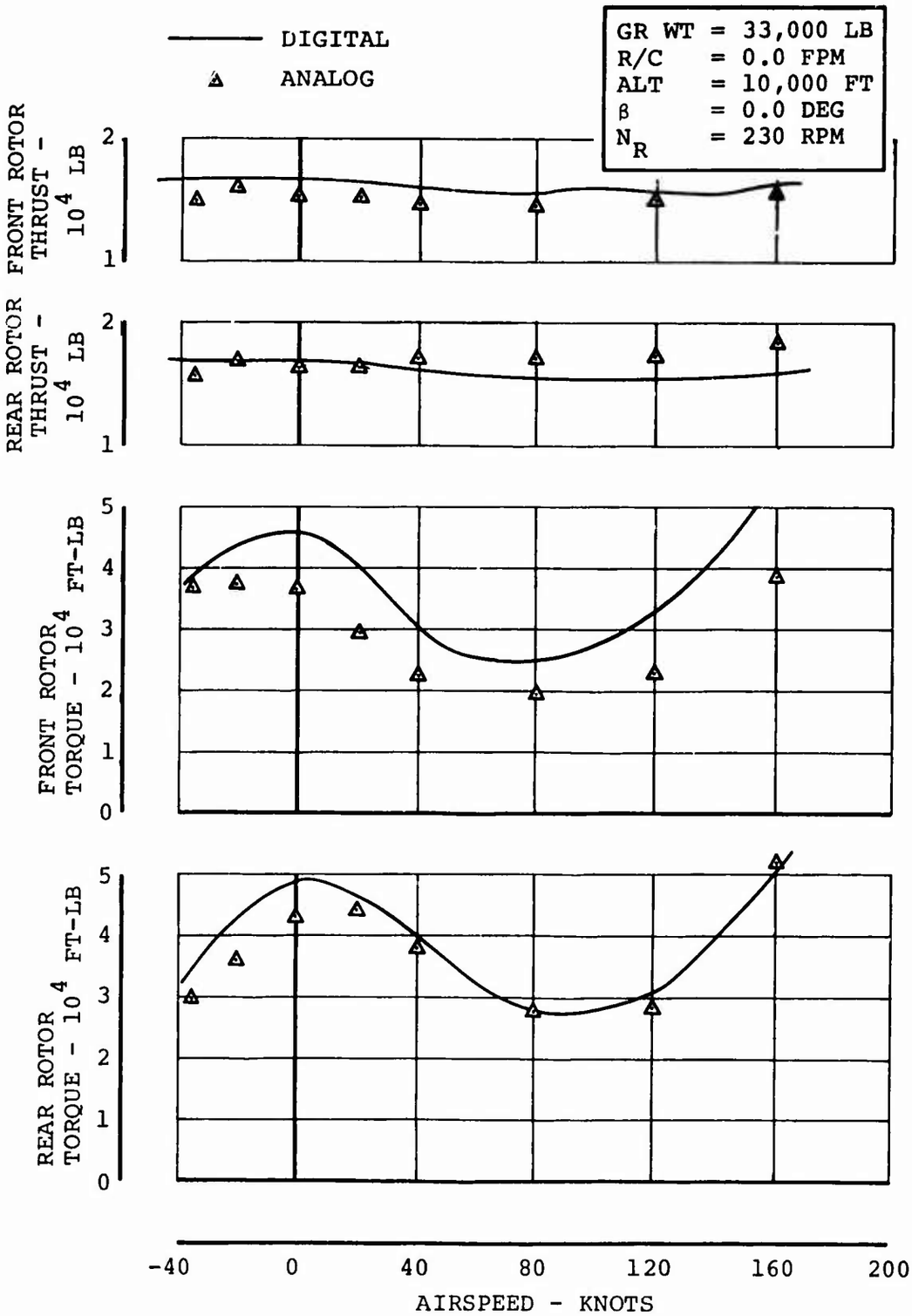

Figure 41. Static Trim Data.

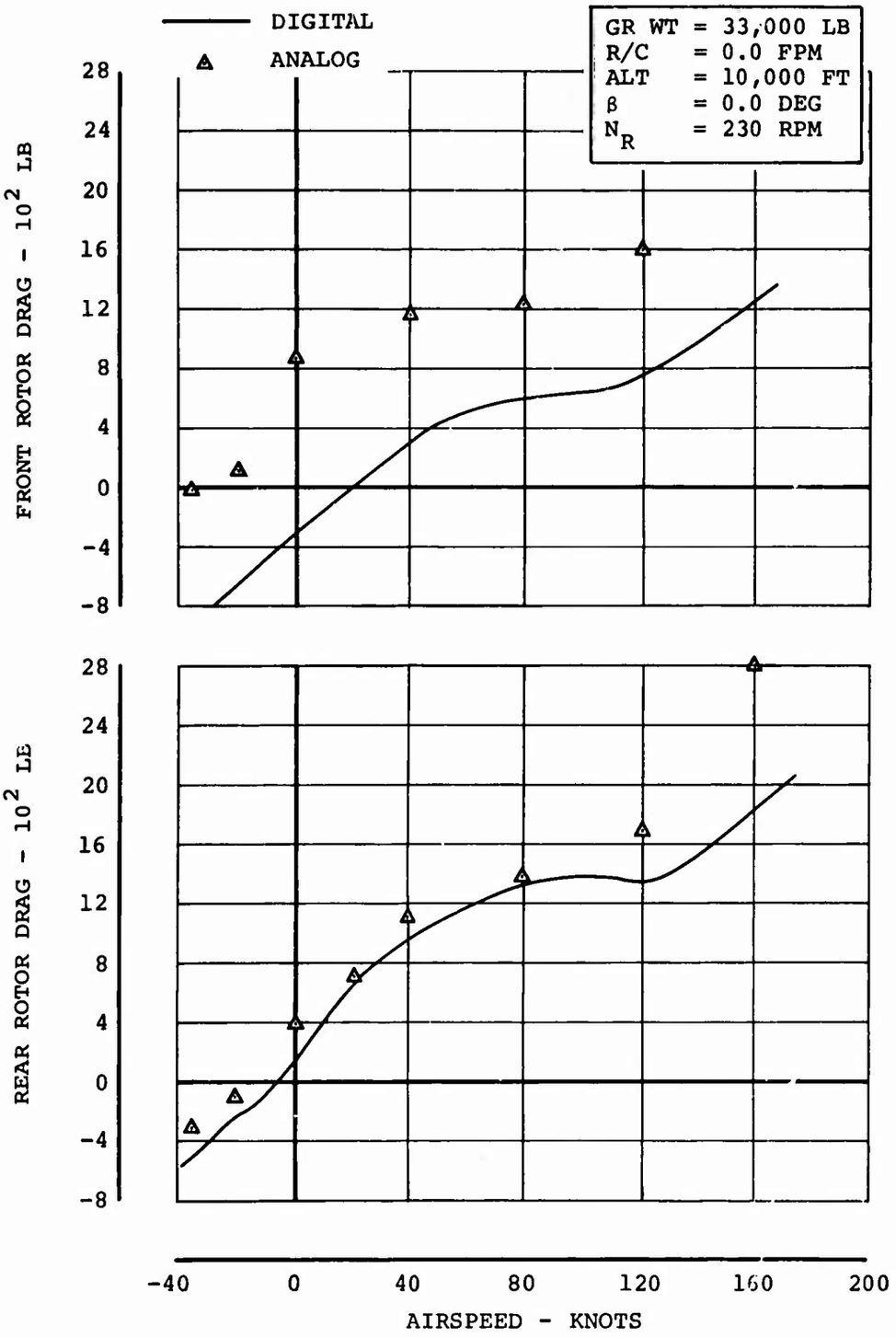

Figure 42. Static Trim Data.

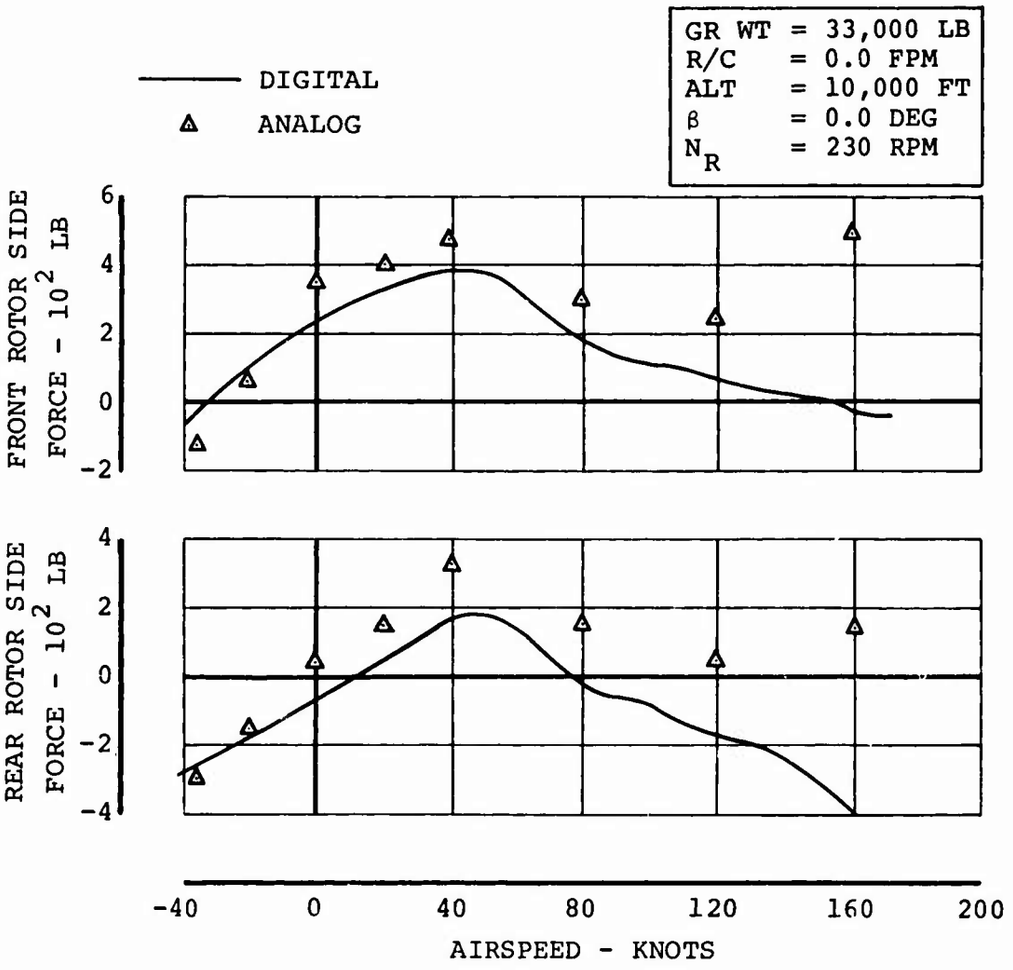

Figure 43. Static Trim Data.

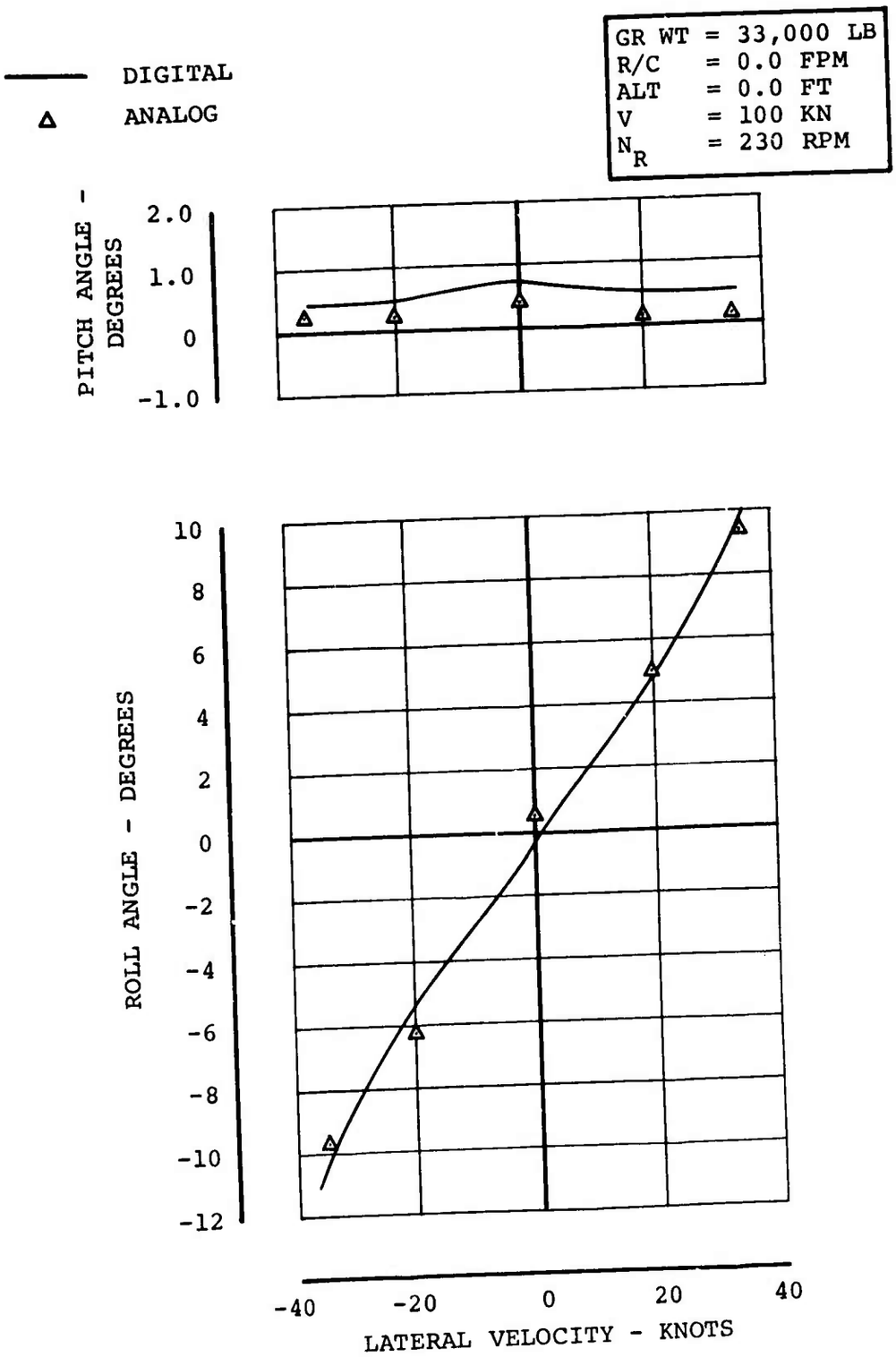

Figure 44. Static Trim Data.

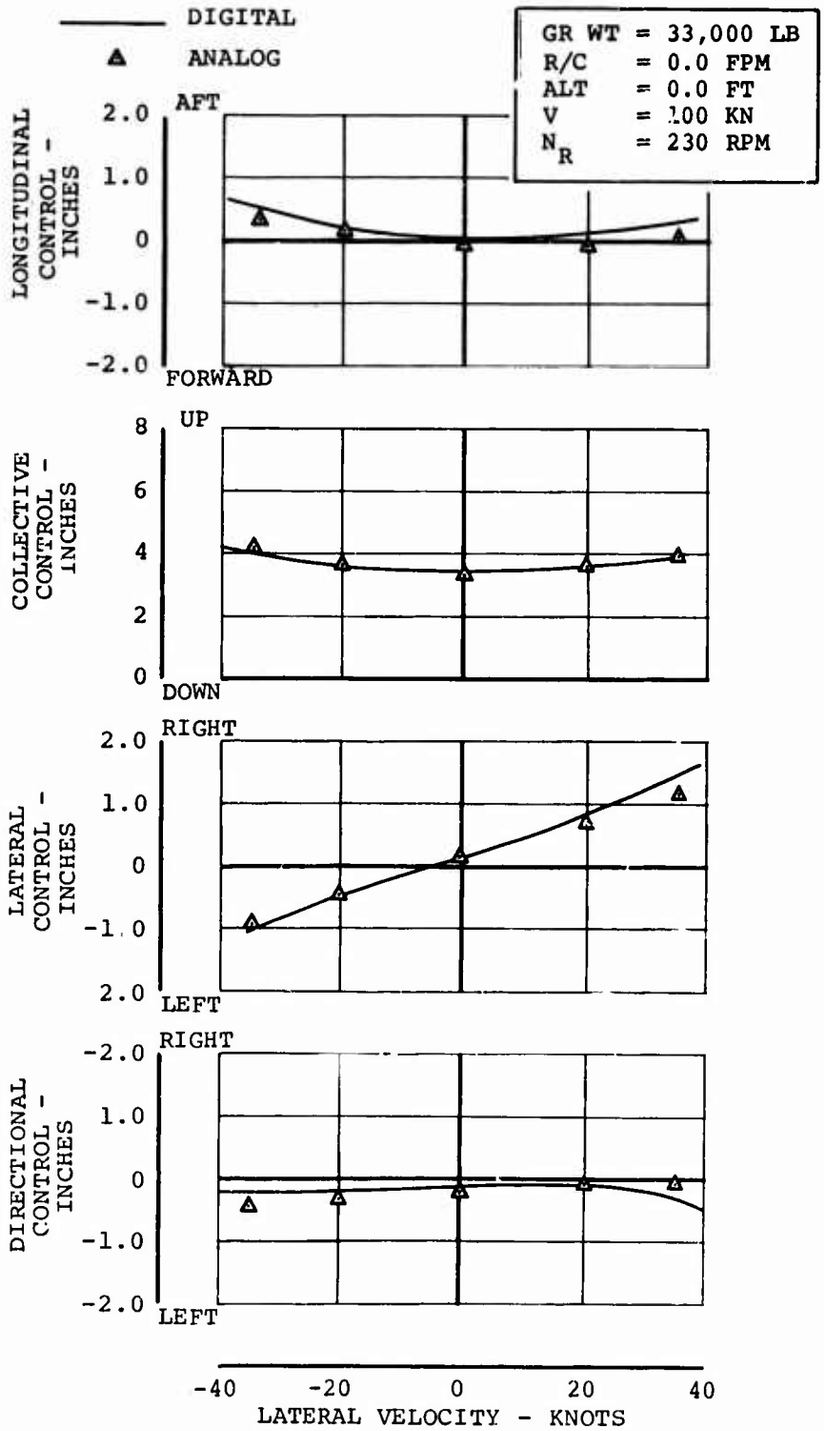

Figure 45. Static Trim Data.

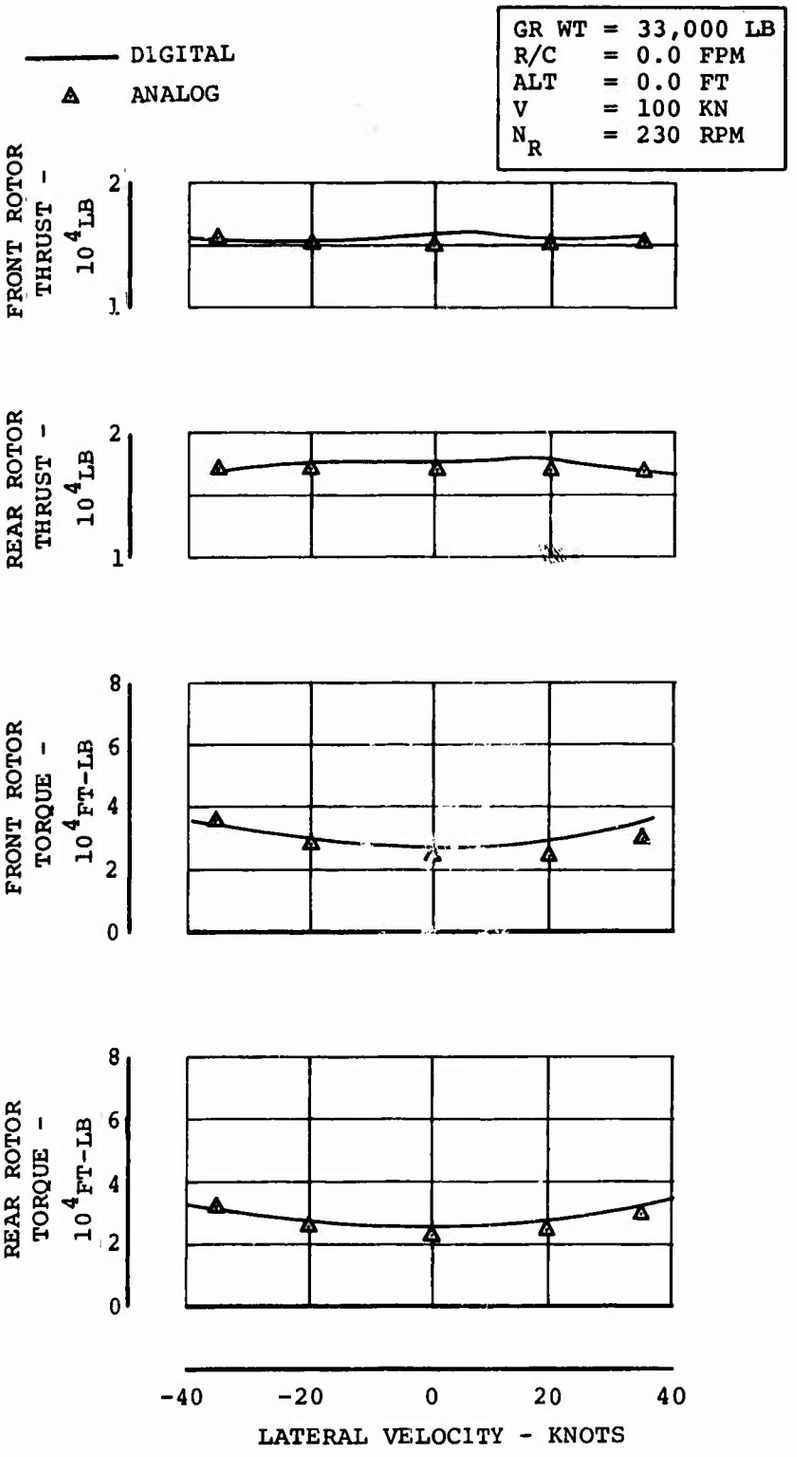

Figure 46. Static Trim Data.

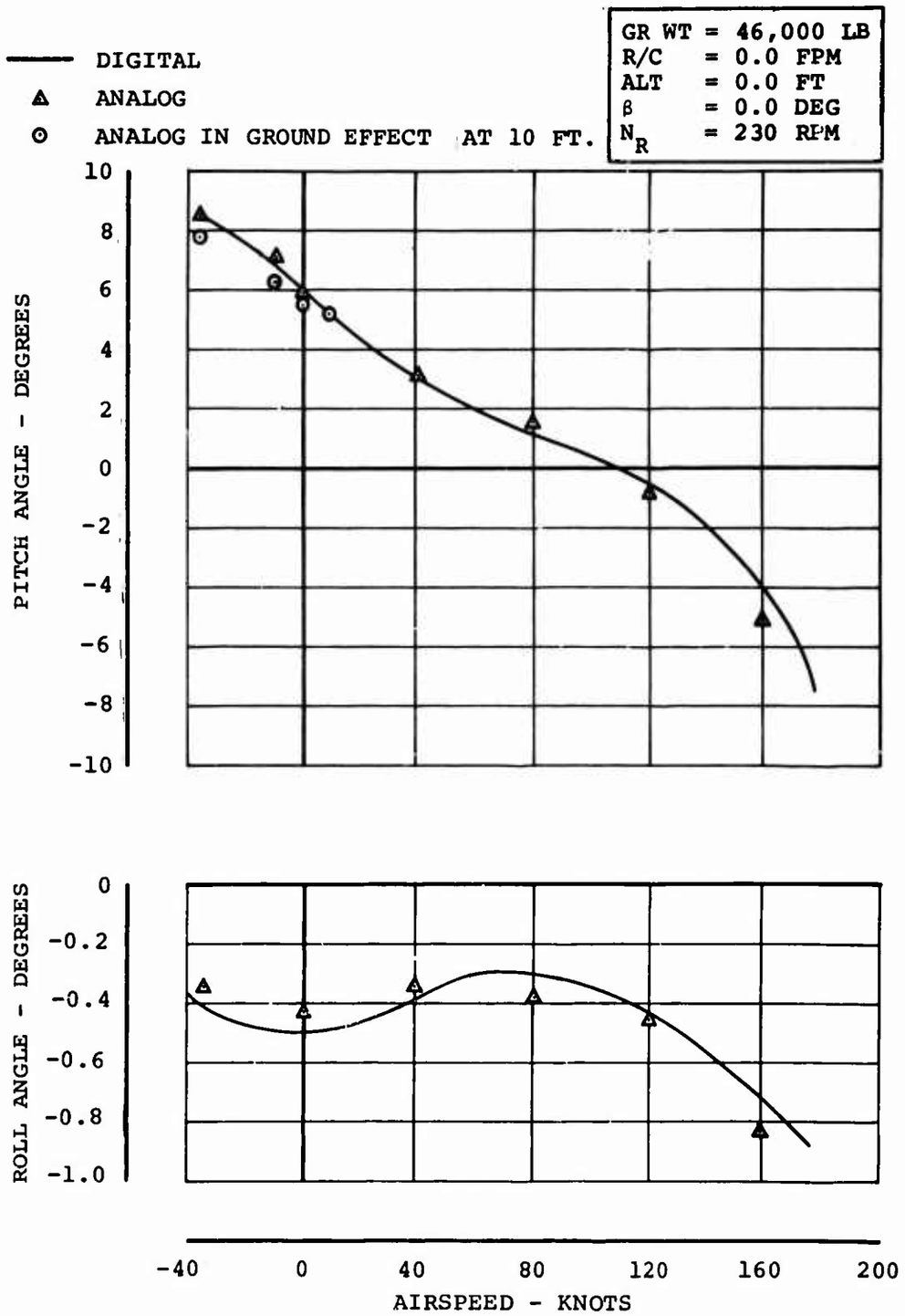

Figure 47. Static Trim Data.

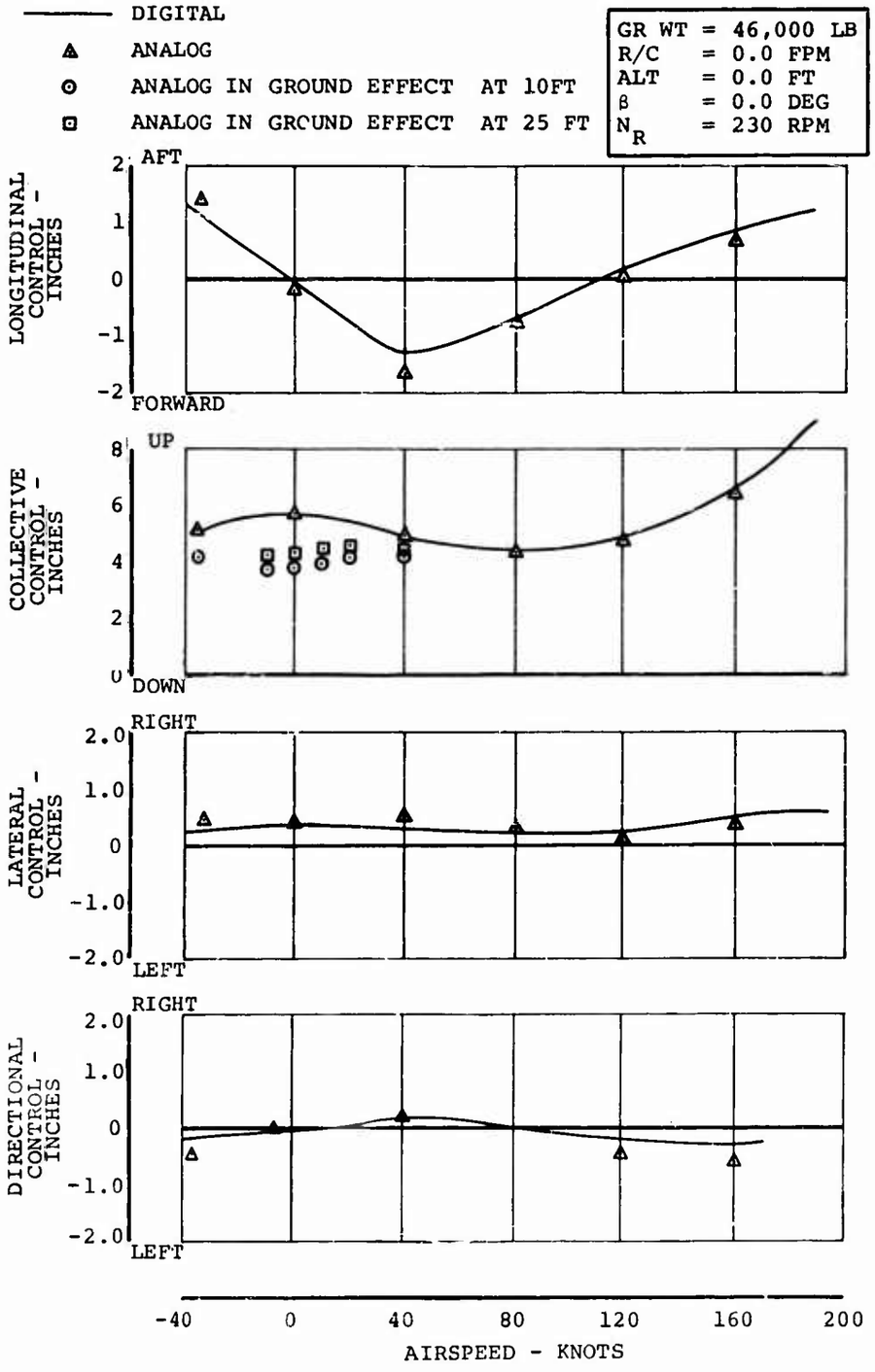

Figure 48. Static Trim Data.

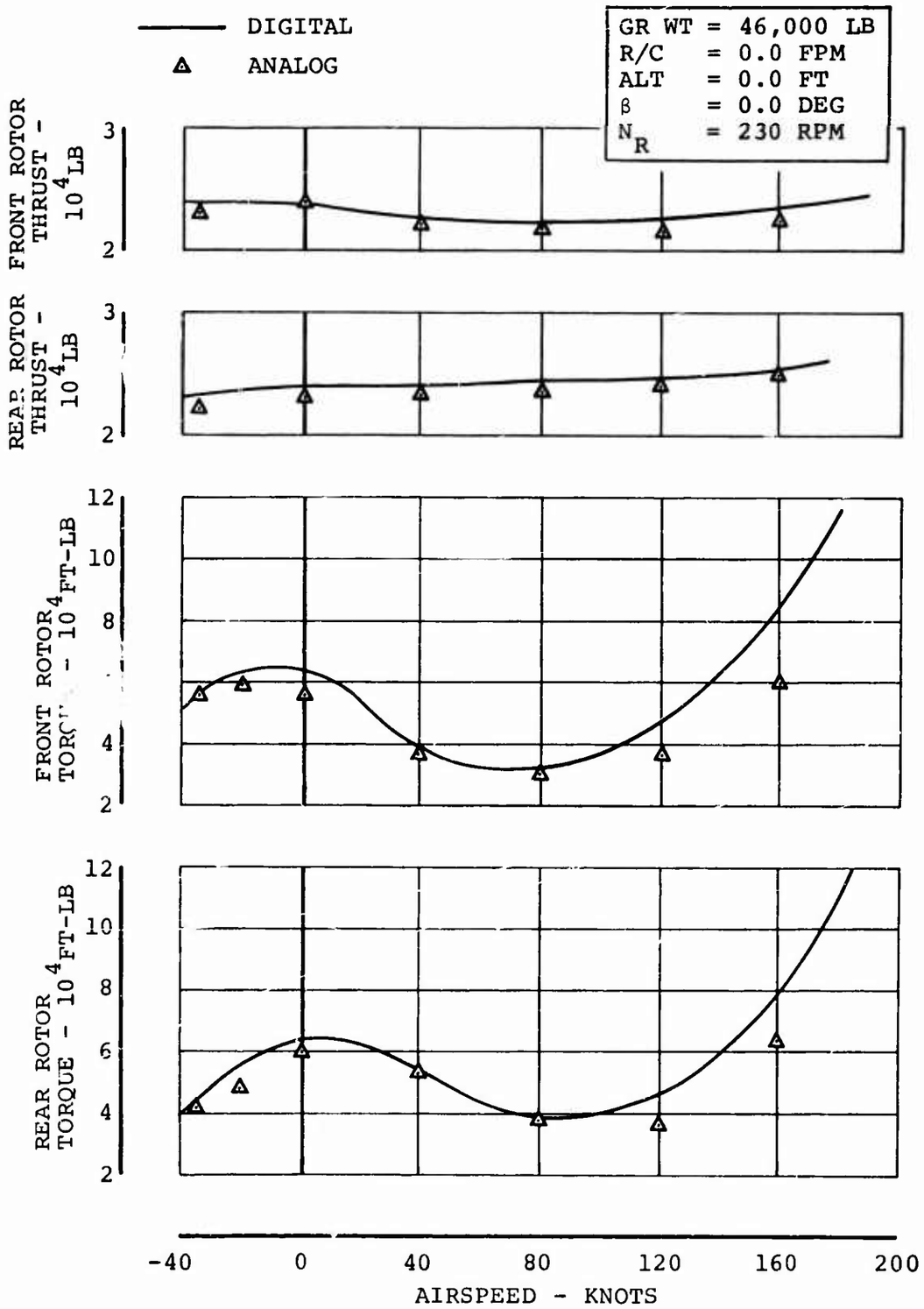

Figure 49. Static Trim Data.

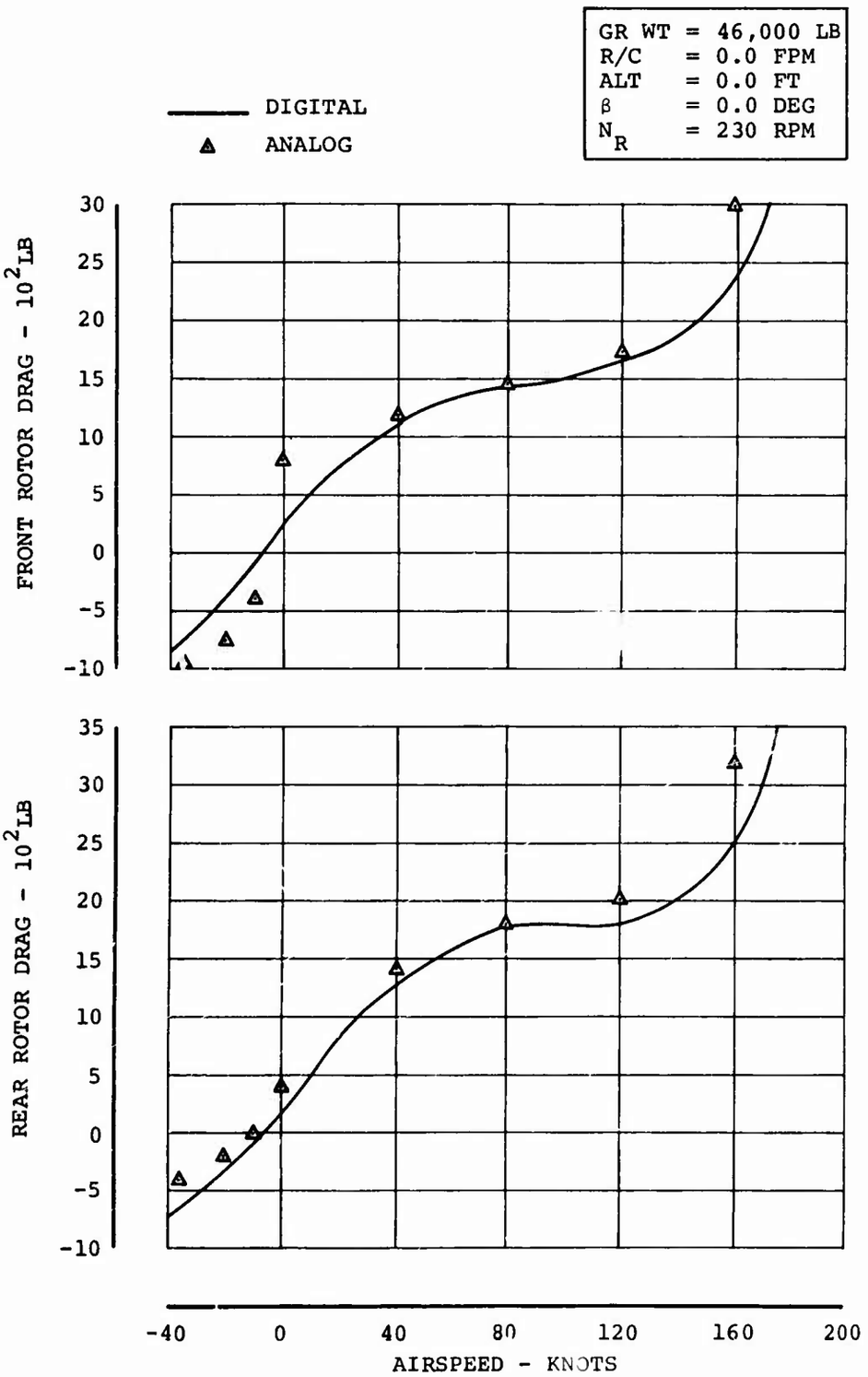

Figure 50. Static Trim Data.

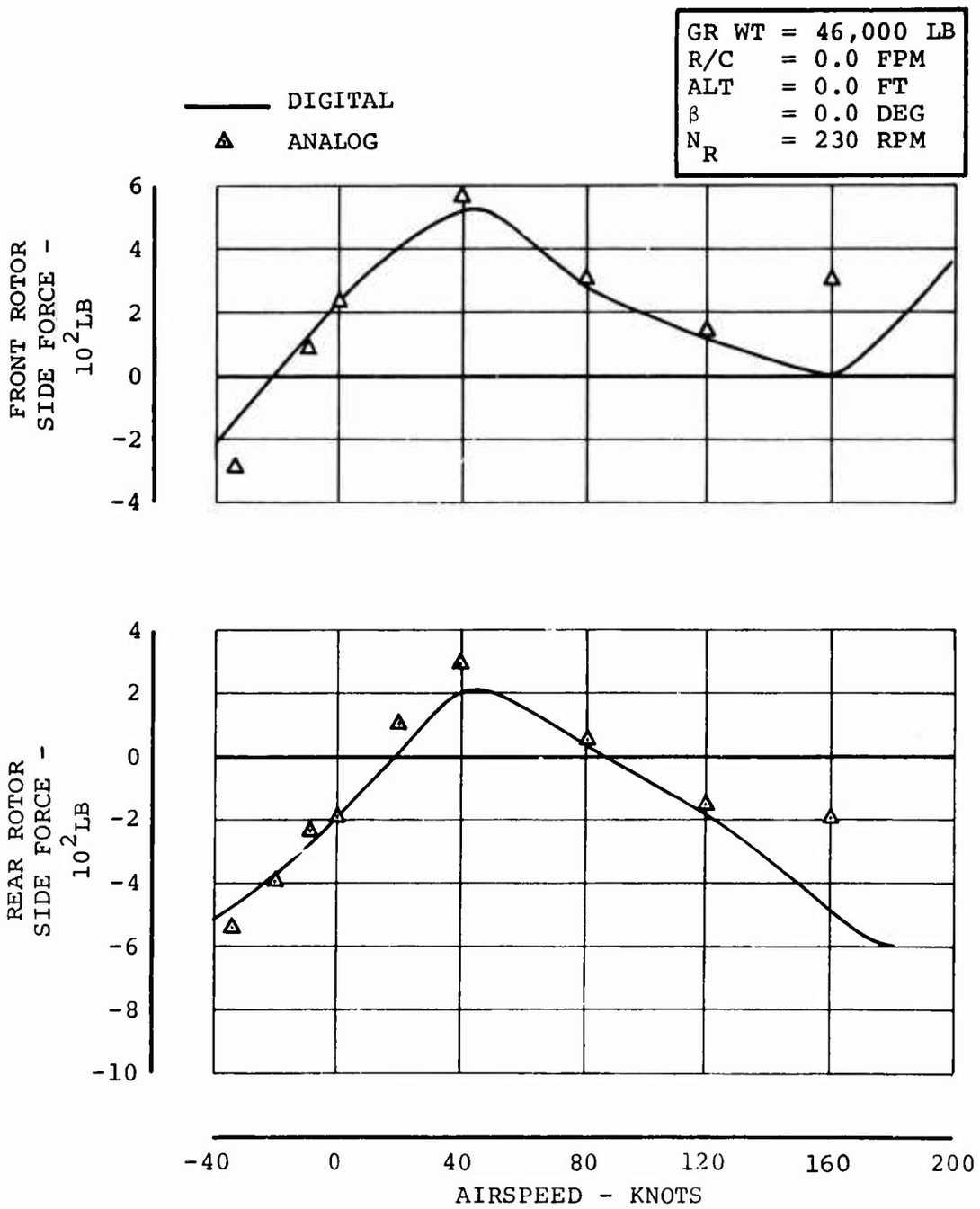

Figure 51. Static Trim Data.

TABLE VII. ISOLATED ROTOR DYNAMICS

Airspeed (kn)	Altitude (ft)	Rotor Speed (rpm)	Angle of Attack (deg)
0.0*	Sea Level	230	-5
100	Sea Level	230	-5
170	Sea Level	230	-5

* Included in this appendix

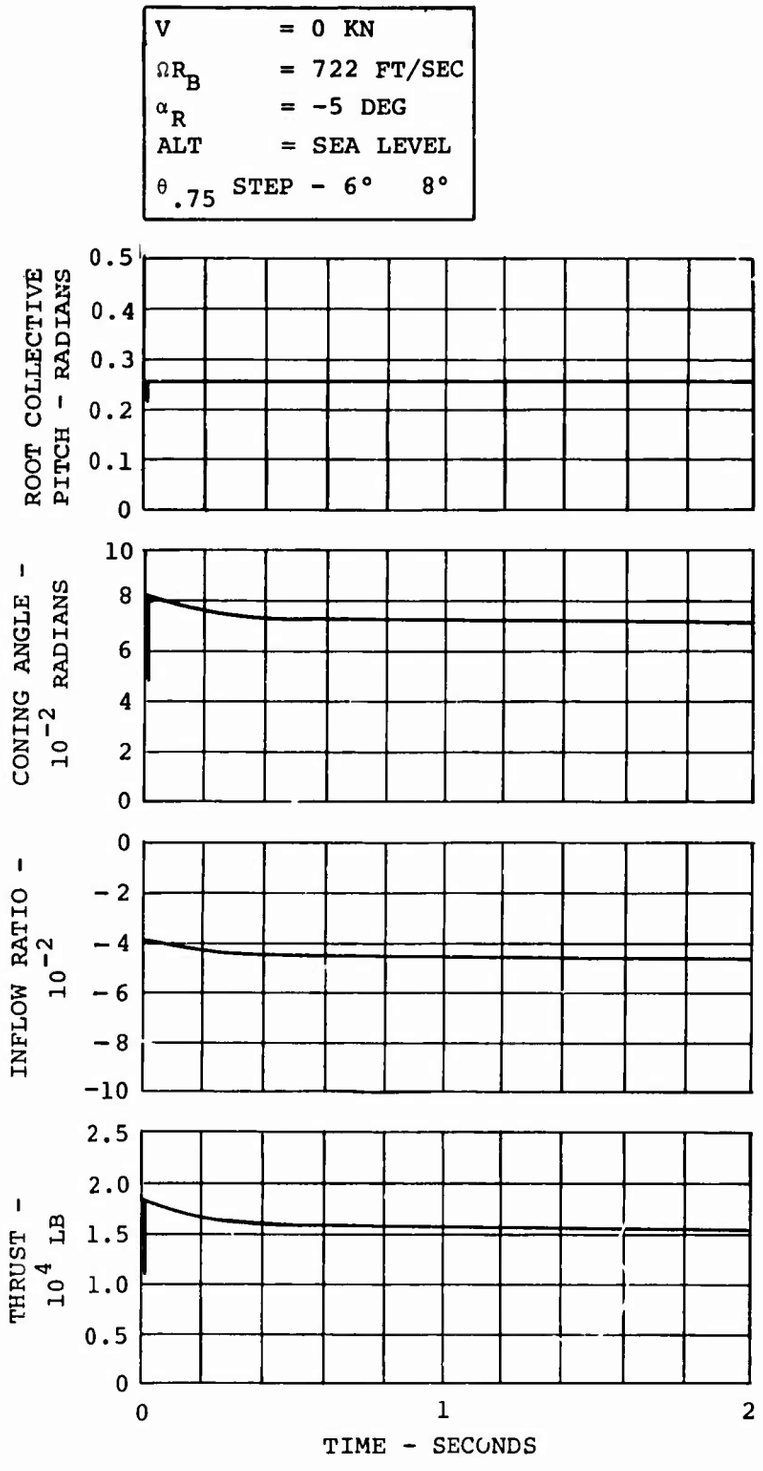

Figure 52. Isolated Rotor Dynamics.

APPENDIX III
UNPILOTED DYNAMIC DATA

Table VIII lists the dynamic data taken for the simulation. The cases which have flight test comparisons and those which are presented in this appendix are indicated. The time histories of the pertinent flight variables are shown for each case. Acquisition and comparison of the data were discussed in the body of this report. The complete dynamic response data package can be found in Reference 3. Eleven responses (Figures 53 through 63) are presented in this appendix.

TABLE VIII. DYNAMIC DATA

Axis	Gross Weight (lb)	Airspeed (kn)	Altitude (ft)	Rotor Speed (rpm)	Pulse Magnitude (in.)	Pulse Duration (sec)
	33,000*+	100	Sea Level	230	+1.0	0.5
	33,000+	132	Sea Level	230	+1.0	0.5
	33,000+	77	10,000	236	-1.0	0.6
Longitudinal	37,000+	74	5,000	235	+0.8	0.5
	37,000*+	127	5,000	236	+1.0	0.5
	37,000+	87	10,000	235	+0.6	0.5
	46,000*+	75	5,000	245	-1.0	0.5
	46,000*+	104	5,000	245	+0.8	0.5
	46,000+	70	8,000	245	+0.8	0.5
Collective	33,000*	100	Sea Level	230	+1.0	Step
	46,000	100	Sea Level	230	+0.5	Step
	33,000*+	35	Sea Level	230	+2.0	0.6
Lateral	33,000	100	Sea Level	230	+1.0	3.0
	37,000+	87	10,000	236	+2.0	0.5
	46,000*+	35	2,000	244	-1.5	0.5
	33,000	0.0	Sea Level	230	+1.0	0.5
Directional	33,000	100	Sea Level	230	+1.0	0.5
	37,000*+	35	10,000	234	+1.6	1.0
SAS Failures	33,000*+	100	Sea Level	230		
SAS Off	33,000	100	Sea Level	230		
Single Engine Failure	33,000*+	115	2,000	225		

* Included in this appendix

\+ Flight test correlation

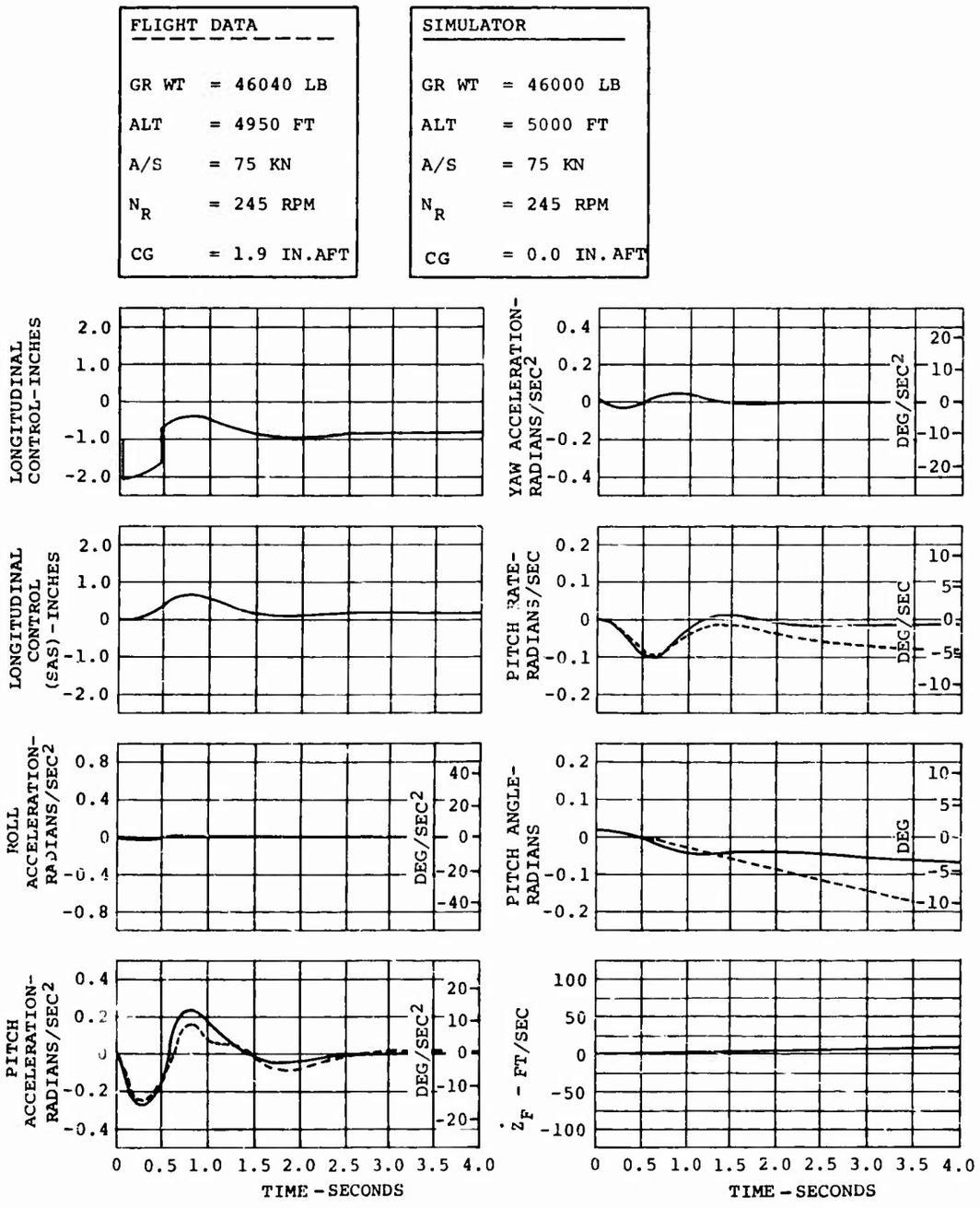

Figure 53. Dynamic Responses - Longitudinal Pulse.

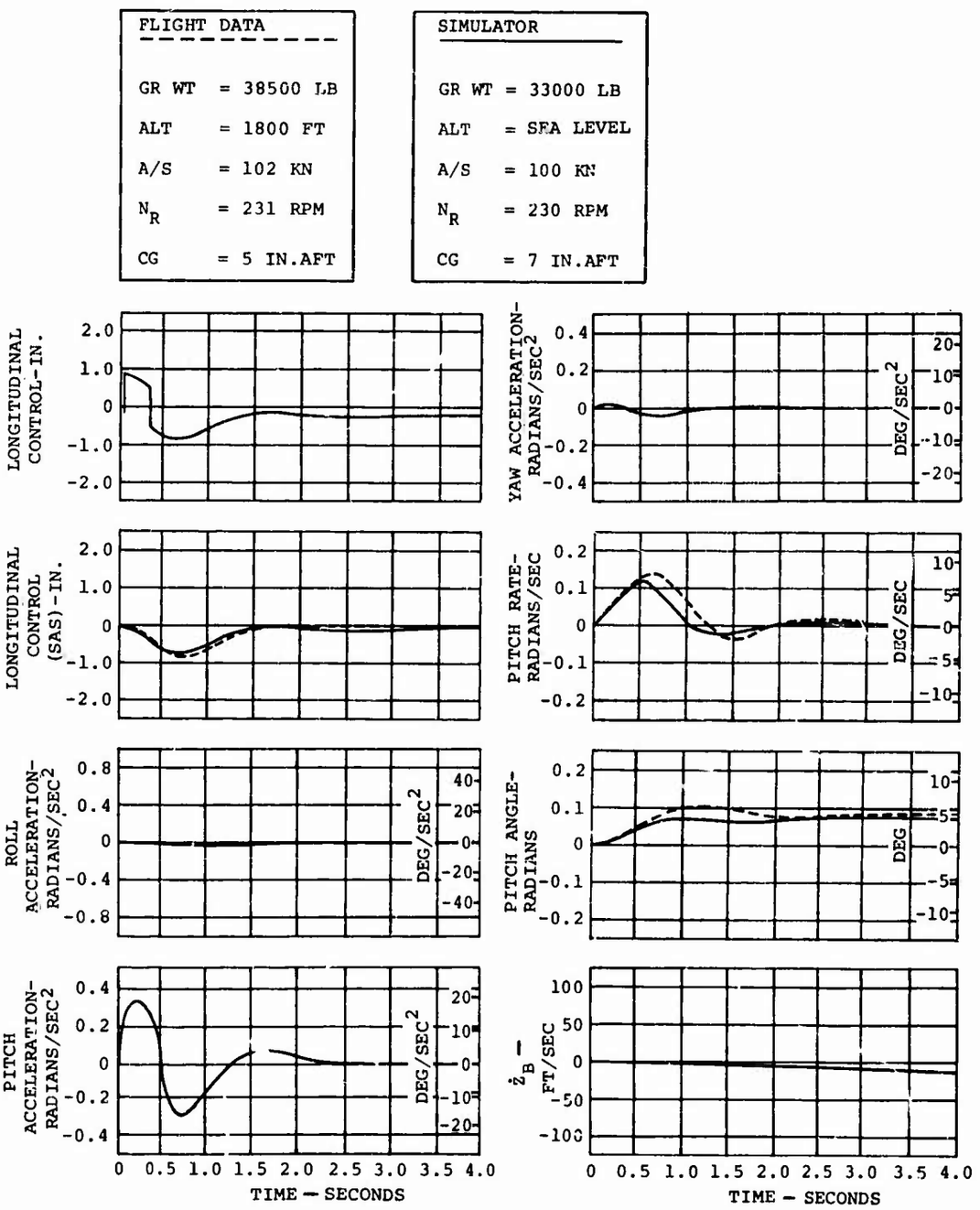

Figure 54. Dynamic Responses - Longitudinal Pulse.

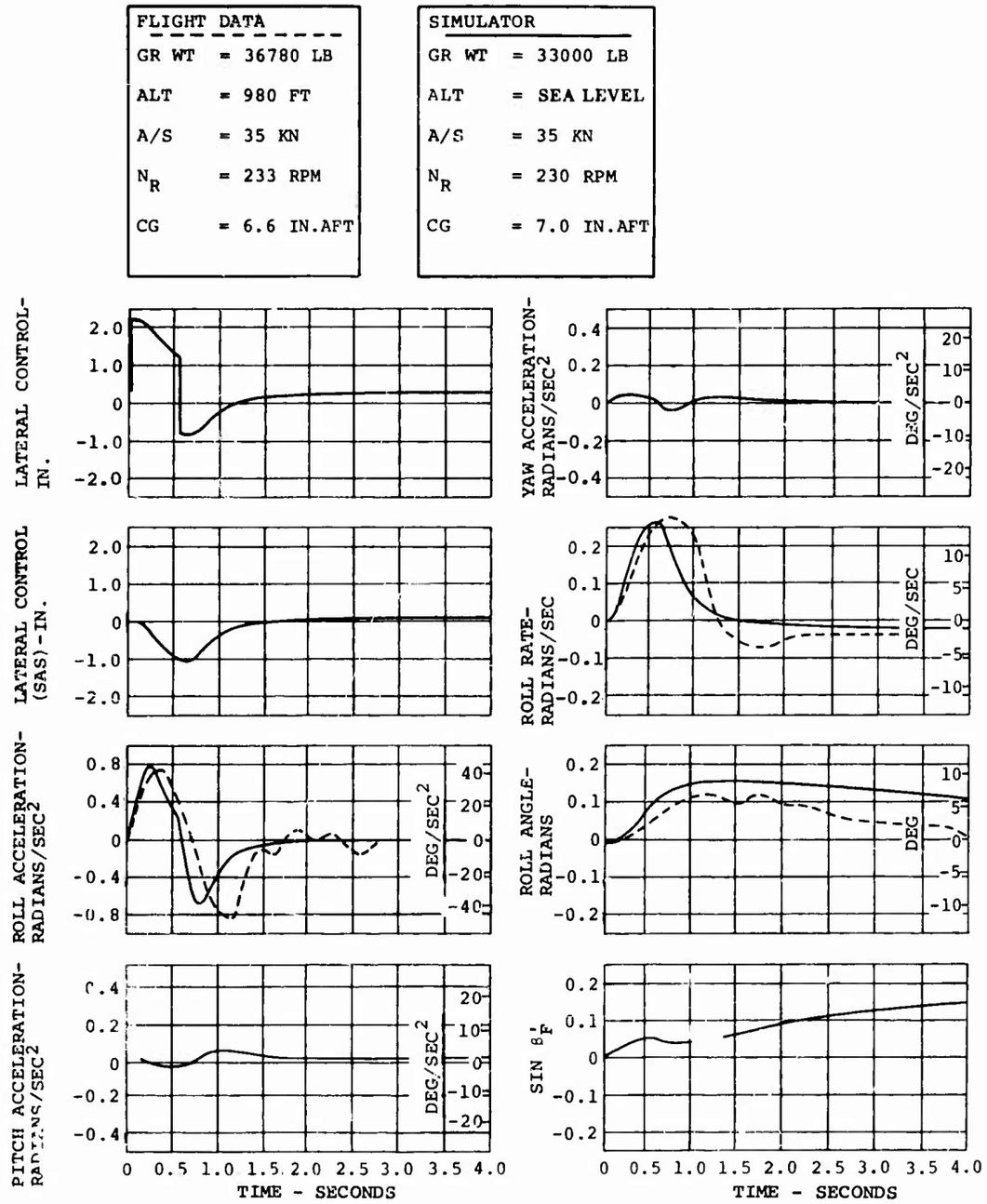

Figure 55. Dynamic Responses - Lateral Pulse.

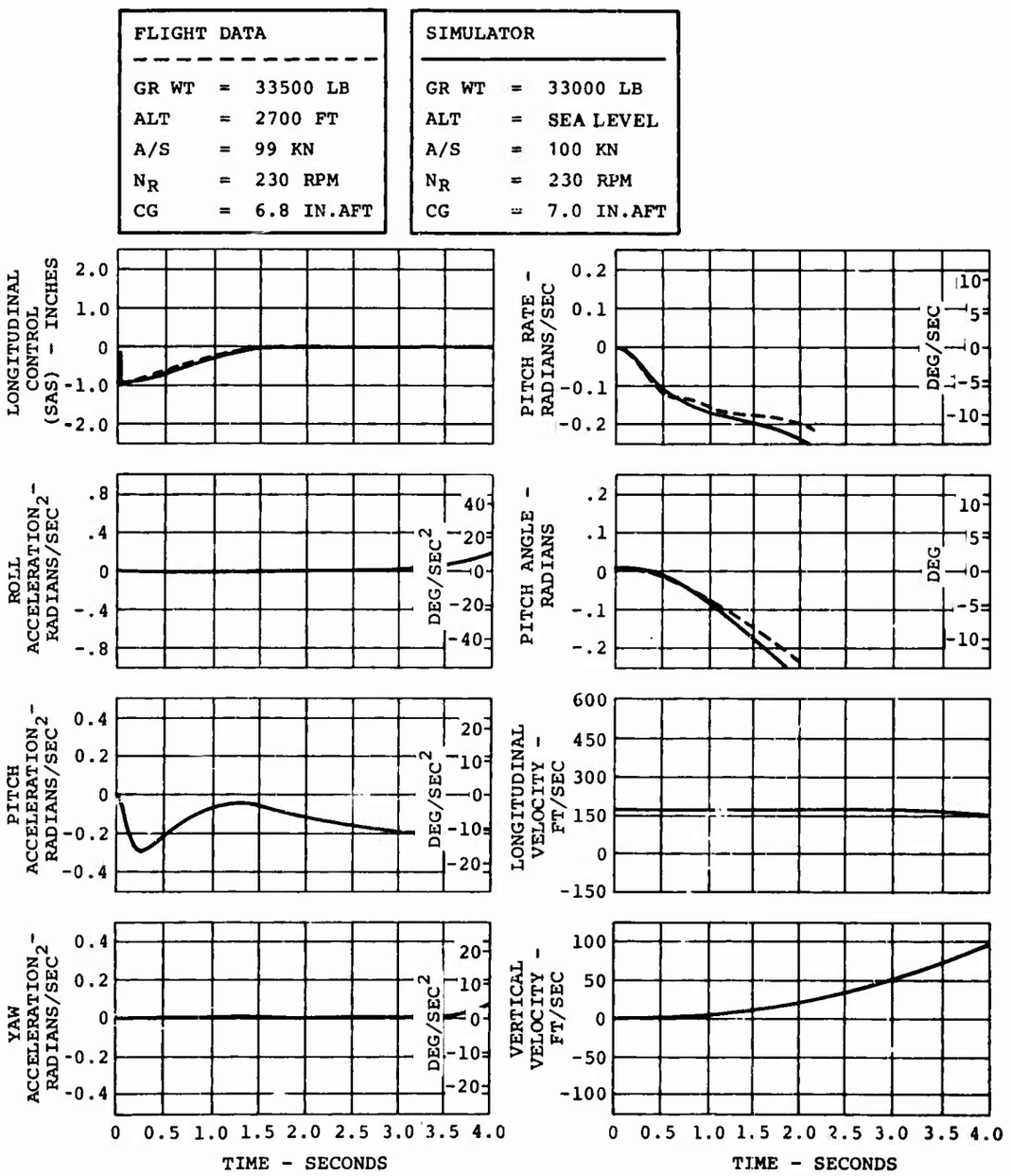

Figure 56. Dynamic Responses - Pitch SAS Failure.

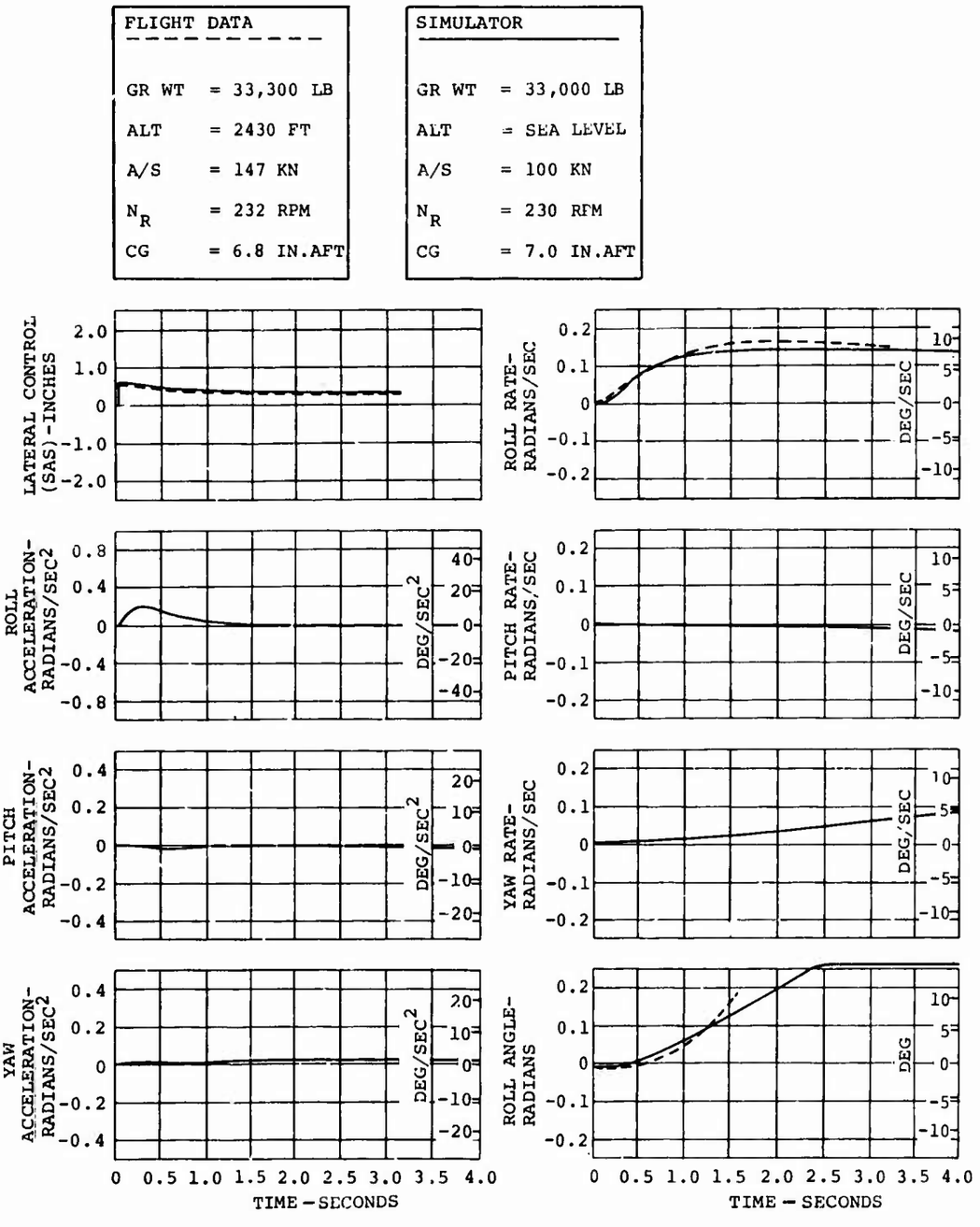

Figure 57. Dynamic Responses - Roll SAS Failure.

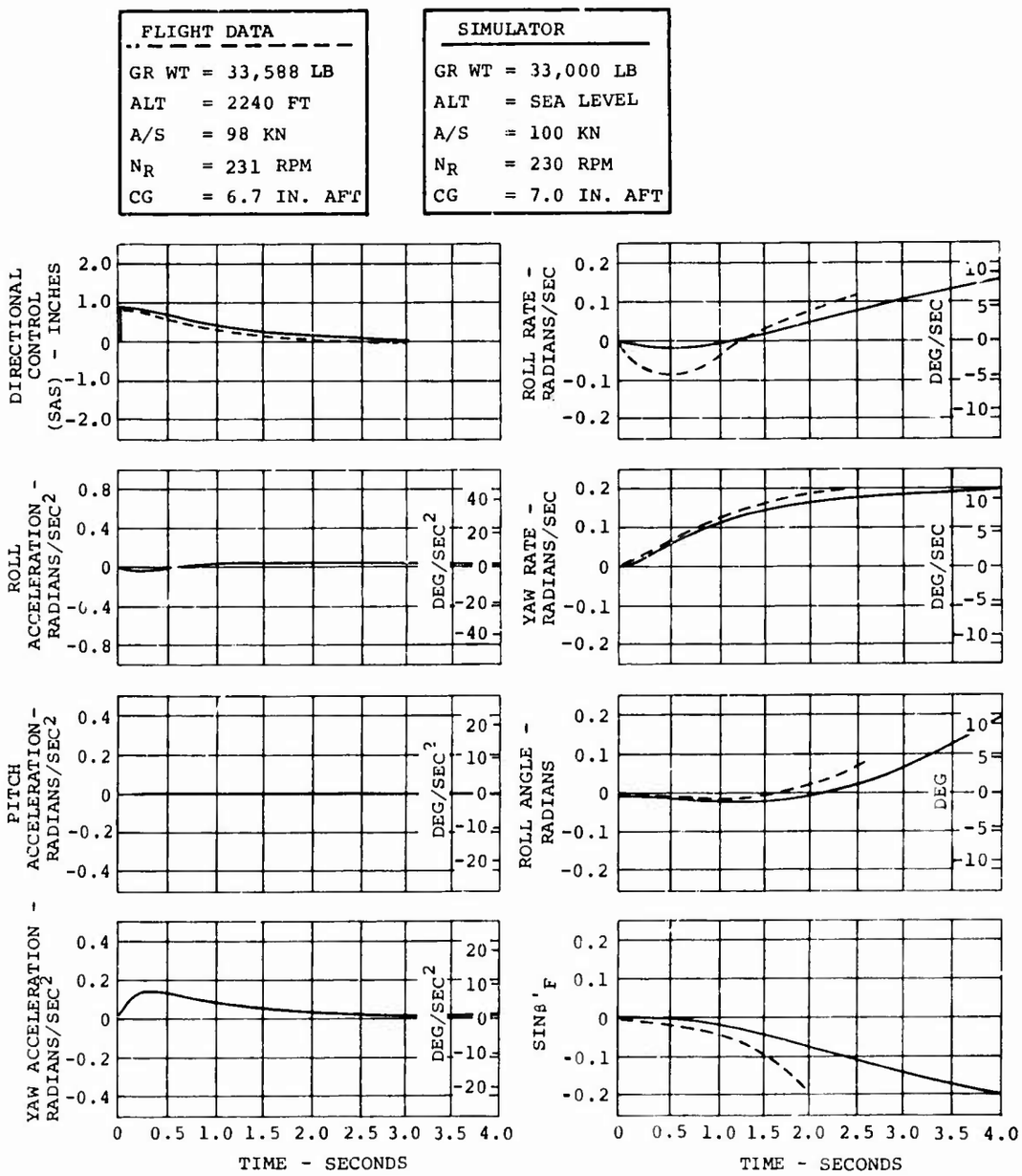

Figure 58. Dynamic Responses - Yaw SAS Failure.

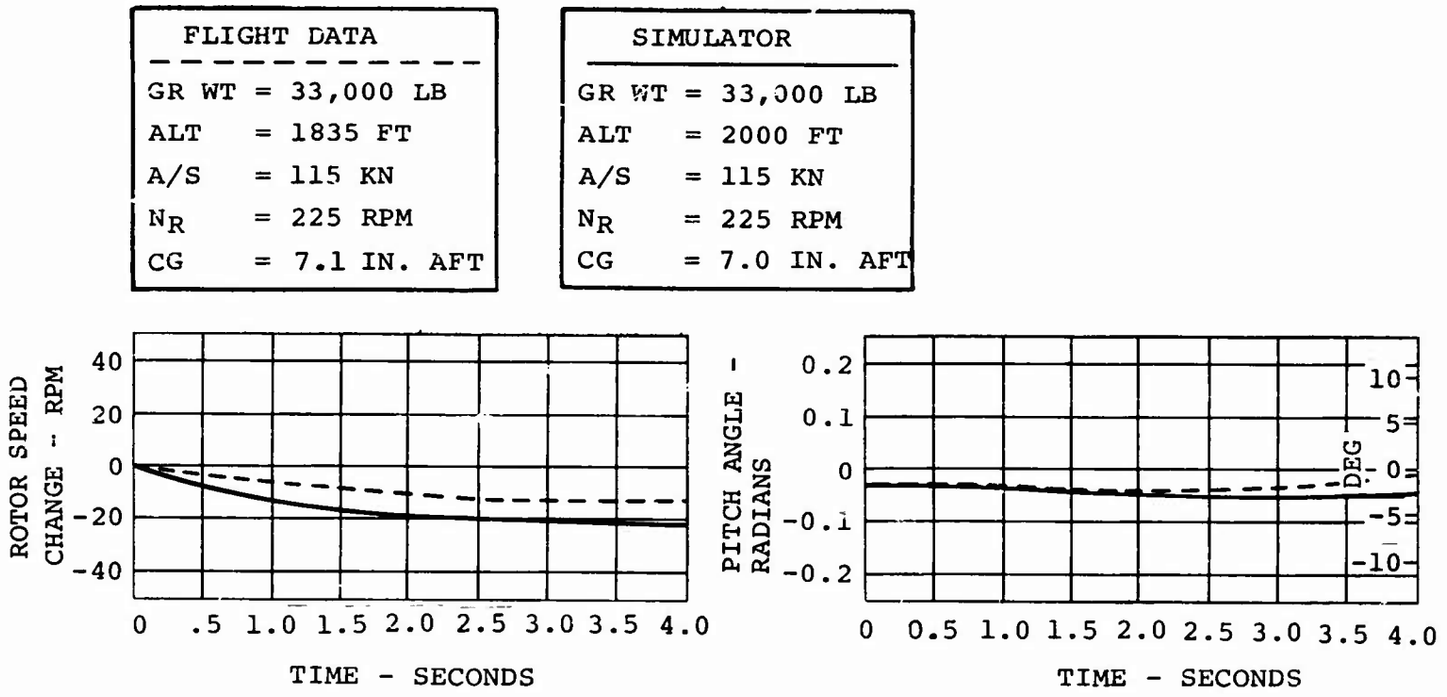

Figure 59. Dynamic Responses - Single-Engine Failure.

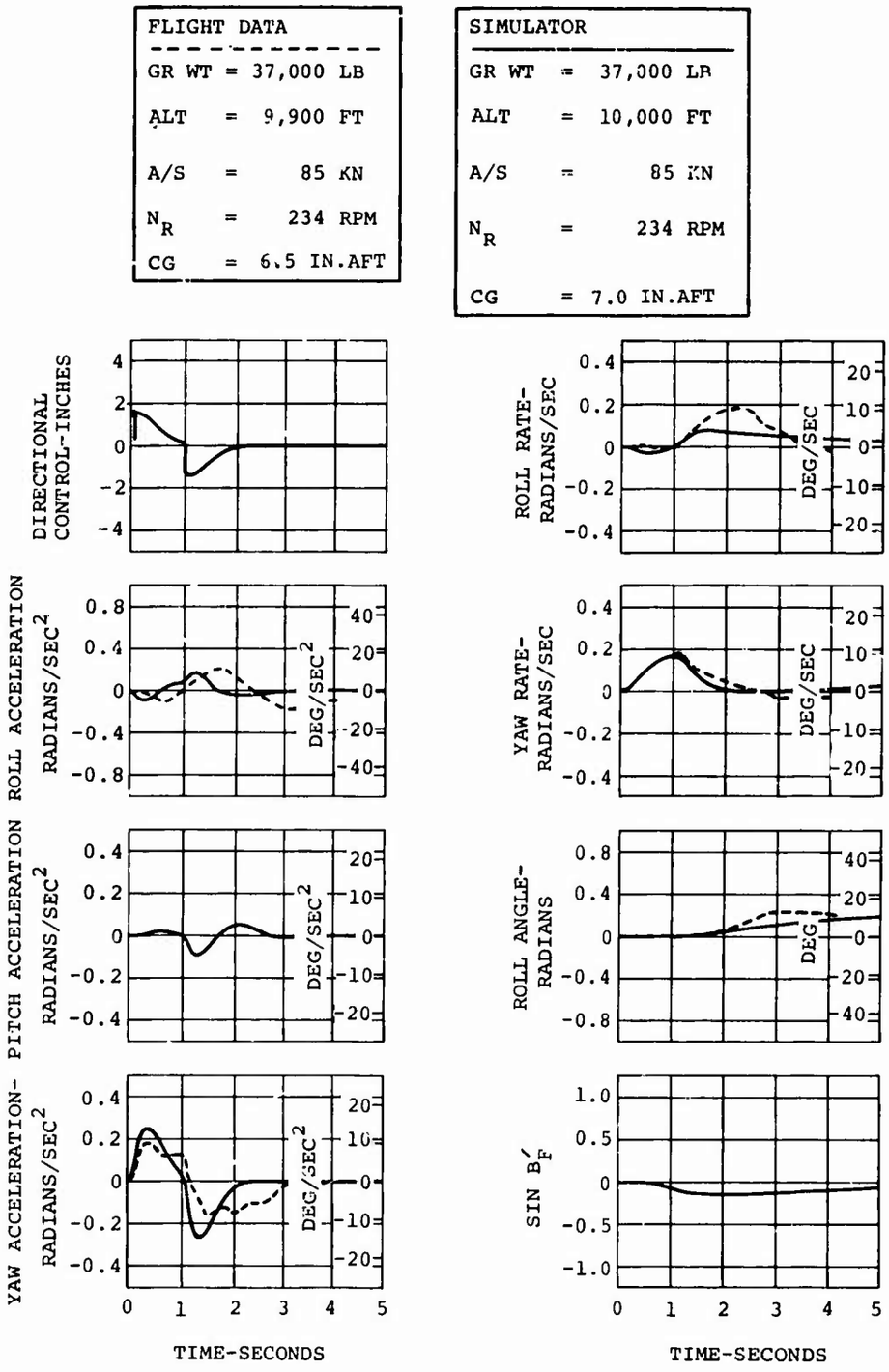

Figure 60. Dynamic Responses-Directional Pulse.

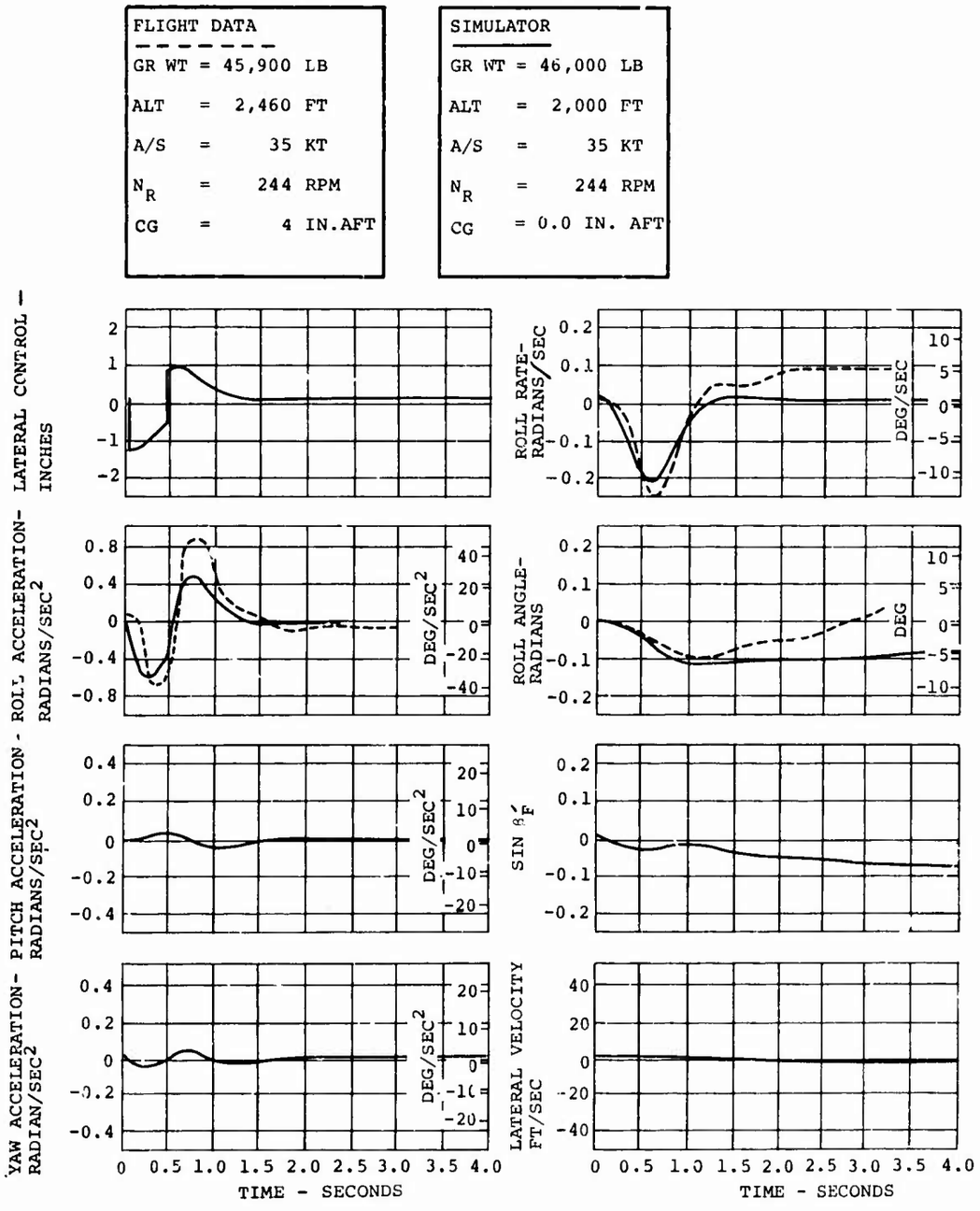

Figure 61. Dynamic Responses-Lateral Pulse.

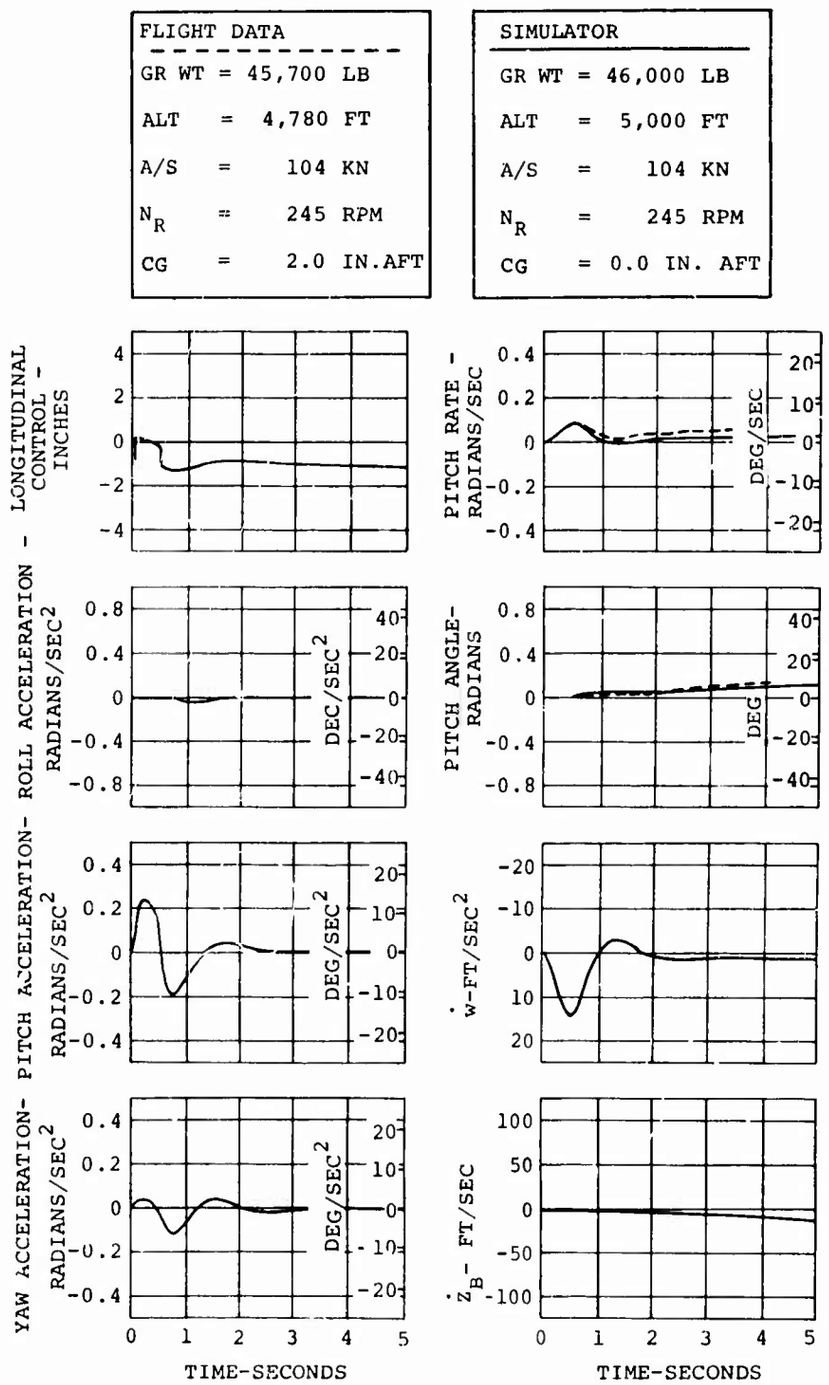

Figure 62. Dynamic Responses-Longitudinal Pulse.

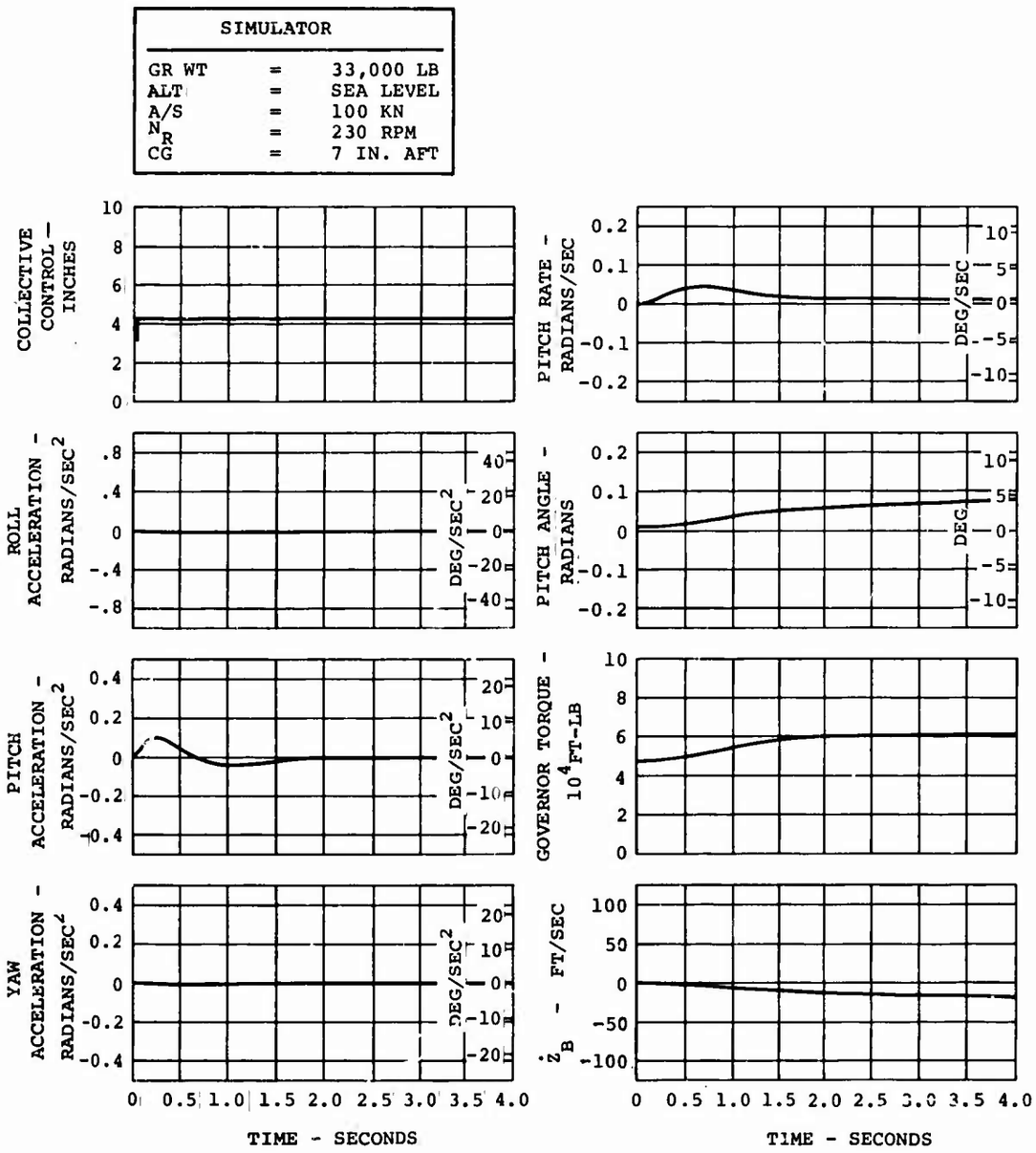

Figure 63. Dynamic Responses - Collective Step.

APPENDIX IV
PILOT VALIDATION DATA

Table IX lists the data recorded during the pilot validation of the simulation with the conventional control system. The cases having flight test comparisons and those presented in this appendix are indicated. Pilot validation with the conventional control system was discussed in the body of this report. The complete data package can be found in Reference 3. Sixteen cases (Figures 64 through 79) are included in this appendix.

TABLE IX. PILOT CONVENTIONAL VALIDATION

Maneuver	Gross Weight (lb)	Trim Airspeed (kn)	Altitude (ft)	Rotor Speed (rpm)
	33,000	0.0	Sea Level	235
	33,000*+	70	2,000	235
Pitch SAS Failure	33,000	130	2,000	235
	33,000	150	2,000	235
	33,000	0.0	Sea Level	235
Roll SAS Failure	33,000	70	2,000	235
	33,000*+	130	2,000	235
	33,000	0.0	Sea Level	235
Yaw SAS Failure	33,000*+	70	2,000	235
	33,000	130	2,000	235
Steady Sideslip				
10KN Lateral Velocity	33,000	80	2,000	235
20KN Lateral Velocity	33,000	80	2,000	235
30KN Lateral Velocity	33,000	80	2,000	235
10KN Lateral Velocity	33,000	150	2,000	235
20KN Lateral Velocity	33,000	150	2,000	235
Hover at 10 Degrees Nose Down IGE	33,000*		300	230
Hover at 10 Degrees Nose Up IGE	33,000		300	230
Hover to Forward Flt IGE	33,000*		300	230
Hover to Rearward Flt IGE	33,000		300	230
Forward Flt at 10 Degrees Nose Down	33,000*	100	500	230
Forward Flt at 10 Degrees Nose Up	33,000	100	500	230
Acceleration	33,000*	100	500	230
Deceleration	33,000*	100	500	230
Autorotation	33,000*		500	230
Climb	33,000*		500	230
Spot Turn	33,000*	0.0	500	230

TABLE IX - Continued

Maneuver	Gross Weight (lb)	Trim Airspeed (kn)	Altitude (ft)	Rotor Speed (rpm)
SAS Off	33,000*	70	500	230
SAS On	33,000*	70	500	230
Light Turbulence	33,000	120	500	230
Moderate Turbulence	33,000	120	500	230
Heavy Turbulence	33,000*	120	500	230
Lateral Start-Stop	33,000	120	500	230
	33,000*	0.0	300	230

* Included in this appendix

\+ Flight test correlation

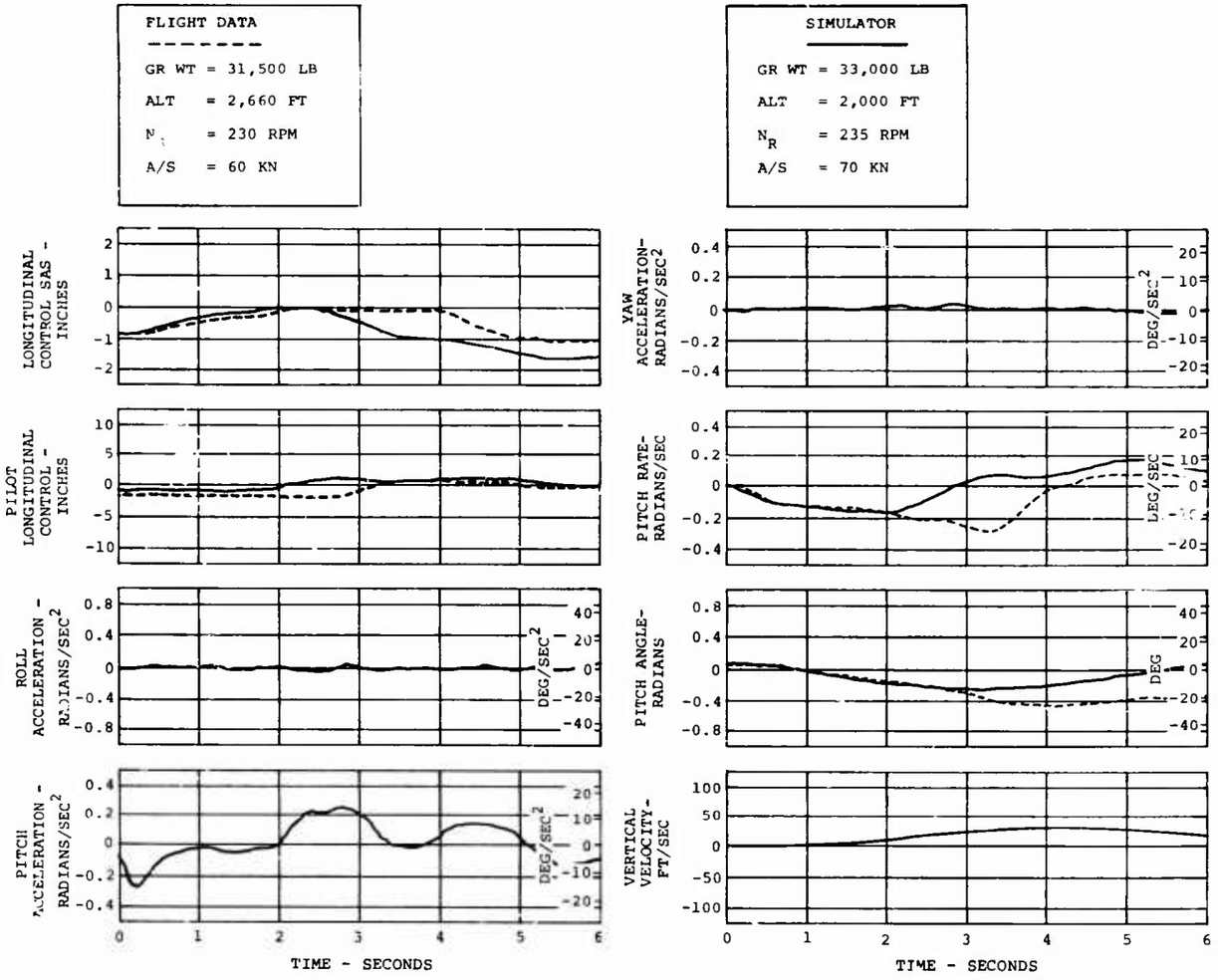

Figure 64. Pilot Validation - Conventional Control System (Pitch SAS Failure).

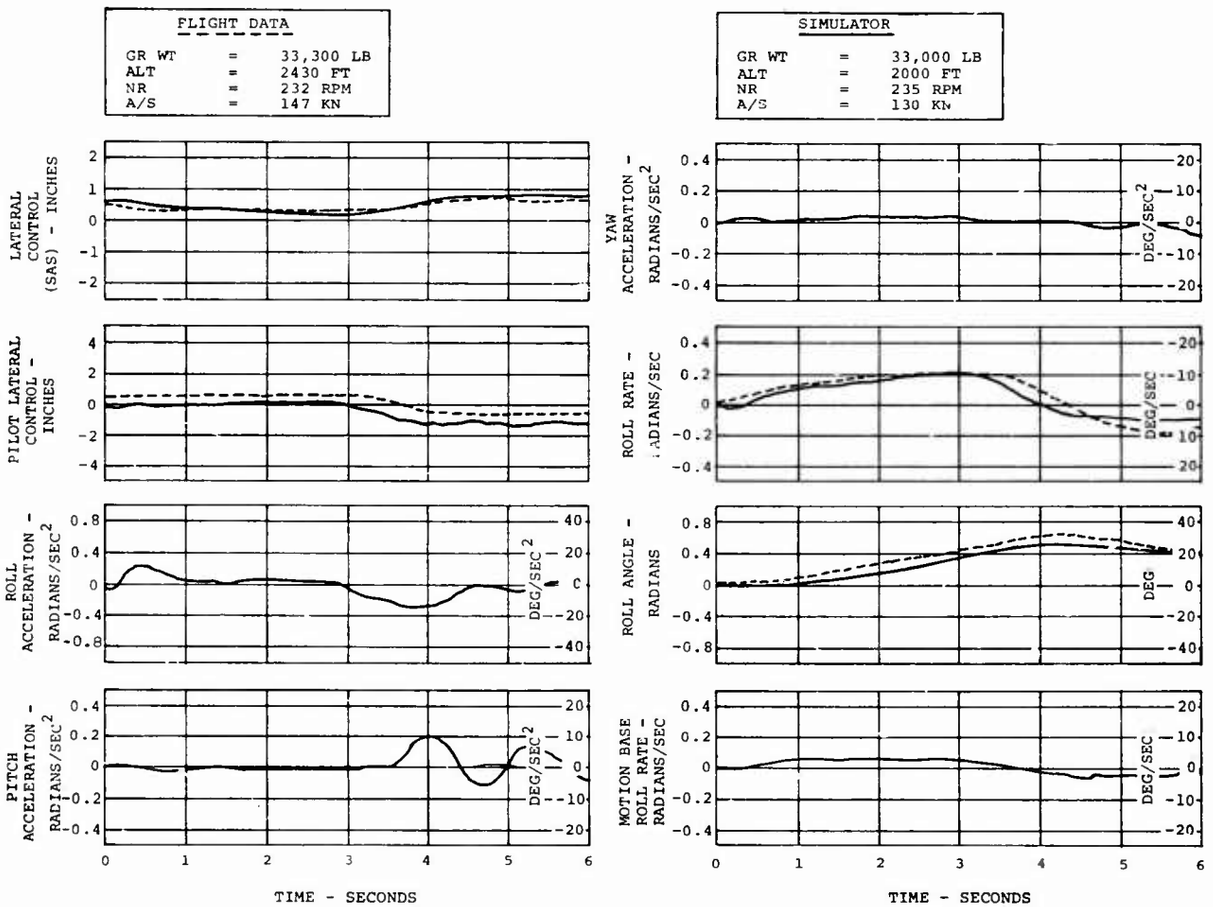

Figure 65. Pilot Validation - Conventional Control System (Roll SAS Failure).

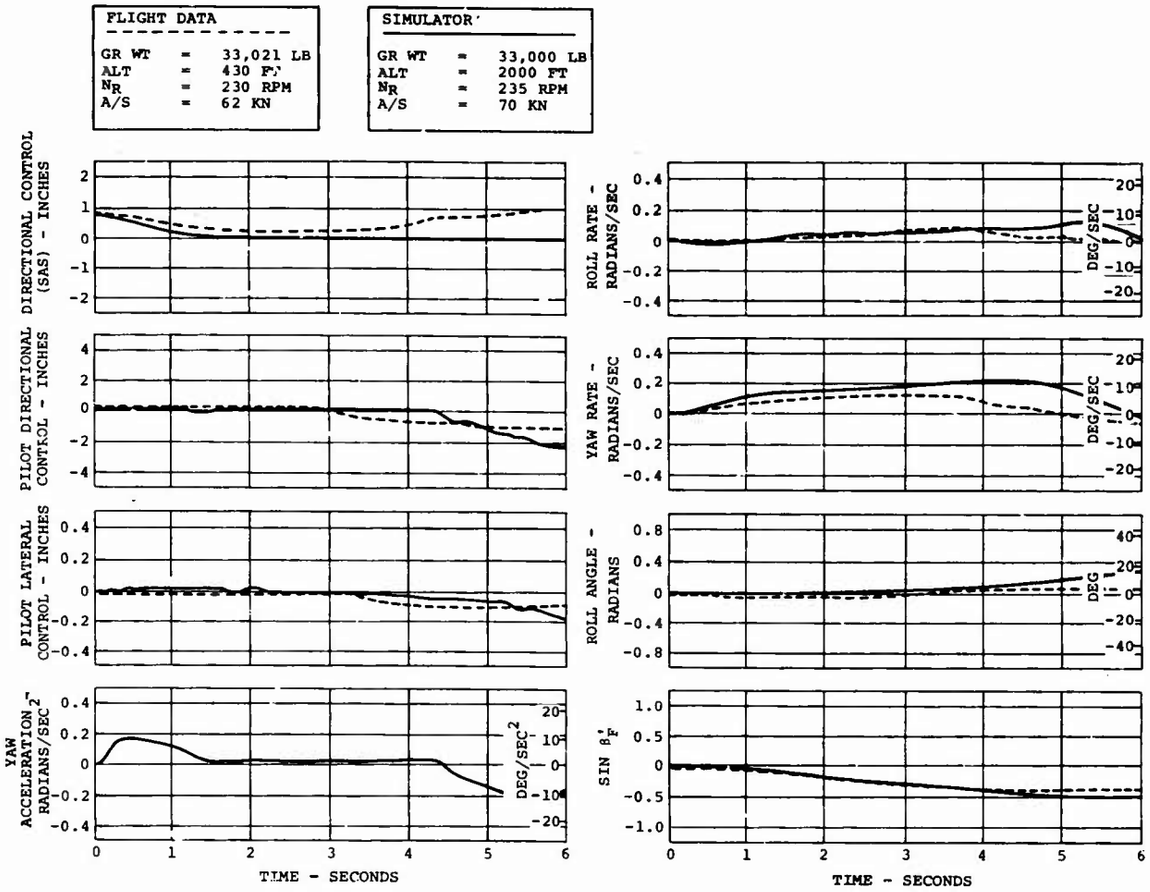

Figure 66. Pilot Validation - Conventional Control System (Yaw SAS Failure).

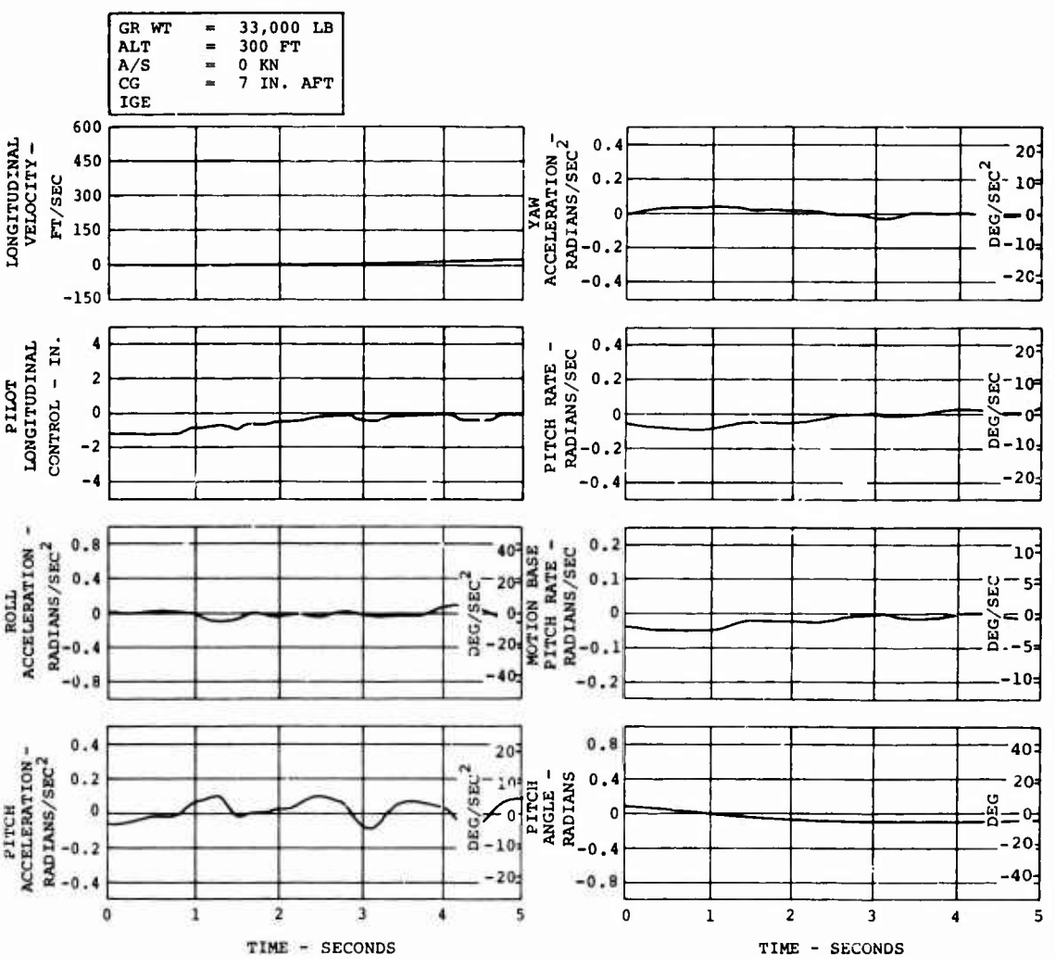

Figure 67. Pilot Validation - Conventional Control System (Hover at 10 Degrees Nose Down).

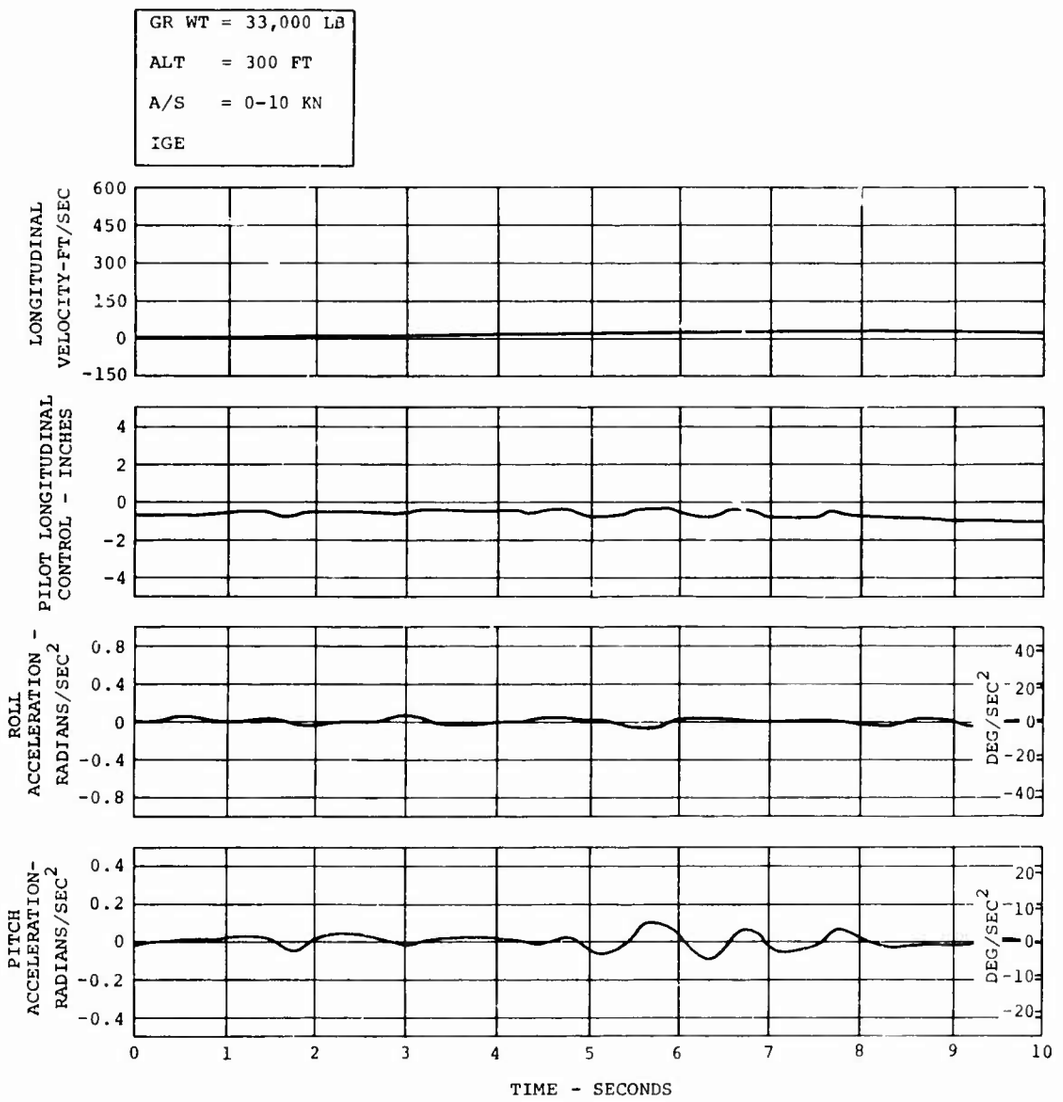

Figure 68. Pilot Validation - Conventional Control System (Hover to 10 Knots) (Page 1 of 2).

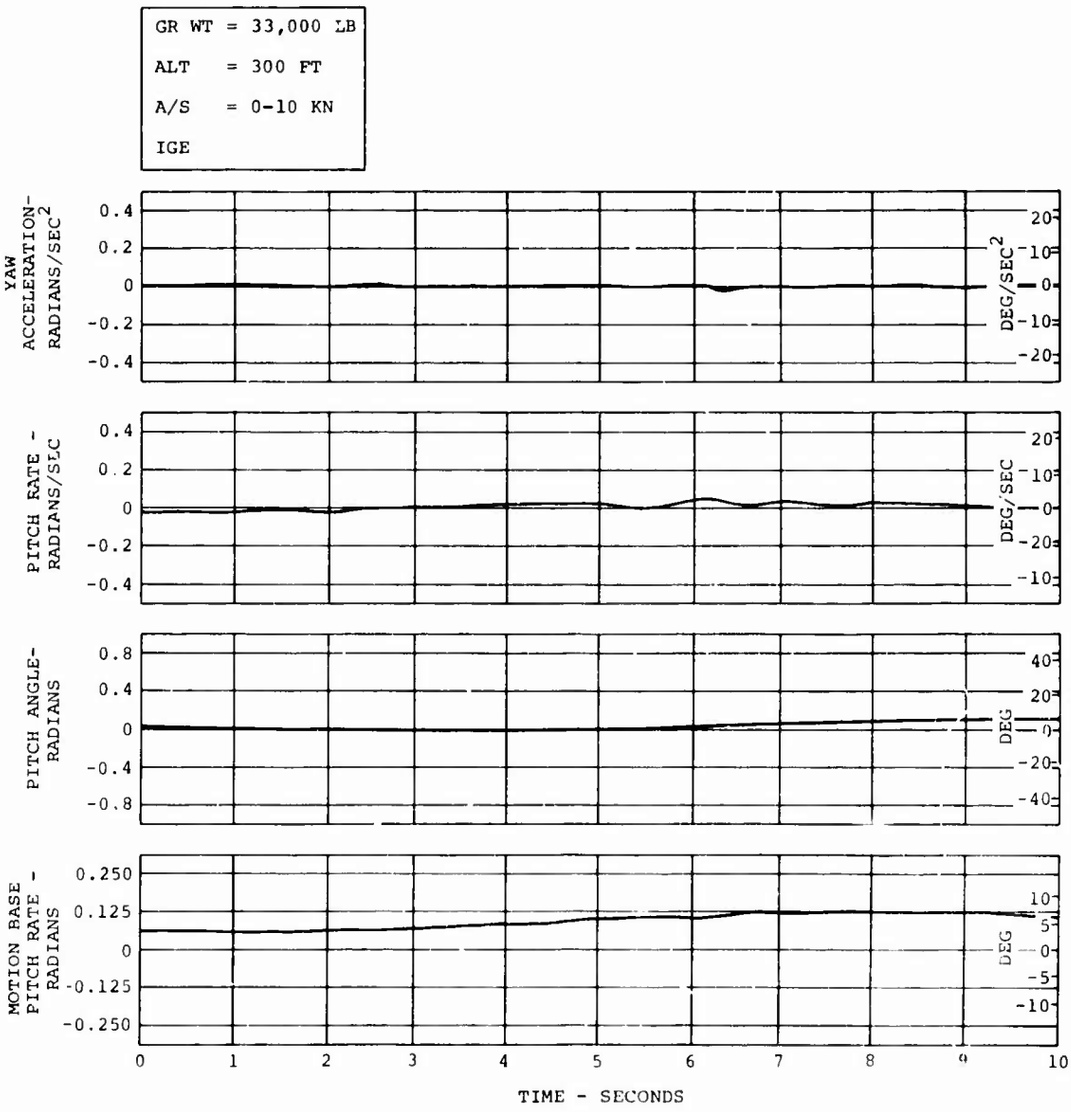

Figure 68. Pilot Validation - Conventional Control System (Hover to 10 Knots) (Page 2 of 2).

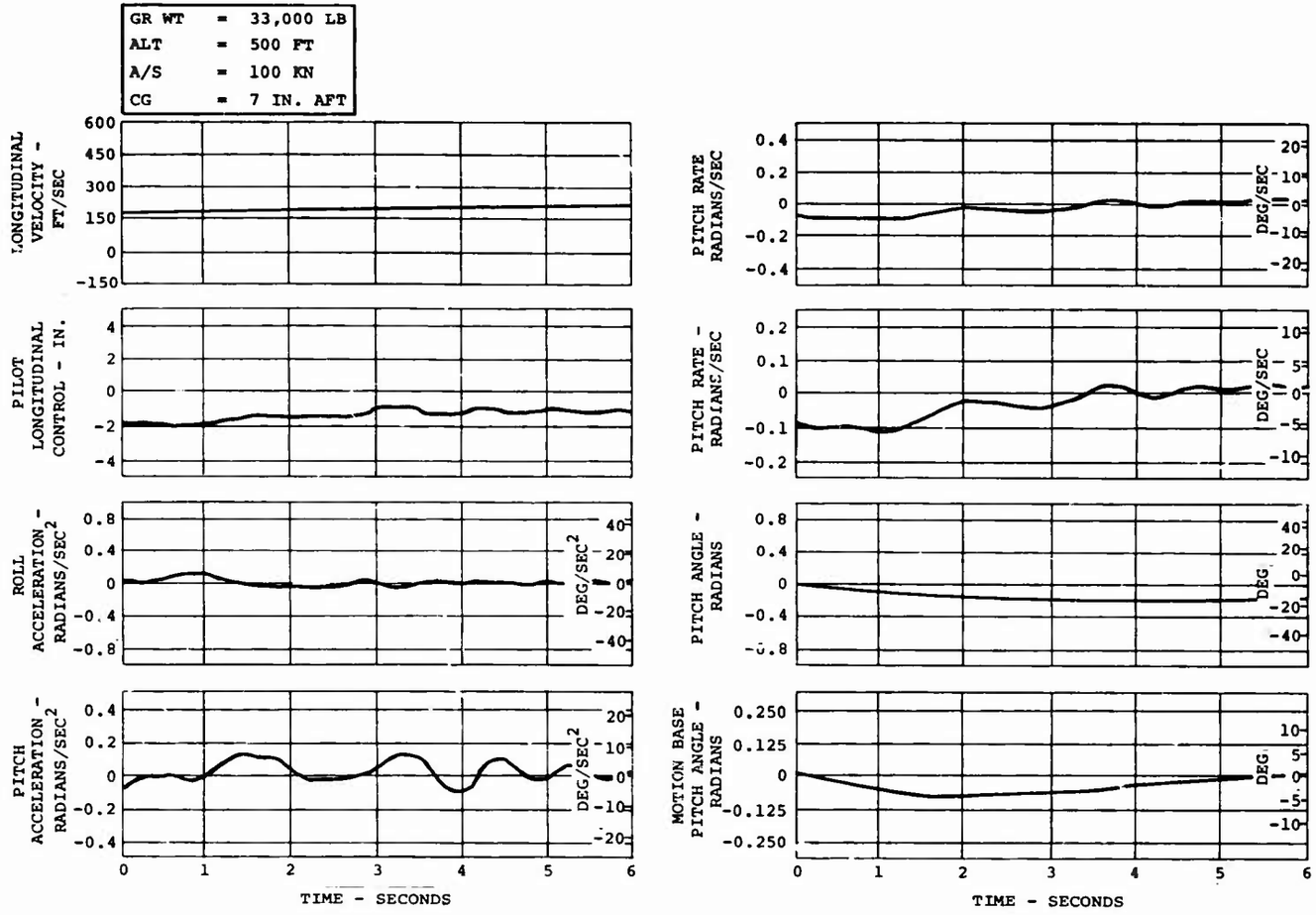

Figure 69. Pilot Validation - Conventional Control System (Forward Flight 10 Degrees Nose Down).

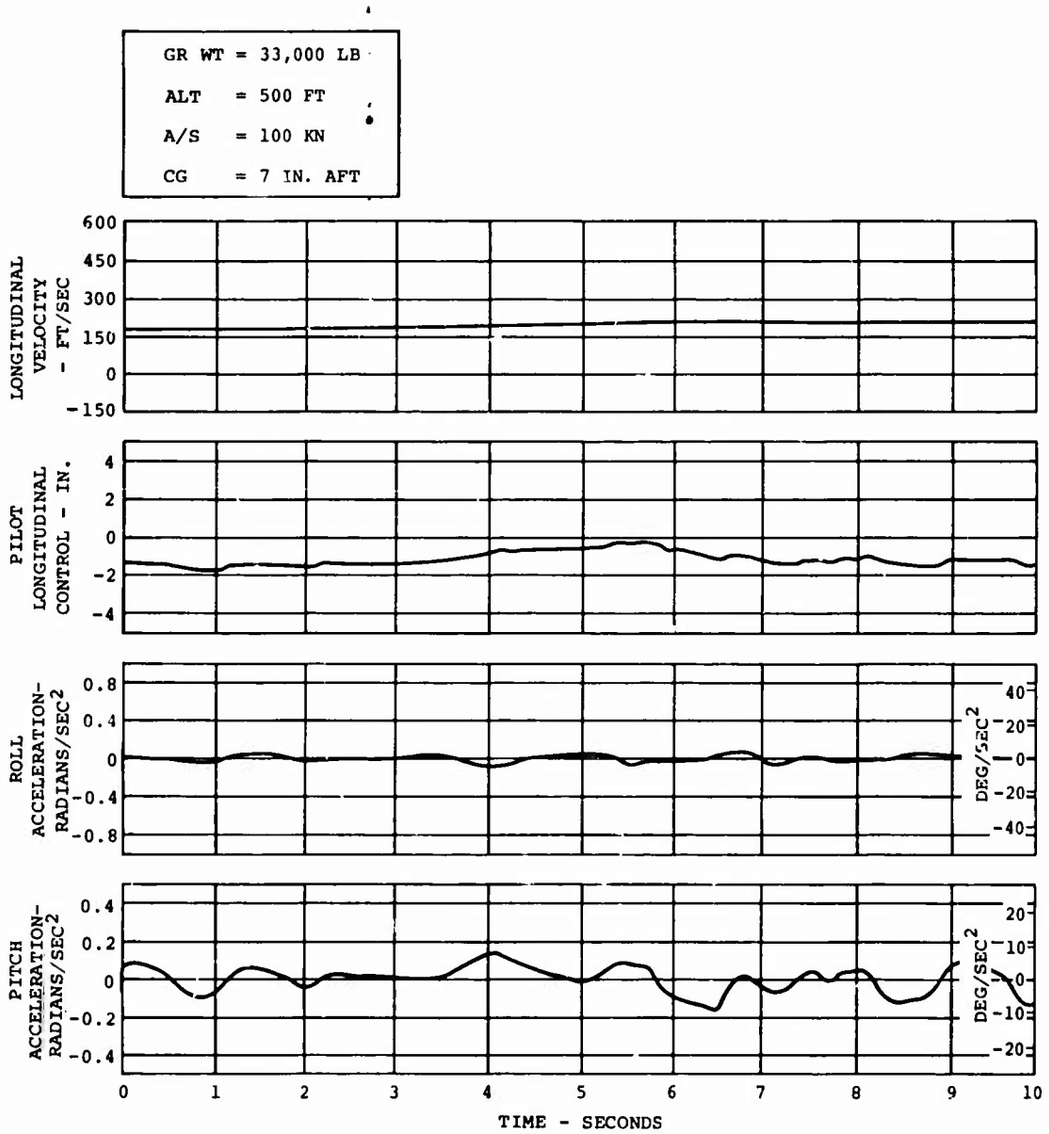

Figure 70. Pilot Validation - Conventional Control System (Acceleration) (Page 1 of 2).

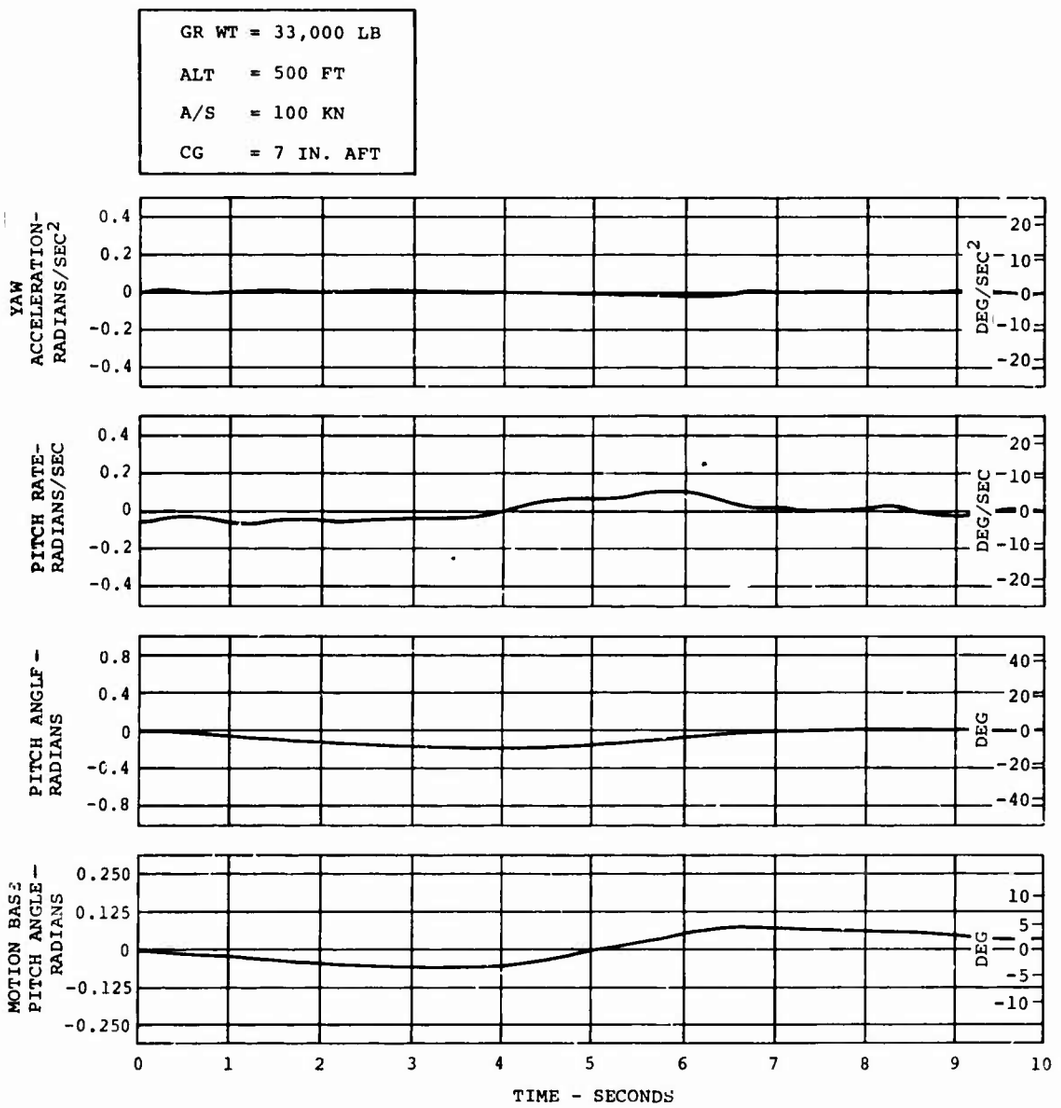

Figure 70. Pilot Validation - Conventional Control System (Acceleration) (Page 2 of 2).

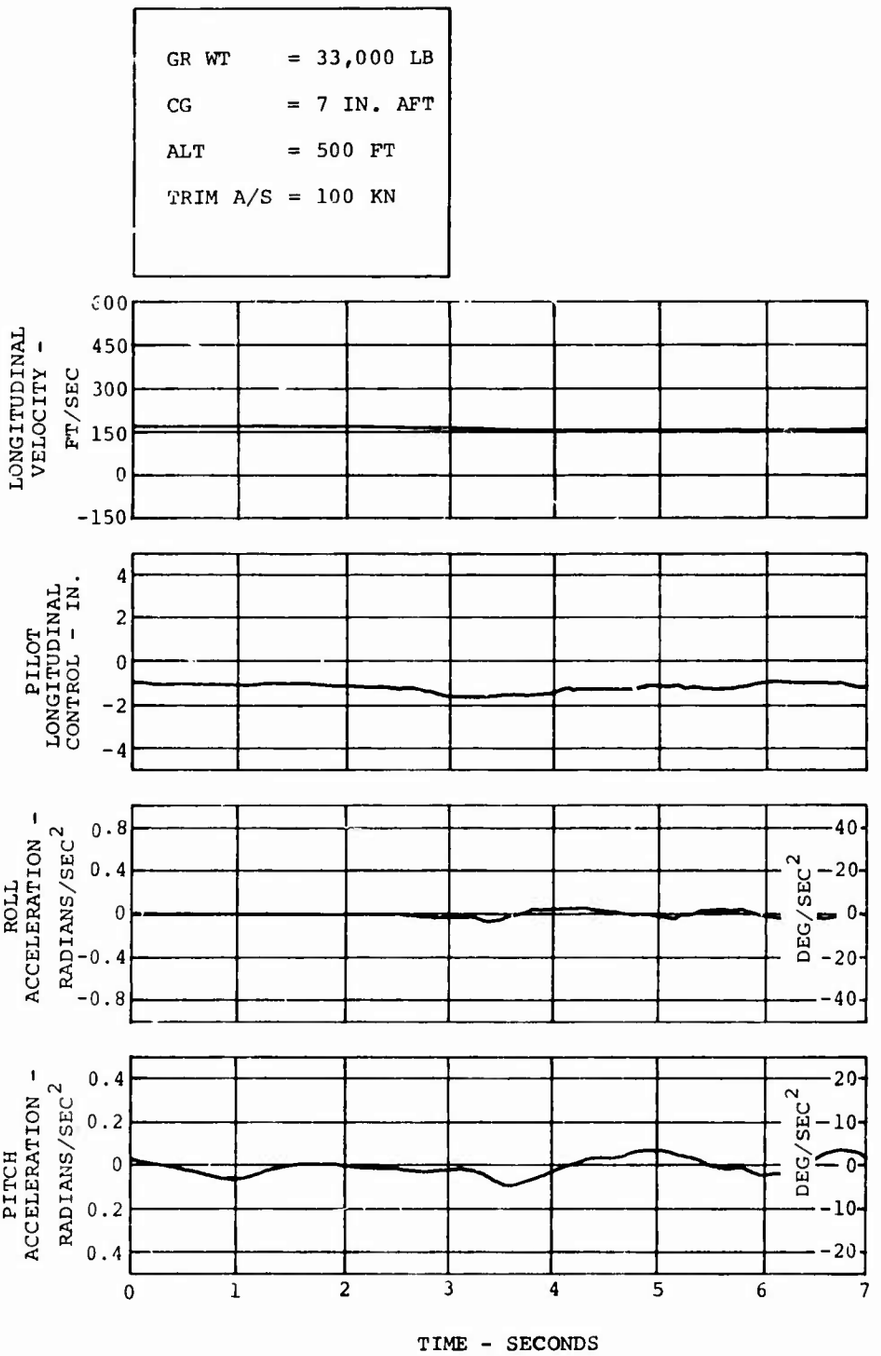

Figure 71. Pilot Validation - Conventional Control System (Deceleration) (Page 1 of 2).

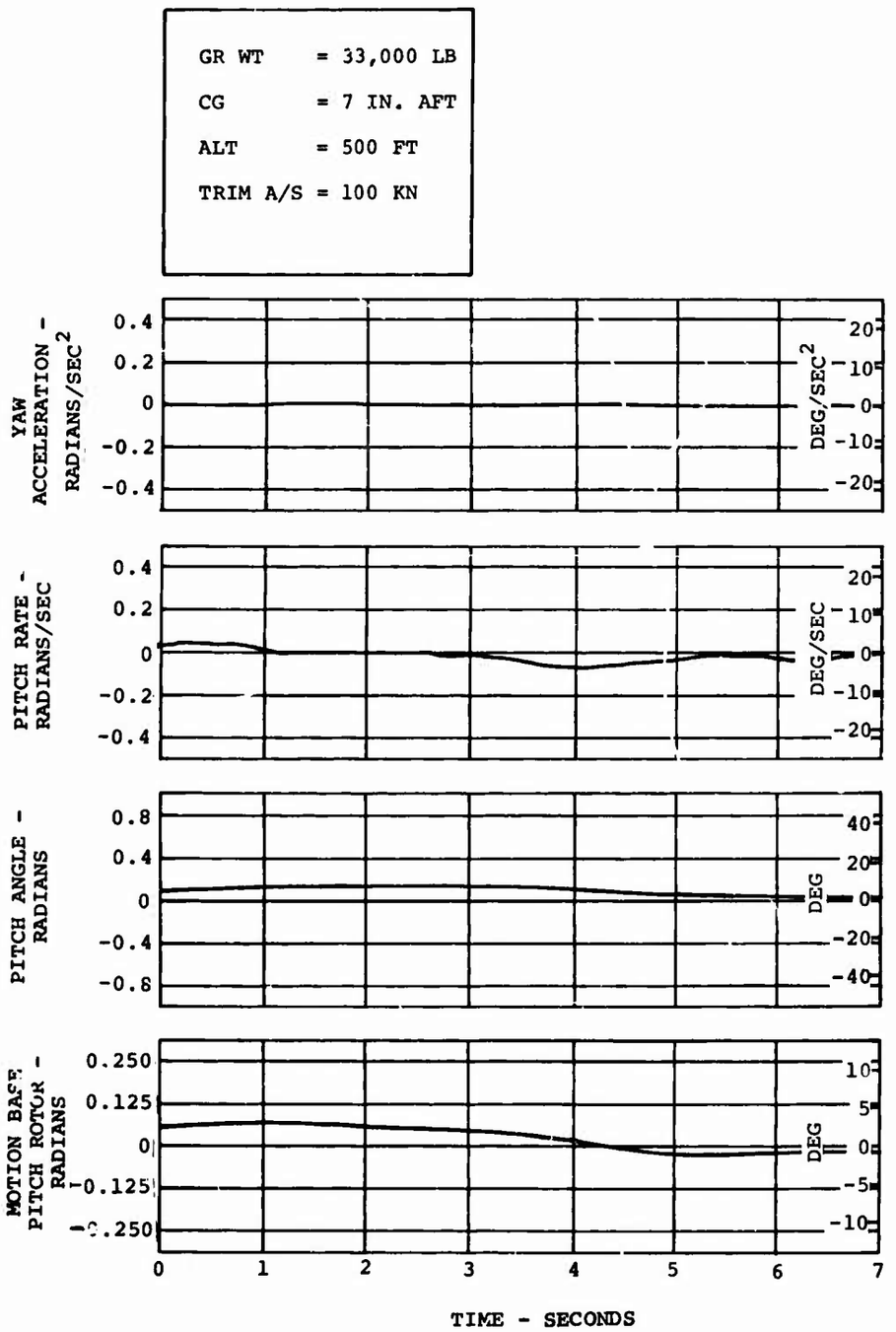

Figure 71. Pilot Validation - Conventional Control System (Deceleration) (Page 2 of 2).

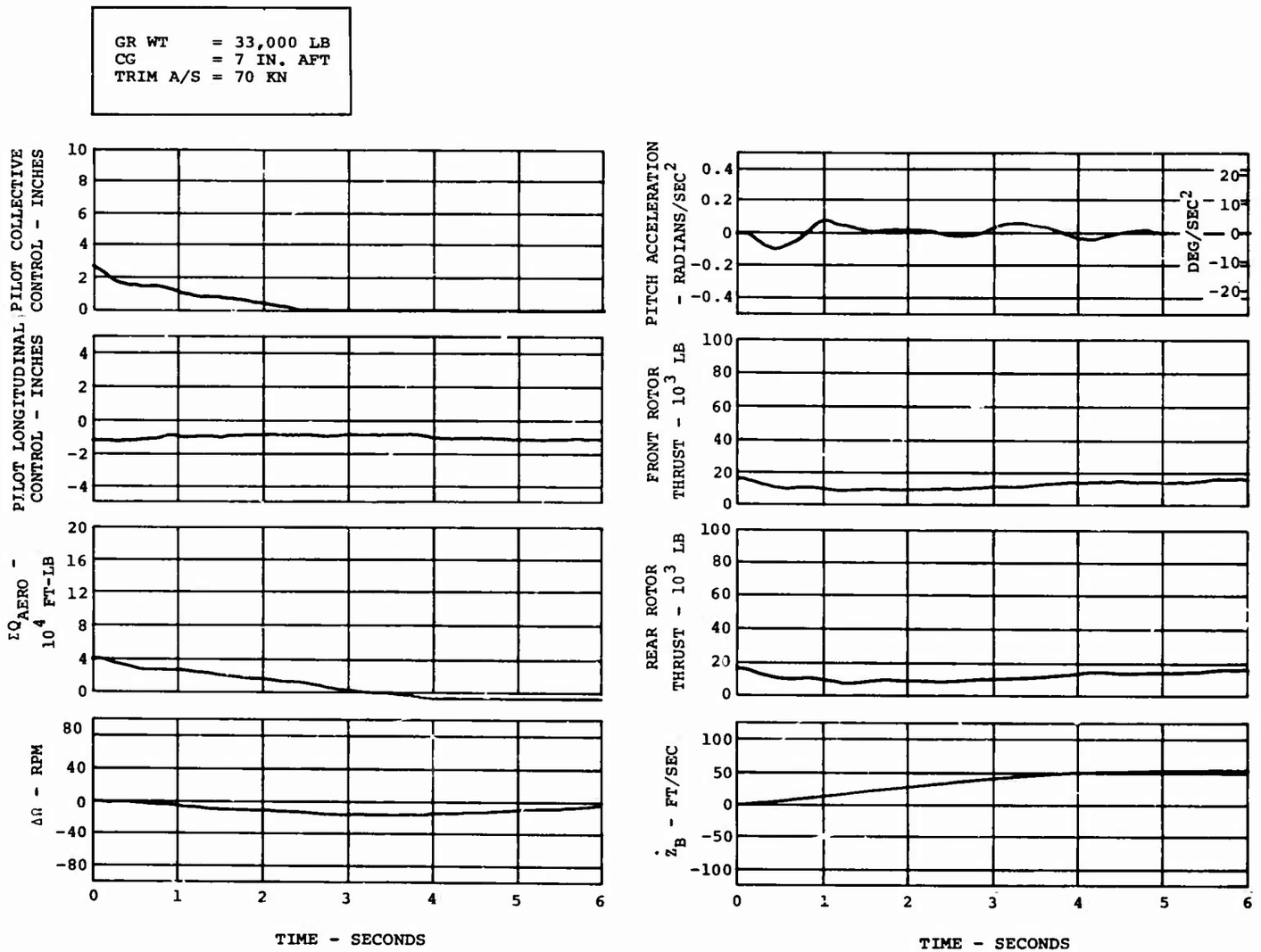

Figure 72. Pilot Validation - Conventional Control System (Autorotation).

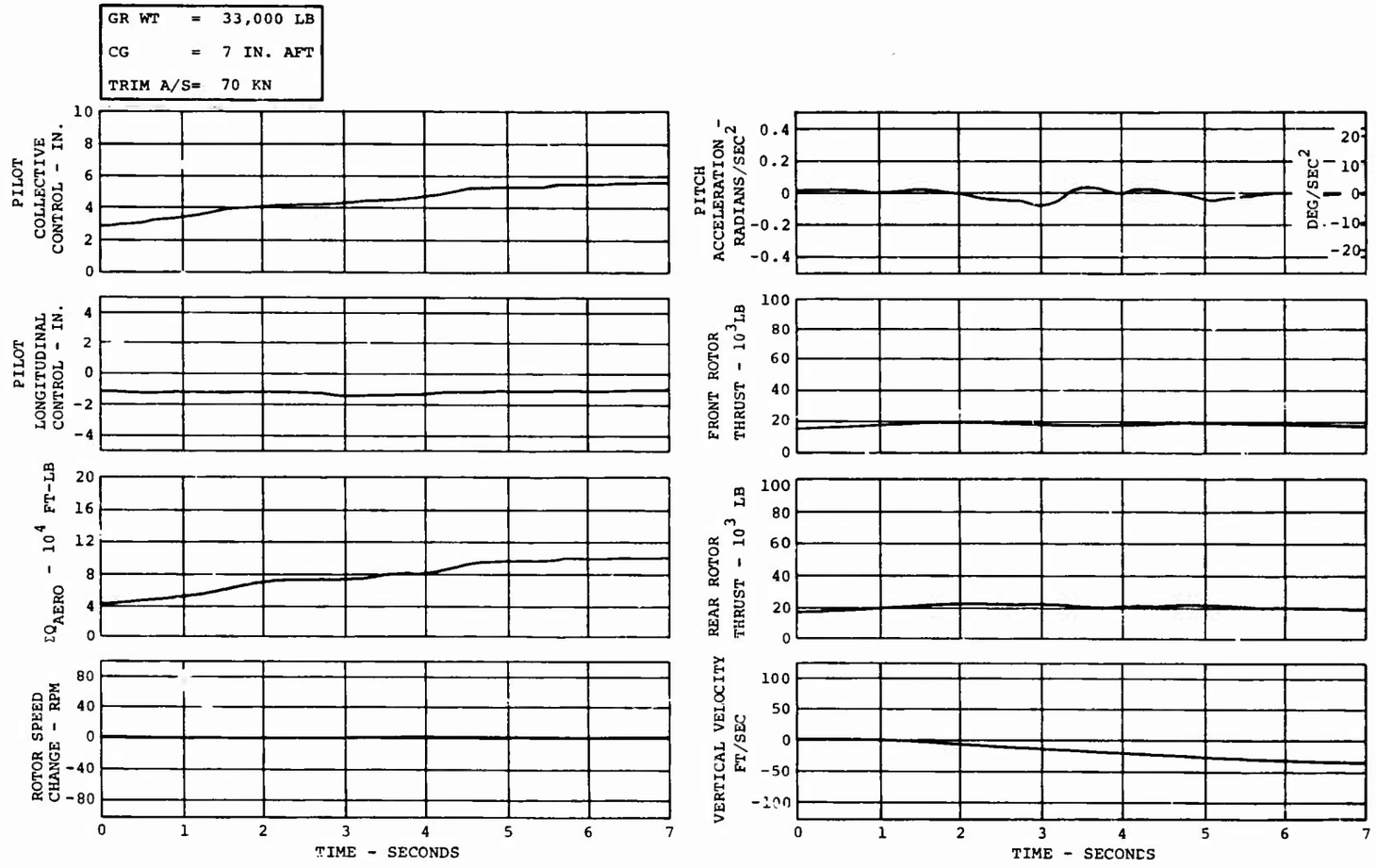

Figure 73. Pilot Validation - Conventional Control System (Climb).

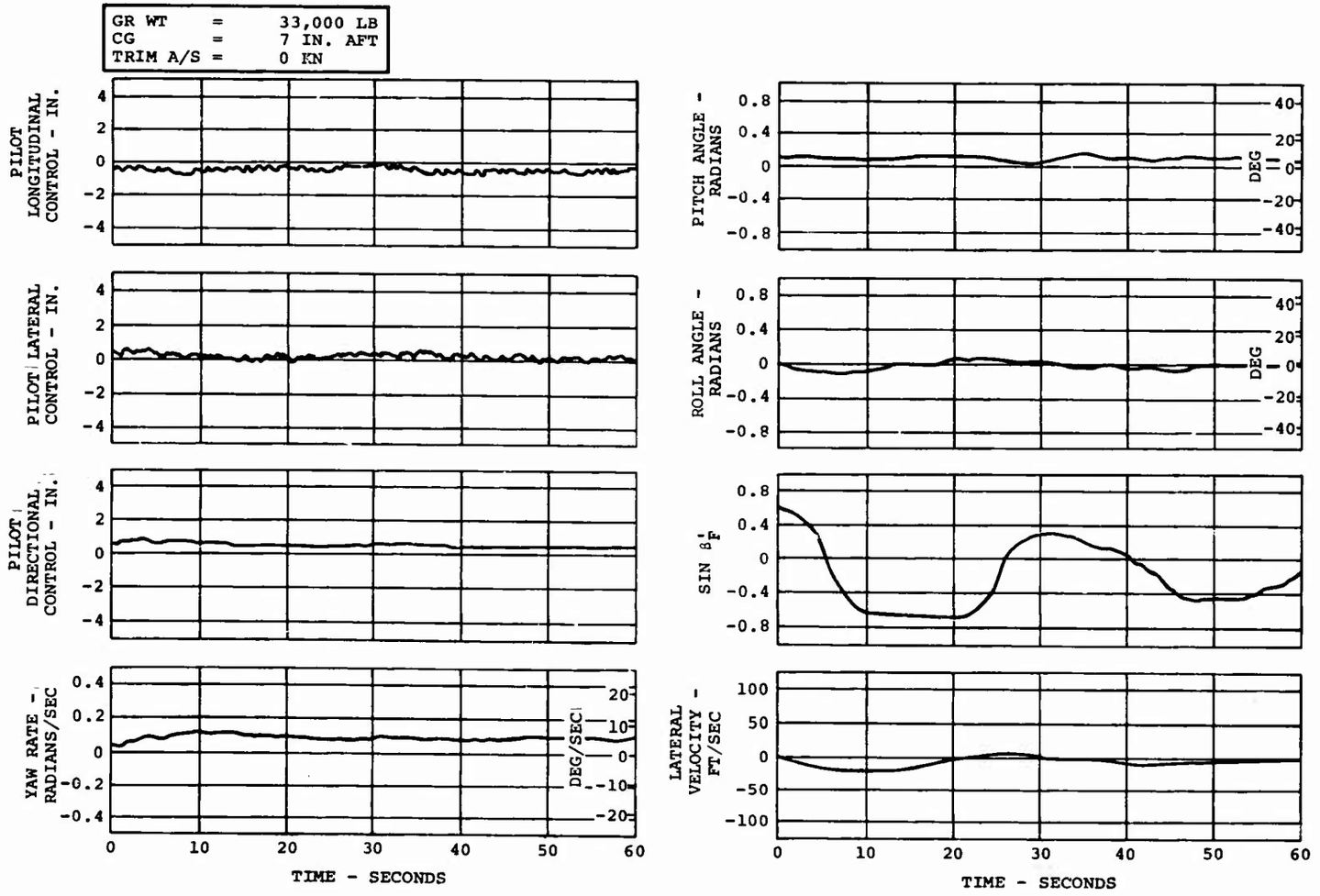

Figure 74. Pilot Validation - Conventional Control System (Spot Turn).

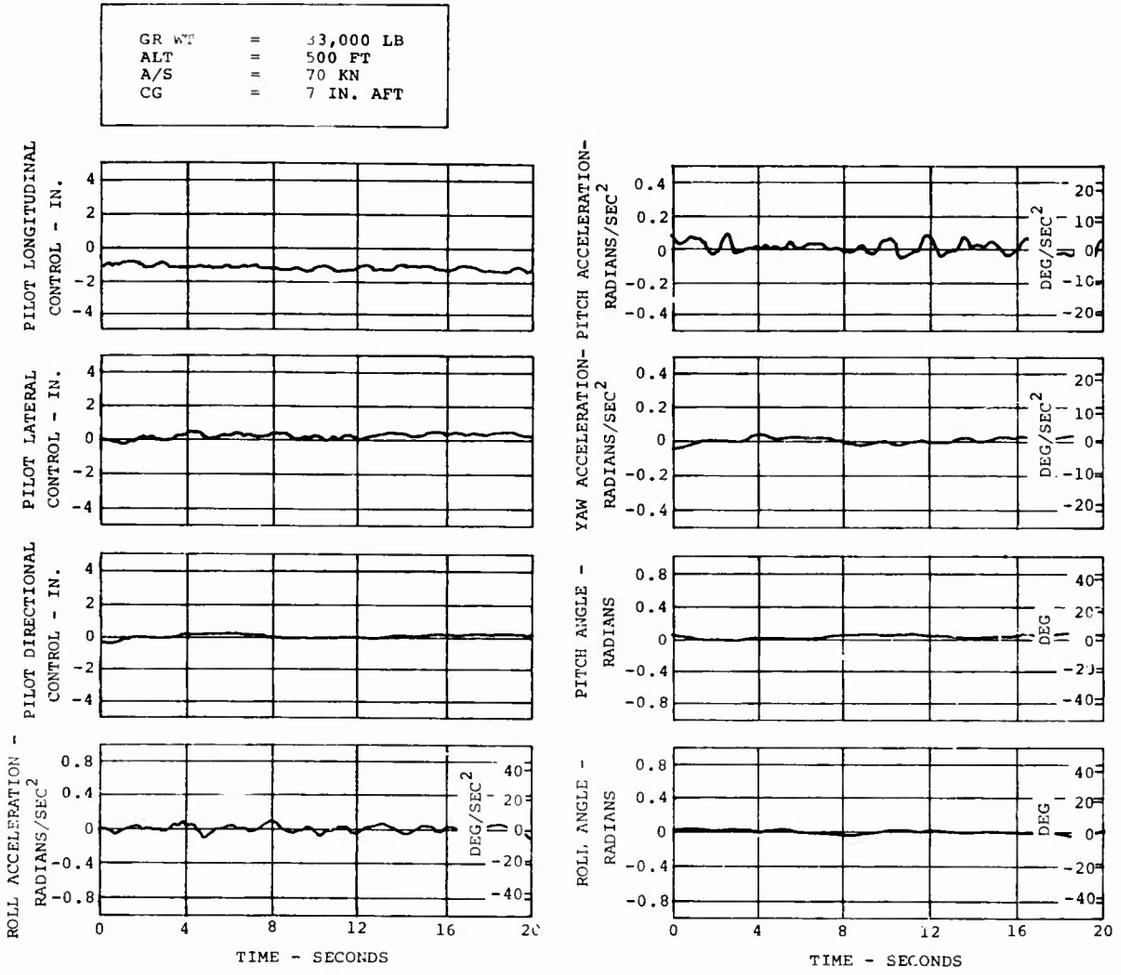

Figure 75. Pilot Validation Conventional Control System (SAS Off).

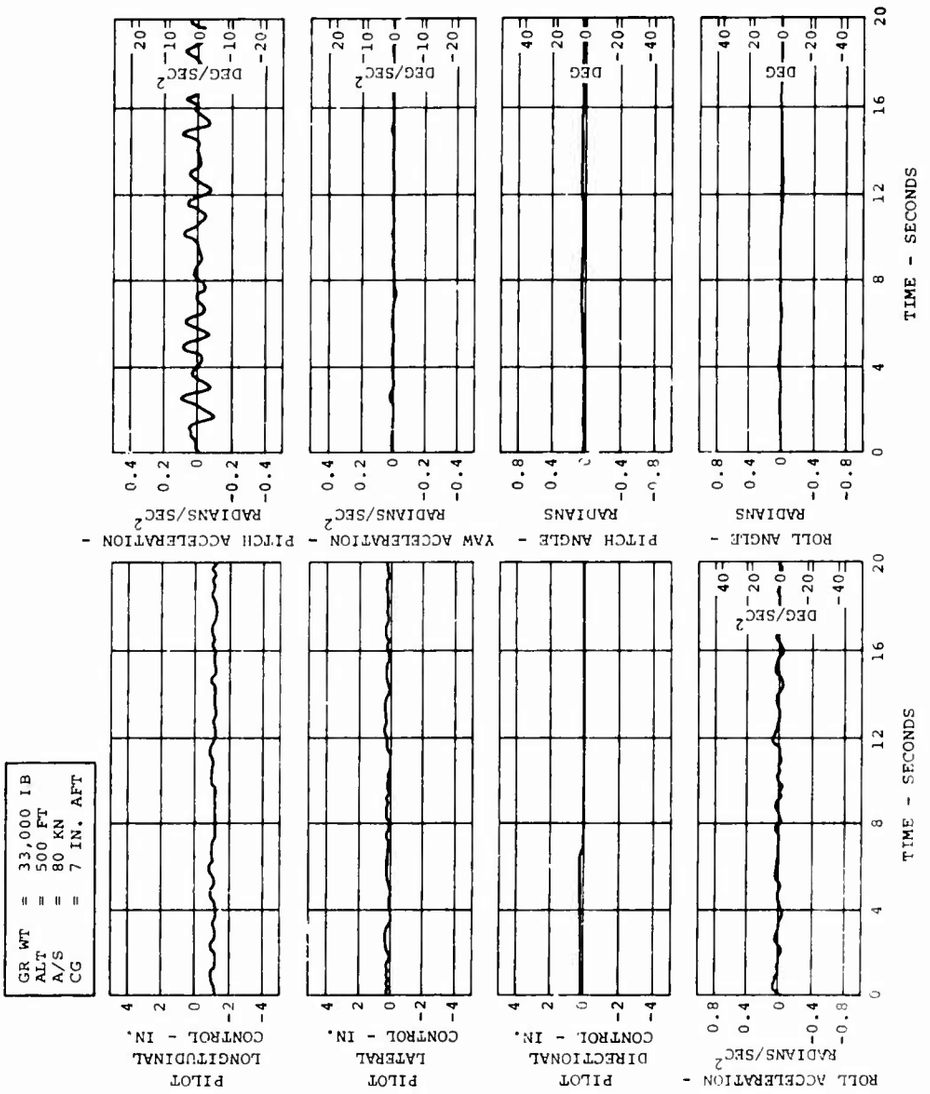

Figure 76. Pilot Validation - Conventional Control System (Forward Flight SAS On).

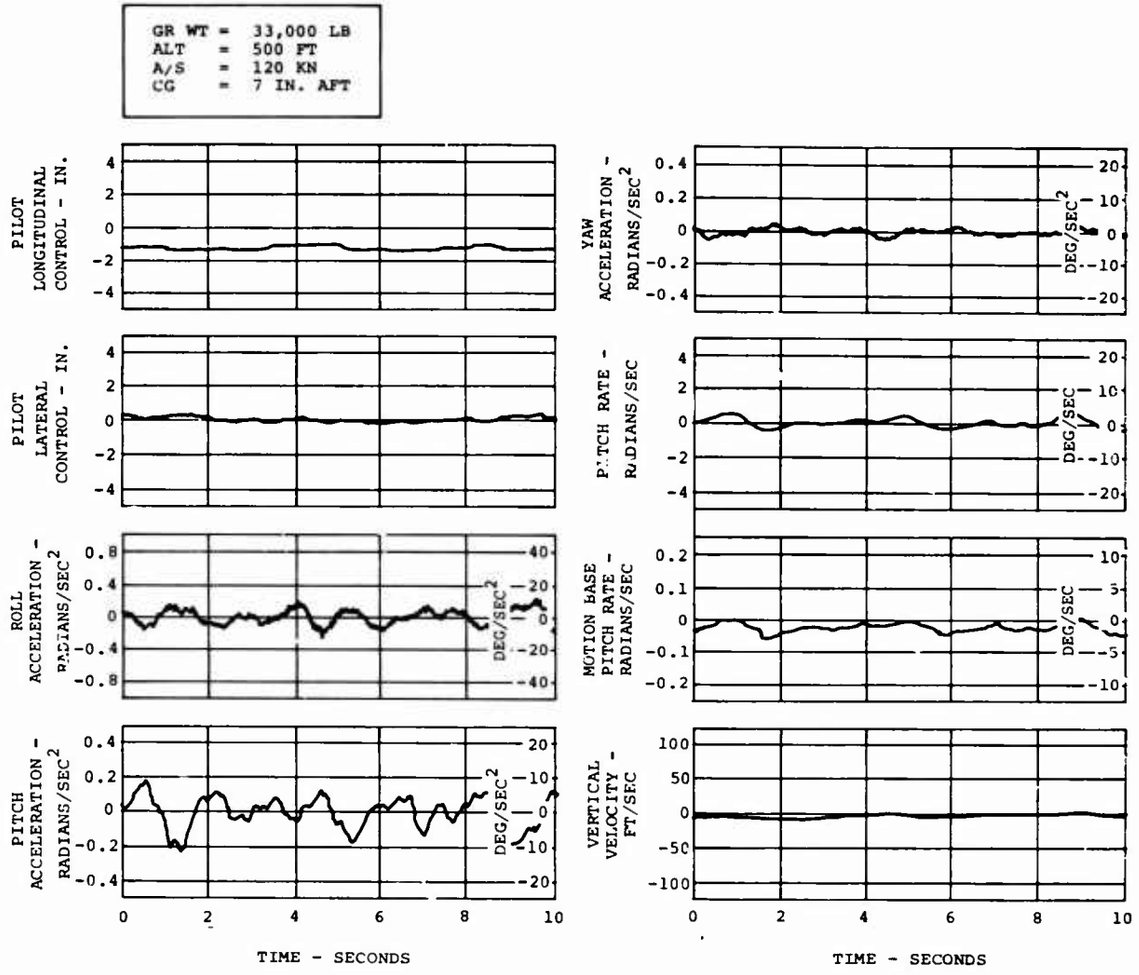

Figure 77. Pilot Validation - Conventional Control System (Moderate Turbulence).

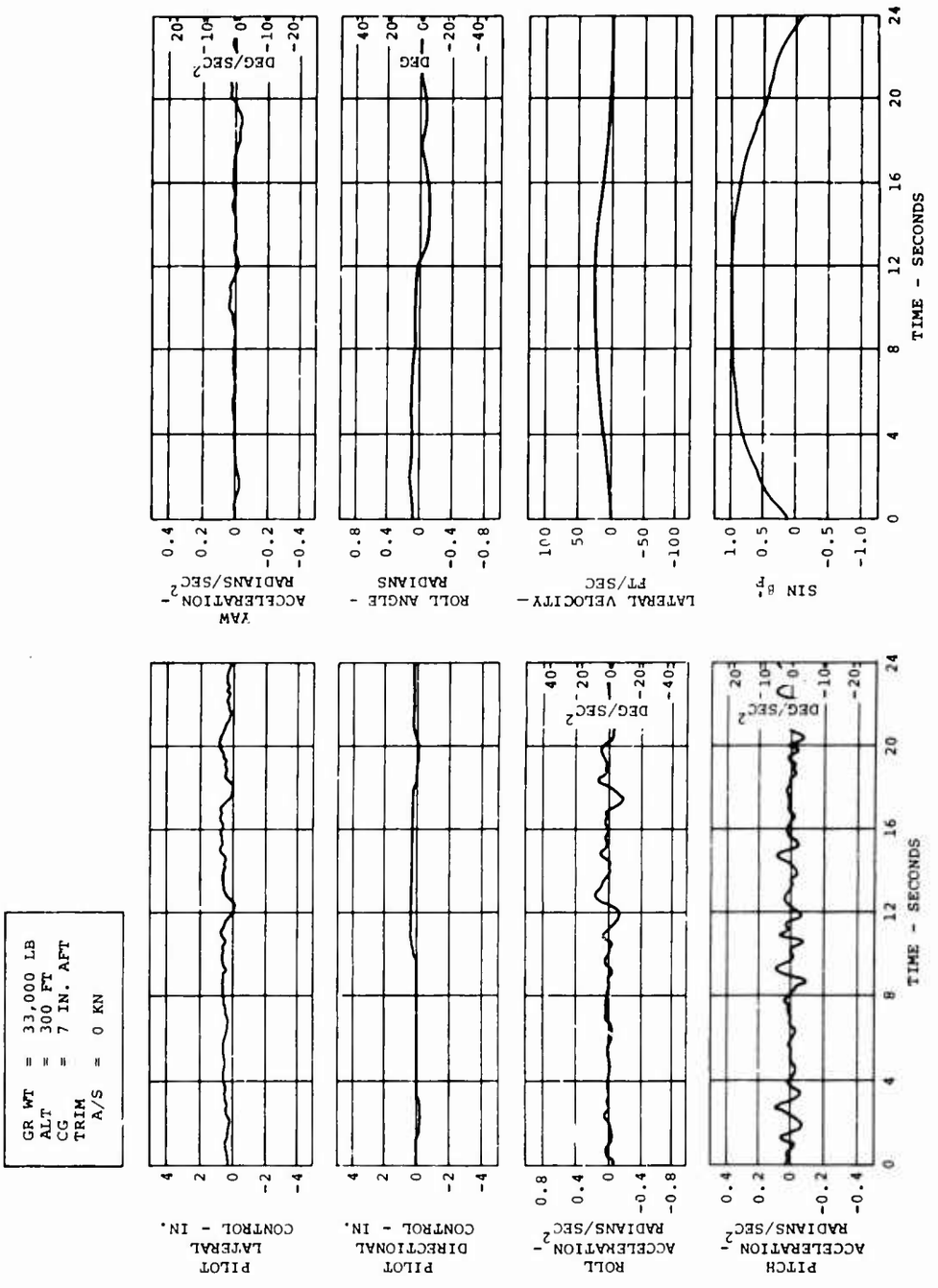

Figure 78. Pilot Validation - Conventional Control System (Lateral Start-Stop).

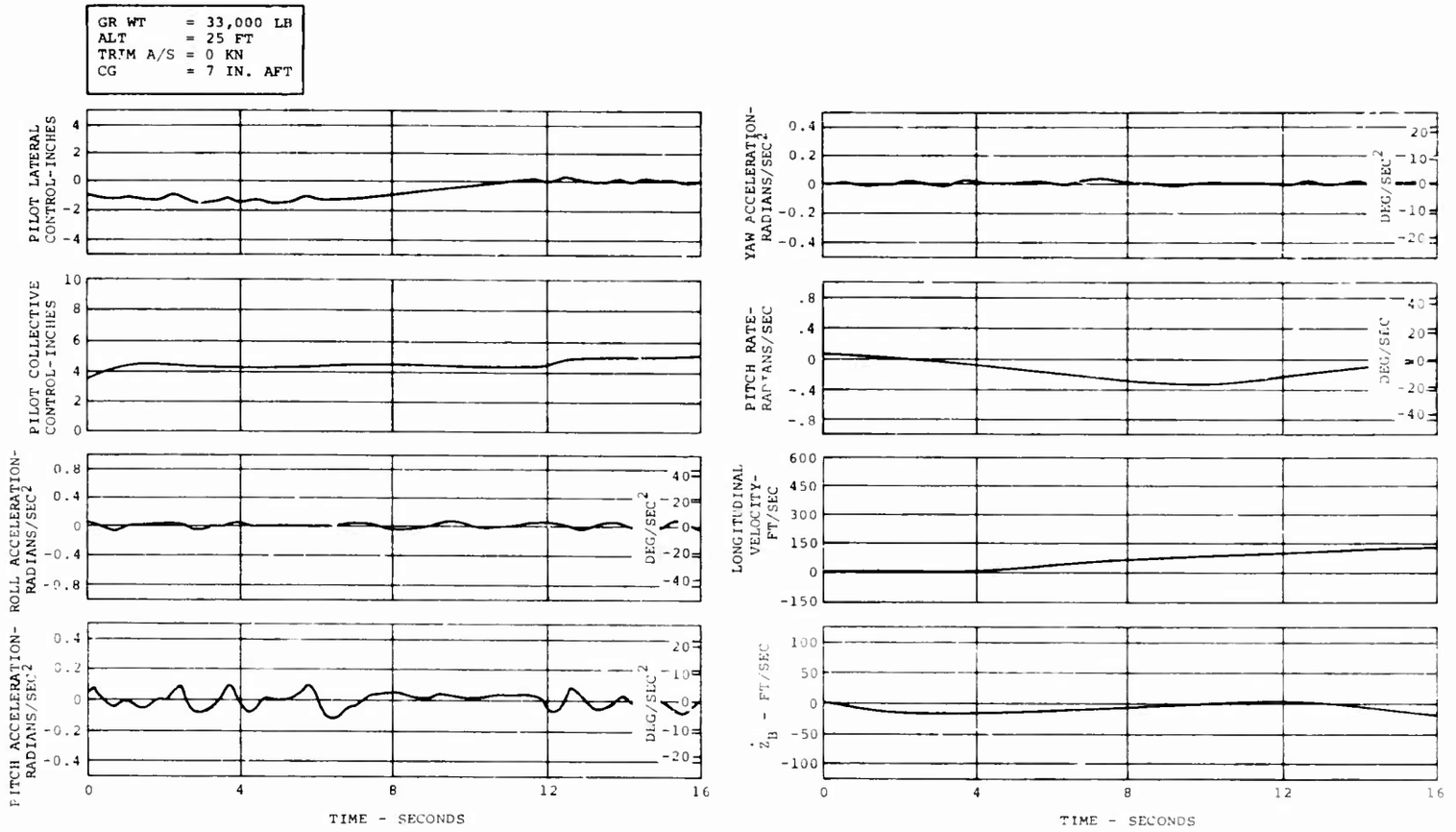

Figure 79. Pilot Validation - Conventional Control System (Acceleration Through Transition).

Unclassified
Security Classification

DOCUMENT CONTROL DATA - R & D

(Security classification of title, body of abstract and indexing annotation must be entered when the overall report is classified)

1. ORIGINATING ACTIVITY *(Corporate author)*
The Boeing Company
Vertol Division - Boeing Center
Philadelphia, Pennsylvania

2a. REPORT SECURITY CLASSIFICATION
Unclassified

2b. GROUP

3. REPORT TITLE
GROUND-BASED FLIGHT SIMULATION OF THE CH-47C HELICOPTER

4. DESCRIPTIVE NOTES *(Type of report and inclusive dates)*
Final Report

5. AUTHOR(S) *(First name, middle initial, last name)*
Nicholas Albion
John R. Leet
P. Austin Mollenkof

6. REPORT DATE	7a. TOTAL NO. OF PAGES	7b. NO. OF REFS
October 1969	156	10

8a. CONTRACT OR GRANT NO.	9a. ORIGINATOR'S REPORT NUMBER(S)
DAAJ02-69-C-0047	
b. PROJECT NO. Task 1F162204A14233	USAAVLABS Technical Report 69-71
c.	9b. OTHER REPORT NO(S) *(Any other numbers that may be assigned this report)*
d.	D8-2418-1

10. DISTRIBUTION STATEMENT
This document is subject to special export controls, and each transmittal to foreign governments or foreign nationals may be made only with prior approval of US Army Aviation Materiel Laboratories, Fort Eustis, Virginia 23604.

11. SUPPLEMENTARY NOTES	12. SPONSORING MILITARY ACTIVITY
	US Army Aviation Materiel Laboratories Fort Eustis, Virginia

13. ABSTRACT

A ground-based simulation of the CH-47C tandem rotor helicopter was constructed and evaluated. The mathematical model provided a fully coupled, large-perturbation representation of the aircraft which was used in conjunction with a five-degree-of-freedom motion base and a wide-angle point light source visual display. The mathematical model was validated by comparing its static and dynamic characteristics with flight test data. A test pilot flew the simulated aircraft to determine the degree of realism achieved and to evaluate the accuracy with which the CH-47 was represented. Representative data and pilot comments are presented in support of the evaluation. The simulation was found to possess sufficient fidelity to be used for investigating control system concepts and the associated handling qualities of the CH-47C.

DD FORM 1 NOV 68 1473 REPLACES DD FORM 1473, 1 JAN 64, WHICH IS OBSOLETE FOR ARMY USE.

Unclassified
Security Classification

14. KEY WORDS	LINK A		LINK B		LINK C	
	ROLE	WT	ROLE	WT	ROLE	WT
Ground-Based Simulation						
Visual Flight Rules (VFR)						
Instrument Flight Rules (IFR)						
Handling Qualities						
Control System Concepts						
Simulator Cockpit						
Analog Computer						
Mathematical Model						